IMPROVEMENTS TO ERGONOMICS AND RELIABILITY OF THE DIGITAL IMAGE ELASTO-TOMOGRAPHY BREAST CANCER SCREENING DEVICE

CLAIRE BEWLEY

A thesis submitted for the degree of
Master of Engineering
in
Mechanical Engineering
at the
University of Canterbury,
Christchurch, New Zealand

January 2017

Acknowledgements

This thesis is dedicated to the late Hope Stark, my grandmother. I never met her, as she fell victim to breast cancer at a young age. Knowing about her fight helped motivate me throughout this research.

I would like to thank my supervisors, Distinguished Professor Geoff Chase and Doctor Matt Signal, for the support and assistance they have given me. Geoff's open door policy, and extremely efficient response time, made it easy for me to progress through my studies. His wealth of knowledge is inspiring and I always appreciated him making time for me in his busy schedule. Matt Signal provided me with countless hours of guidance and ideas. He consistently allowed this paper to be my own work, but steered me in the right direction wherever he thought I needed it.

Thank you also to the technical staff who were always willing to help me when I needed it. In particular, thank you to David Read and Eric Cox. Both of these technicians are extremely approachable, knowledgeable and have given me valuable advice for my thesis and for my future.

I would also like to thank the volunteers who participated in the ergonomic trials I carried out for this research. Without the help from these people, this research would not have been possible. They took time out of their own lives to help me progress with mine, so thank you. I really do appreciate it.

My friends and family, particularly my Mum and two sisters, have always shown a keen interested in my endeavours. Their encouragement and strength throughout my studies has not gone unnoticed. Thank you for the ongoing love and support.

Finally, I would like to thank my partner, Peter Mai, who has been extremely supportive of me during my post-graduate life. He is more than I could ever wish for in a partner. He has helped me stay grounded during my research, and I have been very lucky to have him by my side during this time.

Contents

List of Figures

List of Tables

Abstract

Breast cancer is a major health problem. It has been recognised as the most common cancer among women in both developed, and developing nations. Early detection of breast cancer can significantly reduce mortality, as well as the cost of treatment. Numerous screening systems are used today, but these have limitations including pain or discomfort, high costs and radiation exposure. Digital image elasto-tomography (DIET) is a novel breast screening technique that is non-invasive, low cost and painless. The technology uses tissue stiffness to identify tumours, which are 4-10 times stiffer than healthy breast tissue. Early results from a large clinical trial on a prototype DIET system highlighted two important areas requiring development: ergonomics and the system's breast opening. These two aspects form the focus of this thesis.

During a DIET screening process, a woman must lie prone for up to five minutes for each breast. Any patient motion may lead to reduced quality imaging data. Therefore, the top surface of the DIET system must be ergonomically designed. As part of this research, ergonomic trials were performed on three unique prototype surfaces. Participants were found to prefer a flat surface that gave them an option of where to rest their arms. This surface was developed further with a mechanical loading analysis performed to guide material selection. A design specification has been included for manufacture of the ergonomic surface.

Currently, breast rings isolate the cup of the breast from the chest, and block external light from entering the DIET system. However, breast rings have caused issues during clinical trials, resulting in the need for a new breast opening. A unique shape was chosen for the top surface opening, which allows for imaging all parts of the breast tissue. This shape exposes the patient's chest. Thus, segmentation methods are investigated to isolate the breast cup during imaging. Three phantom breasts with properties that mimic human breasts were created and tested with the new breast opening. When a combination of region and edge detection methods were used, the breast cup was successfully isolated. Additional changes to the DIET system hardware, such as changing the colour of internal components, would reduce the computation required for this process.

This thesis results in a design specification for an improved top surface of the DIET breast screening system. The specification allows manufacture of the ergonomically designed surface, with a unique breast opening shape, for further clinical trials. The improved surface is enabled by improved imaging processes, and is necessary to ameliorate the existing machine's current limitations.

1. Introduction

1.1 Background

Breast Cancer is the most common malignancy among females in both developed and developing regions of the world. It is estimated that 1.67 million women across the globe were diagnosed with breast cancer and over 522,000 women died of the disease in 2012 (Parvin, 2015). Breast cancer is also the most deadly cancer for New Zealand (NZ) women, with more than 2,700 cases diagnosed and more than 600 deaths every year (Hayes, Richardson, & Frampton, 2013). The 2,800 breast cancer cases in NZ, during year 2011, represented 28% of all female cancer registrations, the highest proportion of any cancer among NZ women (Ministry of Health, 2013).

The breast is made of mammary glands that produce milk, as well as fatty tissue. The glandular tissue of the mammary gland consists of lobes, each containing lobules, which have ducts protruding from them towards the nipple (Martini & Nath, 2009). The anatomy of the breast is depicted in Figure 1.1.

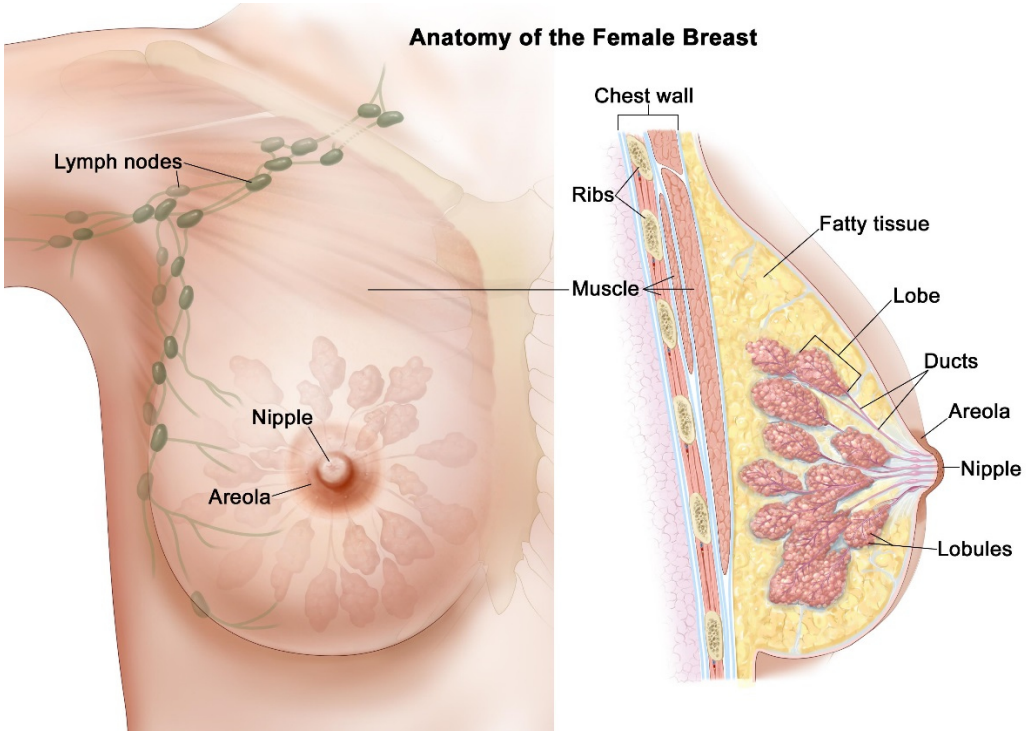

Figure 1.1: Breast anatomy (Institute, 2013)

Breast cancer is a malignancy occurring within mammary gland caused by abnormal growth and uncontrolled cell division. The stages of breast cancer are defined:

1. **Stage 0**: At this early stage, the cancer is non-invasive meaning there is no evidence that the cancer cells, equally, the non-cancerous abnormal cells, are migrating from the part of the breast where they originated, or invading neighbouring tissues. There are two types of stage 0 cancers:
    a. Ductal Carcinoma in Situ (DCIS): Occurs on the lining of the breast ducts.
    b. Lobular Carcinoma in Situ (LCIS): Occurs within the lobules.

2. **Stage I, II and III**: Cancer cells start to become increasingly invasive during these later stages. The cells begin to break through to neighbouring tissue and tumours can increase in size. Cancerous tissue can also spread through to the lymph nodes during these stages.

3. **Stage IV**: At this late stage, invasive breast cancers cells have spread beyond the breast and lymph nodes and into other organs of the body, such as the lungs, skin, bones, liver or brain (Cowell et al., 2013).

The five year survival rate, for women in developed nations, with each of the stages is summarised in Table 1.1. Clearly, earlier detection will improve the likelihood of treatment being successful.

Table 1.1: 5-Year survival rates for women with varying stages of breast cancer (Society, 2015)

Stage	5 Year Survival Rate
0	100%
I	100%
II	93%
III	72%
IV	22%

1.2 Breast Cancer Detection Methods

Early detection of breast cancer has a significant effect on the survival rate of a patient. Most cases of breast cancer are found through self-examination (Valea & Katz, n.d.), although the use of clinical screening with mammography has increased in recent years with aging demographics and public health campaigns to raise awareness (Feig, 2006). The average diameter of an abnormality detected by feeling for a lump is 22mm (W. a. Berg et al., 2004), whereas mammograms can detect abnormalities as small as 2mm in size (W. a. Berg et al., 2004). However, the average size detected with mammography is 14.5mm, and these statistics include those found first via manual palpation and then confirmed with a mammogram (W. a. Berg et al., 2004).

Detecting smaller abnormalities typically means the cancer has been found at an earlier, non-invasive, stage. Early detection of breast cancer leads to a 95% five year survival rate (Michaelson et al., 2002). However, when a cancer is detected at the latest stage, the five year survival rate drops to 15% (Michaelson et al., 2002).

There are currently three types of technology commonly used for breast cancer detection:

1. **Mammography (breast x-ray):** Currently, mammography is the conventional method of breast cancer screening and is regularly used in most developed nations. The New Zealand Breast Cancer Foundation states the ten-year survival rate for breast cancer patients is 92% if the cancer was detected by mammogram, but only 75% if a lump is the first sign (New Zealand Breast Cancer Foundation, 2015). Mammograms can detect cancers as small as 2mm in diameter. However, the average cancer size detected with a mammogram is 14.5mm (W. a. Berg et al., 2004).

   While mammography can detect some breast cancers, it has limitations including performance, cost, radiation exposure and patient discomfort. The use of x-rays also require specialised premises, adding further costs and restrictions of access that can limit screening compliance. The cost of equipment and personnel alone puts mammography out of reach for most developing nations. Mammography is also limited to screening women over the age of 45 when the breast tissue is typically less dense, primarily due to risks of radiation exposure. However, mammography is less robust as a screening tool in dense breasts (W. a. Berg et al., 2004).

   Despite these limitations, mammography is the current typical standard of screening care.

2. **Ultrasound:** Sound waves are used to detect changes in tissue density with ultrasound technology. Typically, ultrasound is used to determine whether an abnormality is solid or contains fluid. Therefore, ultrasound is used in conjunction with a mammogram, rather than replacing it as a screening tool. While an ultrasound does not rely on x-ray imaging and is relatively low cost, this screening method is less reliable than alternative screening options (Valea & Katz, n.d.),(W. A. Berg et al., 2008). In addition, ultrasound is heavily dependent on the availability of skilled operators.

3. **Magnetic Resonance Image (MRI):** MRI uses a magnetic field and radio waves to create detailed images of breast tissue. The reliability of using MRI as a breast screening method is still being evaluated (W. A. Berg et al., 2008). Regular screening with MRI is exclusively recommended to women at high risk of breast cancer, and is to be used in conjunction with mammogram technology. Early tests show that MRI screening may be more sensitive for picking up breast cancer. However, MRI is a much more expensive tool than conventional mammograms (Dempsey, Condon, & Hadley, 2002), and its time and cost limit its use in high throughput screening.

Each breast screening method has inherent limitations. To make breast screening available to all women, regardless of age or location, there is a great and growing need for additional breast screening modalities that address some/all of these limitations. In particular, an ideal screening method would remove limitations around age and x-ray invasiveness, cost and portability, where current tools are primarily in expensive, radiation proofed fixed locations, which can affect compliance and reduce screening efficacy.

1.3 Digital Image Elasto-Tomography (DIET)

The digital image-based elasto-tomography (DIET) technology is a non-invasive, low cost, painless breast cancer screening system that works well on both dense and less dense breast tissue. The DIET system operates by assessing breast tissue stiffness. In particular, cancerous tissue has been shown to be 3 – 13 times stiffer than surrounding tissue (Samani, Zubovits, & Plewes, 2007). This contrast in stiffness is much larger than the contrast in radio-density (between 1.05 – 1.10) measured in mammography (Kashif, 2013).

The DIET system detects abnormalities within breast tissue by applying a small mechanical vibration to the breast, while observing and processing images of the breast surface motion response. The system consists of an array of digital cameras synchronized with strobe lights, as in Figure 1.2. These cameras are used to capture sinusoidal surface oscillations at pre-set phases relative to the input motion, as the response is at the same frequency. The input is sinusoidal low amplitude mechanical actuation directly applied to the breast. The breast surface motion can then be evaluated directly to determine the presence of stiffer cancerous lesions based on how stiffer tissue modifies the progress of shear ware in the tissue (Kashif, Lotz, Heeren, & Chase, 2013). Equally, it can be put into an inverse reconstruction algorithm to more directly calculate the distribution of internal stiffness of the breast (Kashif, Lotz, Heeren, et al., 2013), (Van Houten, Peters, & Chase, 2011).

The initial goal is to have the DIET machine detect a 10mm mass, equal to or better than the current mammogram average (W. A. Berg et al., 2008). Detecting abnormalities at this size has been shown to lead to 15 year survival rates of over 85% (Michaelson et al., 2002). In addition, it could serve all ages, as it does not require x-ray dosing, and could be used equally as a pre-screening tool prior to mammography. Finally, it's low-cost and portability could be used to enhance screening compliance and numbers in a cost-effective manner.

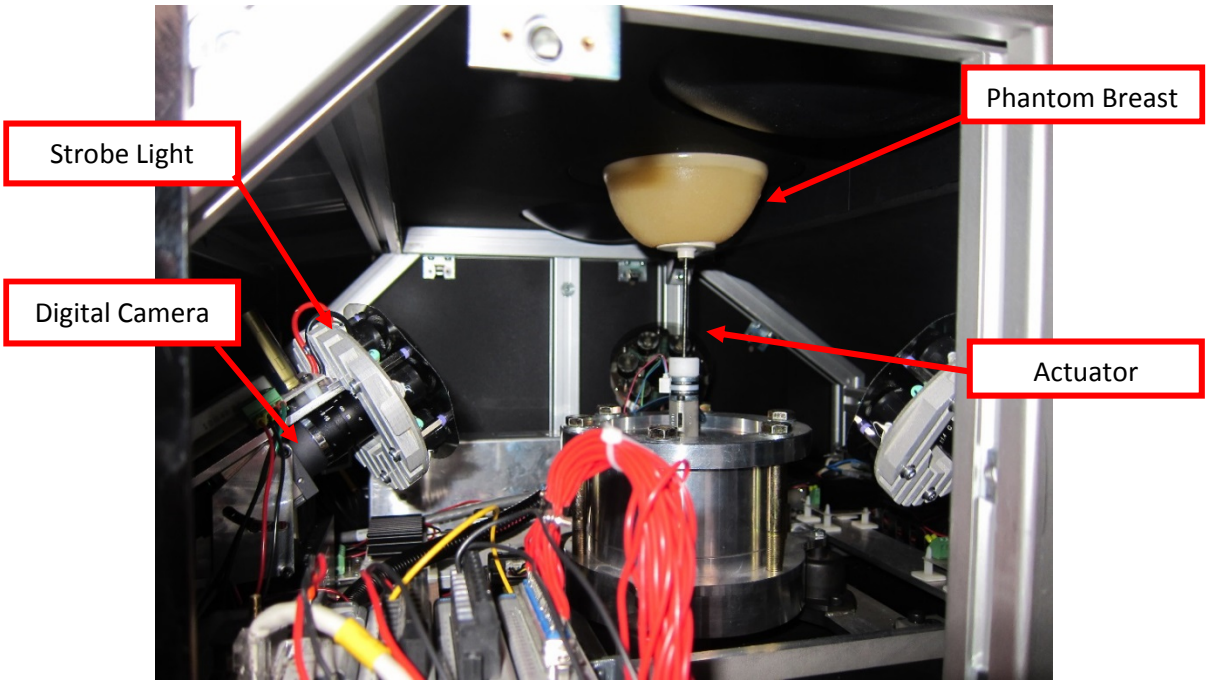

Figure 1.2 Internal components of DIET machine

The DIET technology is currently in a working prototype state and is undergoing a clinical study at Canterbury Breastcare to assess performance and limitations. The trial recruits both healthy volunteers and those that have recently had a screening/diagnostic result showing the presence of an abnormality. The process involves participants lying face down on the surface of the system with one breast hanging pendant into the system, as illustrated in Figure 1.3.

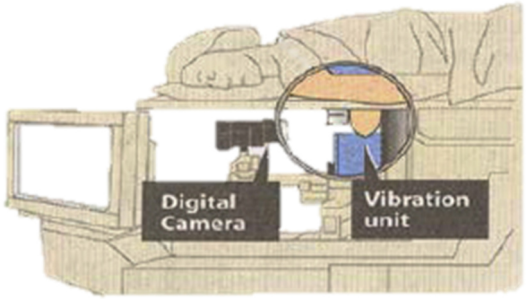

Figure 1.3: Schematic of DIET breast screening system

In the current design, an appropriately sized interchangeable breast ring is used to provide a boundary between the woman's breast, as close to the chest as possible, and the underside of the support surface. Inside the system, a mechanical actuator is positioned below the centre of the suspended breast, before the actuator is raised and a small vertical preload applied to the breast. The actuator then vibrates the breast vertically at an amplitude of less than 1mm, over a range of frequencies.

During the cyclic vibration, multiple images of the breast surface are taken. These images are post-processed to detect motion from which it is possible to determine the presence of an abnormality. The total time to image each breast using the DIET system is approximately five minutes, although it is anticipated this imaging time will be significantly reduced in a commercial system. The patient then changes position so their other breast is screened and the process is repeated.

1.4 Research Issues and Scope

While early stage clinical testing of the system has successfully detected breast abnormalities, two important areas of development have been exposed. The first is the ergonomics of the machine and its ease of use, which could be improved. The second is the breast opening. These two areas of development are the focus of this research thesis, as improvements in these areas will impact the imaging and thus the detection capability of the system.

1.5 Research Objectives

1.5.1 Breast Opening

The current DIET system uses several interchangeable breast rings for two main reasons: **1**) To isolate the cup of the breast from the rest of the chest; and **2**) To block light from entering the system, causing motion measurement noise errors due to the sensitivity of the cameras used for imaging. The current breast rings have highlighted two main challenges with using a 'multi-ring' breast ring system.

The first problem relates to clinical work flow. The sizing and changing of incorrectly sized breast rings consumes time and requires operator skill. Often what appears to be the correct sized ring when a patient is standing, may not be the best size breast ring when the patient lies down. In this case, the patent would have to then stand up again to have the ring size adjusted. This process takes time and makes the screening process less streamlined for both the patient and operator. Additionally, if a poorly sized breast ring is chosen, it can cause wrinkles on the breast surface which may limit the usability of the resulting imaging data.

The second problem is that the breast rings limit the area of breast being imaged by the machine. The result of this issue means that some abnormalities will not be able to be detected in regions of the breast that are not visible to the cameras. In particular, these areas are near the chest wall, where manual detection and mammography are also very poor in finding tumours (Ampil et al., 2012), (Dibden et al., 2014).

Because of these two problems, further research into the machine's breast opening is required. Since the opening interacts with the imaging, any changes made to the opening will require changes to the imaging algorithms as well, and a reassessment of their performance. Hence, these issues reflect a system wide impact and need for redesign that considers all of these factors.

Research Objective 1: Develop machine top surface opening to remove the need for interchangeable breast rings

1.5.2 Ergonomics of the System

For the system to perform optimally, women are required to lie very still during the imaging process. Any undue motion could result in poor data quality or potentially false positive/negative screening results. Feedback from clinical studies to date have indicated that the top surface of the DIET machine is not comfortable for all women, and on occasion has resulted in women adjusting their position during an imaging session. Therefore, to ensure the integrity of all data it is very important that the ergonomics of the system are improved.

Research Objective 2: Improve ergonomics of the DIET surface.

1.6 Thesis Organisation

The order of this thesis follows the progression of work completed to achieve the objectives outlined in Section 1.5. Any relevant prior work related to each design step, and any relevant initial research, is discussed at the beginning of each chapter. Chapter 2 of this thesis describes the concept design and prototype production of the ergonomic surfaces and breast opening for the DIET system. Chapter 3 details the ergonomic trials, including the ethical requirements required to carry out the trials. Chapter 4 explains methods used to produce phantom breasts which includes details on the material choice, skin colour choice and how the size and shape of the breasts were chosen. Chapter 5 examines the impact of changing the breast opening size and shape. In this chapter the detection of the edges

of the breasts were discussed, in particular how different colours of breast skin effected the edge detection process. Chapter 6 describes detailed design of the final surface which includes a mechanical loading analysis and material selection. Finally, Chapter 7 presents overall conclusions of the research.

2. Concept Design and Prototyping

2.1 Breast Opening

2.1.1 Breast opening background

The existing DIET system requires breast rings for two reasons: **1**) Isolating the breast tissue from the rest of the chest; and **2**) Blocking light from entering the system. However, due to clinical workflow constraints and a suboptimal area of breast being imaged, there has been need for a review of the opening of the DIET surface. Ideally, there will be a solution providing a "one size fits all" approach, where any woman will be able to lie on the machine without adjustment required to account for breast shape or size. Additionally, the breast opening should be sized to allow for the imaging of all parts of the breast, particularly near the chest wall.

2.1.2 Breast opening requirements

The DIET system consists of 5 digital cameras and synchronized strobe lights that capture surface oscillations when 10 – 100 Hz of low amplitude mechanical actuation is applied to the breast (Kashif, 2013). Several images are captured during sinusoidal steady state response at each frequency, all at different phase angles relative to the input motion. A strobe light system is used in conjunction with the cameras to avoid the need for expensive high frame rate cameras and to reduce the impact of motion on image quality (Van Houten et al., 2011). Figure 2.1 shows how controlled strobe lighting was used to capture the full range of breast surface motion. Because of the need for strobe lighting, it is essential that no light pollution leaks around the opening during a screening.

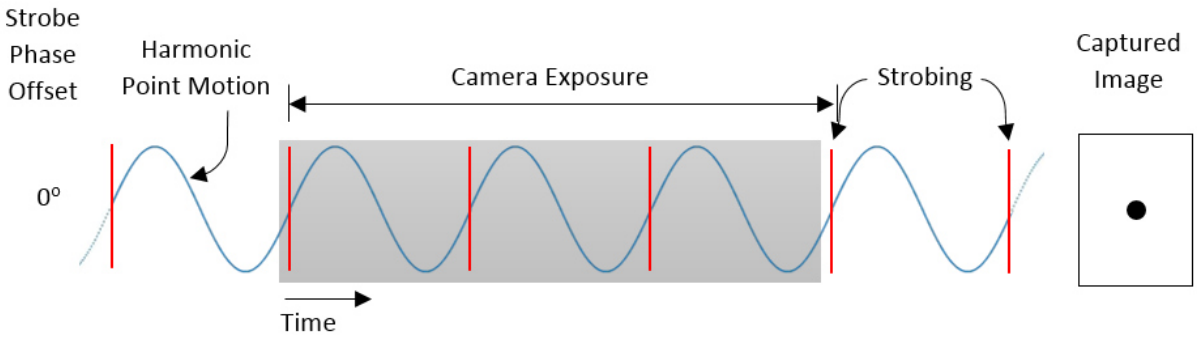

Figure 2.1: Schematic of camera exposure and strobing (Kashif, 2013)

The current DIET machine uses a model-based shape-from-silhouette method to reconstruct three dimensional models of the breast surface (Botterill, Lotz, Kashif, & Chase, 2014). Each of the five

cameras in the machine take 2-D images of the breast such that the entire breast is imaged. This process relies on each 2-D image overlapping, illustrated in Figure 2.2. Thus, the breast opening must be designed such that the breast remains central to all five cameras.

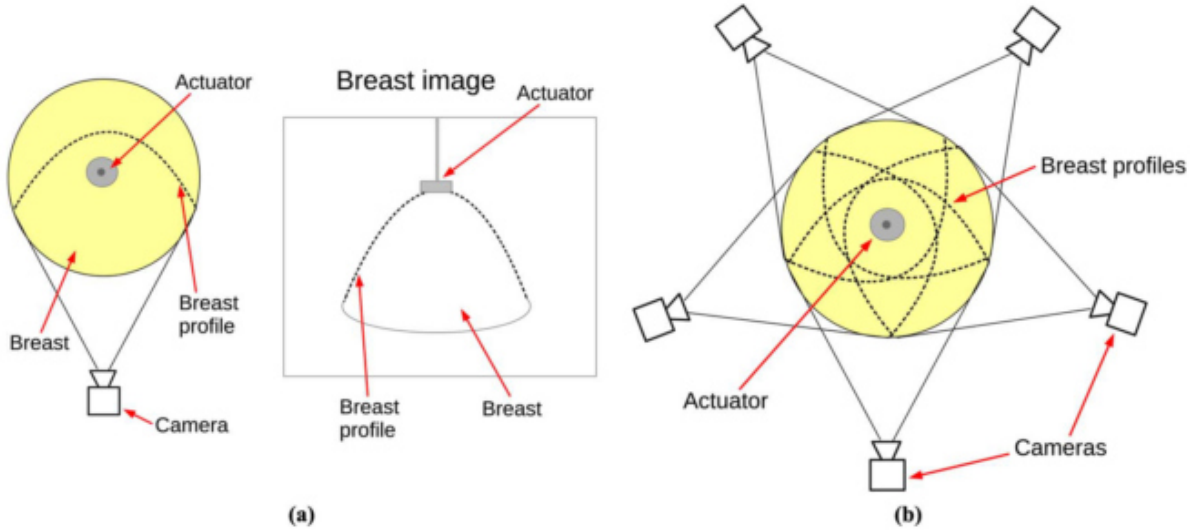

Figure 2.2: Schematic of breast in DIET system. (a) Each camera captures the breast from one side to give a 2-D profile. (b) Breast shown centrally such that the entire breast is captured (Botterill et al., 2014)

The shape from silhouette method finds an object's outline in each image to construct a 3-D surface. The current system relies on a breast boundary between the breast and the background, shown in Figure 2.3, which works well when no chest wall is exposed. Variations will need to be made, for cases where the chest wall is exposed, such that differences between the images in the sequence are used to find the boundary.

The breast surface is represented in spherical, polar coordinates where the origin is fixed at the centre of the machine's circular hole (Botterill et al., 2014). As the shape of the opening is likely to change, the origin of the coordinate system will also have to be altered, directly impacting the resulting imaging methods. This case is a simple example of the interaction between the design and the imaging methods that are fundamental to the DIET process.

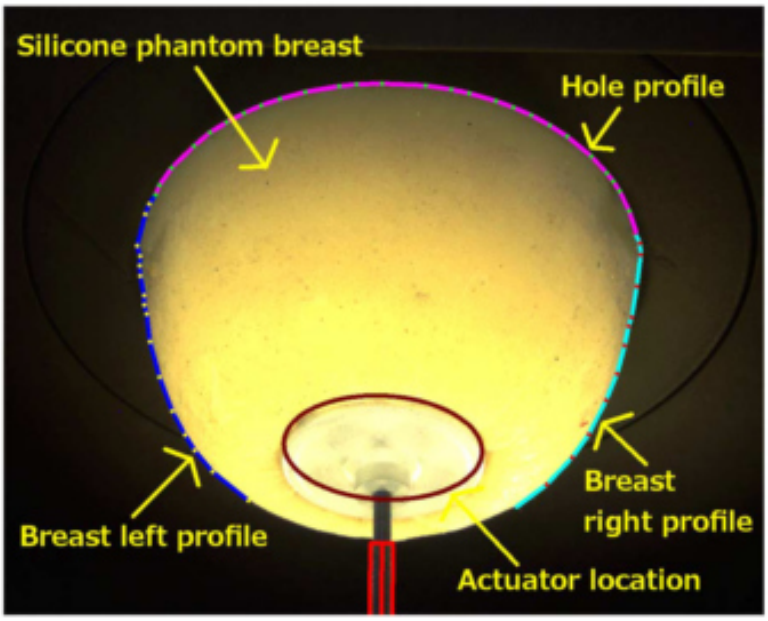

Figure 2.3: Phantom breast segmentation (Botterill et al., 2014)

As the rings are proposed to be removed, the opening must be large enough to accommodate the 95th percentile breast size. Most statistical data on the size of breasts relate to the cup and back size of a bra. The methodology of sizing bras varies significantly between bra manufacturers and are defined differently in each country. The cup and back size is determined by measuring bust girth and underbust girth respectively. This method of breast measurement is not detailed enough to truly represent the geometries of the breasts.

Additionally, anthropomorphic data specific to the breast, in adequate detail, are not available in most ergonomic textbooks. However, a study was carried out in Hong Kong to determine the three dimensional measurements of 456 Chinese women's breasts aged between 20 and 39 (Rong, 2006). The results from this study form the bases of the size limitations for the breast opening. Table 2.1 and Figure 2.4 show key measurements of breasts being used for this research thesis.

Table 2.1: Three dimensional breast measurements (cm) (See Figure 11) (Rong, 2006)

	Name	Percentile 5th	50th	95th
5	Shoulder width	30.00	33.00	35.59
6	Chest width	26.00	28.67	32.66
7	Bust width	25.00	27.66	31.05
8	Underbust width	24.00	26.33	29.66
10	Bust depth	19.43	22.50	26.63
12	Median chest depth	17.00	19.45	22.88
13	Bust point width	16.33	19.00	22.33
23	Horizontal distance between inner-most bust point	0.67	1.70	3.02
24	Centre breast depth	0.61	1.65	3.49
25	Centre bridge height	3.69	5.46	7.00
26	Inner arc total length of right breast root	9.13	10.80	13.20
27	Total arc length of right breast root	19.00	21.90	26.10
28	Width of breast	10.33	12.16	14.29
29	Base of breast	12.42	14.35	16.69

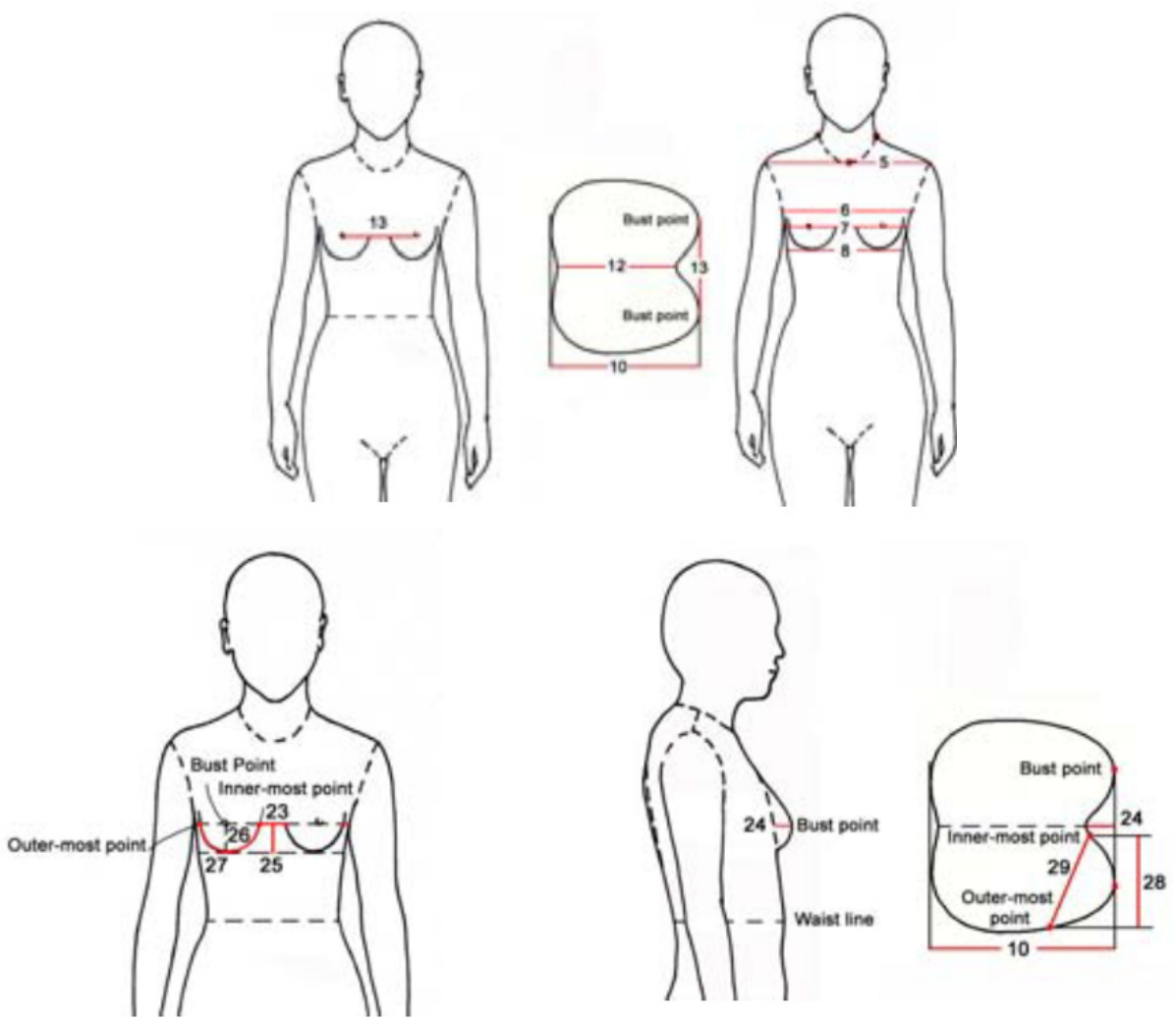

Figure 2.4: Dimensions taken to obtain three dimensional breast measurements (Rong, 2006)

Dimension 29, from Table 2.1, provides the most important measurement for determining the size of the breast opening. To allow for the growing population and because the sizes of Chinese women's breasts may differ from other ethnicities, the actual breast opening will be slightly larger than 16.69cm in diameter.

To summarize, the following constraints on the new breast opening are defined:

- Light cannot penetrate the breast opening.
- Breasts are to be located central to the five cameras of the DIET system.
- The breast opening is to be larger than 16.69cm in diameter.

2.1.3 Shape of breast opening

The existing DIET system has a circular breast opening into which a circular breast ring can be fitted. This simple design works well on some breast shapes/sizes, while also separating the breast tissue from the surrounding chest wall. However, this opening shape also limits the imaging area of the DIET system to the cup of the breast.

Importantly, this screening limitation is also present in existing breast screening systems such as mammography (Dibden et al., 2014). Specifically, the extent of the mammary tissue extends beyond the cup of the breast, as shown in Figure 2.5. Additionally, cancers do occur within the mammary tissue outside of the cup area and are not likely to be picked up in existing breast screening systems or in the current design of the DIET system.

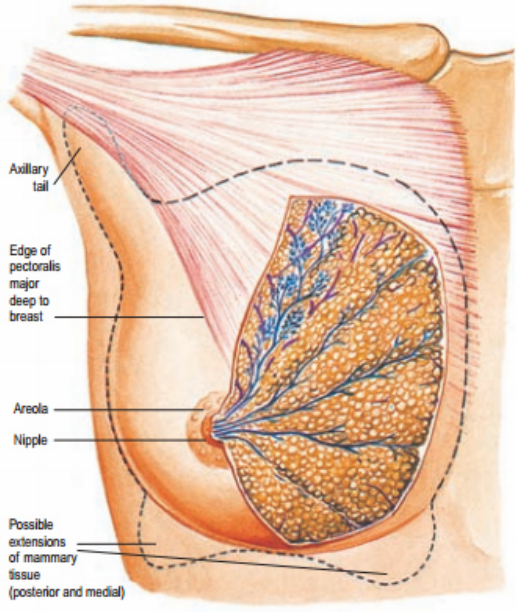

Figure 2.5: Extent of mammary tissue (Valea & Katz, n.d.)

In particular, Carcinoma in Axillary Tail of Spence (CATs) affected approximately 1.1% of breast cancer patients in a study of 839 women with breast cancer (Ampil et al., 2012). Of the ten women with CATs, physical examination and breast imaging failed to reveal the tumour in the breasts. Eight of the ten women had stage II or III cancer, which might be expected given the difficulty of detecting these cancer locations.

At these late stages, the cancer may be classified as inoperable. However, the cancers can still be treated to reduce the size of the cancer before surgery is considered. The outcome of the treatment is highly dependent on how far the cancer has spread (National Breast Cancer Foundtion, 2016). The estimated five-year survival rate of women with CATs is 67% (Ampil et al., 2012). This rate is much lower than the 95% five-year survival rate if detected by mammogram, and lower still than the 75% five-year survival rate if a lump is the first sign. Due to the much lower survival rate of patients with CATs, the opening should be designed to capture this area.

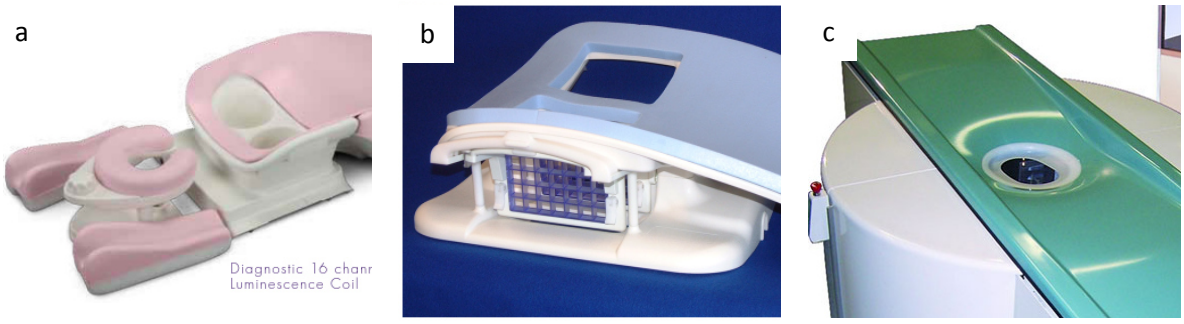

Figure 2.6: Existing breast screening surfaces with differing breast opening shapes: (a) Circular openings on the Siemens Breast Array Coil, (b) Rectangular opening on the Invivo™ Biopsy Breast Array Coil, and (c) Oval opening on the Koning™ Breast CT

Existing breast screening machines have circular, rectangular and oval holes, as shown in Figure 2.6. These medical screening surfaces give inspiration to the design of the breast opening for the DIET system. Table 2.2 shows the options examined for the breast opening shape of the DIET system. Four important conditions were considered when assessing the viability with the DIET system:

1. **Simplicity of design:** A simple design would allow for cheap manufacturing of the surface with use of standard manufacturing practice
2. **Scope to capture Tail of Spence:** The ability to screen this area of the mammary gland may lead to earlier diagnosis of CATs and therefore, a higher survival rate
3. **Likelihood of light pollution:** It is important to prevent light pollution, allowing images to be exposed with minimal noise.

4. **Overall ergonomics:** The opening must be comfortable for the patient, otherwise poor quality data may be obtained.

Table 2.2: Options for breast opening shape for the DIET surface (red cells represents non-desirable conditions).

	Option 1: Circular	**Option 2: Oval**	**Option 3: Teardrop**
	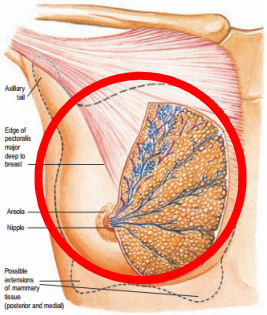	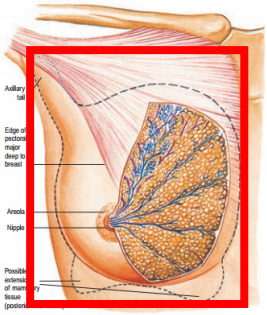	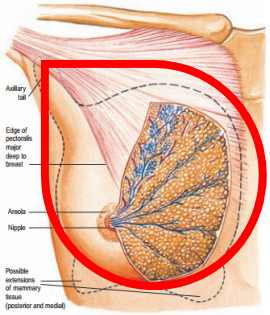
Simple Design (Nice to have)	Yes	Yes	No – complex curves may require non-standard manufacturing methods
Captures Breast Tail (Nice to have)	No – exept in the case of smaller women	Yes	Yes
Likely to have light pollution (Required)	No	Yes – light may leak below the armpit	No
May be uncomfortable (Required)	No	Yes – May be pushing on clavial	No

While Option 1 and Option 3 both have an equal number of undesirable conditions, a shape that allows for screening of the entire breast tissue has the potential to have more benefits over having a simple design. Therefore, the tear drop type shape is the chosen shape for the new breast opening on the DIET system. To allow for both breasts to be screened, the tear shape will be flipped, such that the shape is vertically symmetric.

2.1.4 Size of breast opening

Dimensions of breast tissues, which were discussed in Section 2.1.2 have been used to determine the size of the breast opening. Figure 2.7 shows a summarised sketch of the dimensions of the breast. The figure defines the basic dimensions considered in this research. The dimensions of the 5th, 50th and 95th percentile breast size have been summarised in Table 2.3. Of particular interest is Dimension B which is the diameter of the breast as this will give an outer diameter required to allow a “one size fits all” breast opening.

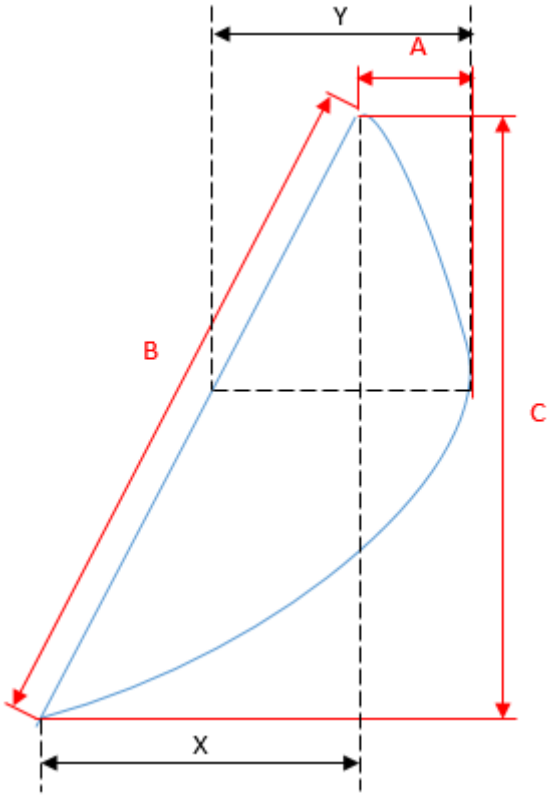

Figure 2.7: Simplified dimensions of breast (Red = Dimension from Table 1)

Table 2.3: Summary of breast dimensions for 5th, 50th and 95th percentile breast size

	A	B	C	X	Y
5TH	0.61	12.42	10.33	6.90	4.06
50TH	1.65	14.35	12.16	7.62	5.46
95TH	3.49	16.69	14.29	8.62	7.80

The data used to obtain these values was from a study of 456 Chinese women who were between 20 and 39 years of age (Rong, 2006). To account for differing breast sizes between ethnicities and to allow for the growing population, a 10% increase in breast diameter has been made.

Figure 2.8 shows the proposed size and shape of the breast opening. This opening will negate the need for breast rings, will allow for up to the 95th percentile women to be screened, and will allow for the machine to screen the all mammary tissue, including at the Tail of Spence. The design has been adapted from Option Three in Table 2.2. However, it has been made symmetric to suit both left and right breasts.

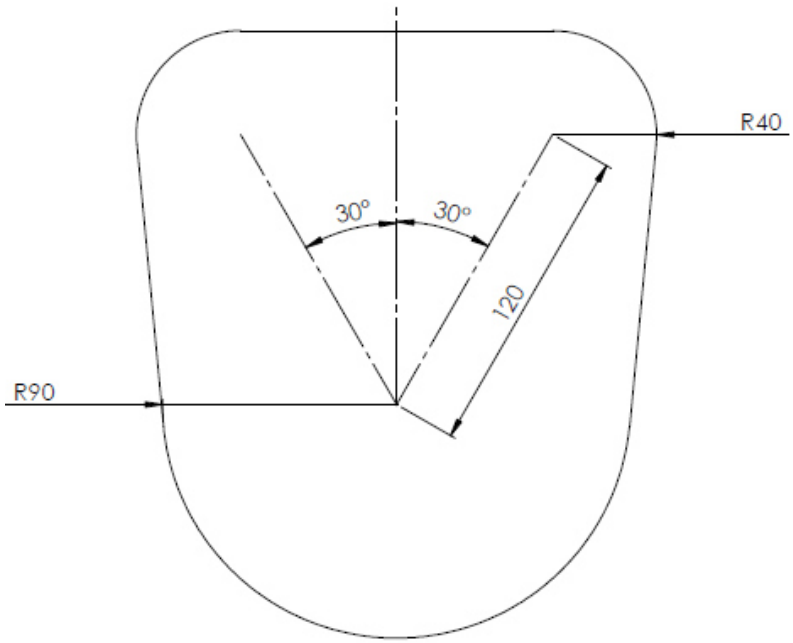

Figure 2.8: Shape and dimensions of breast opening

2.2 Ergonomics of Surface

The DIET system requires women to lie face down on the surface of the machine with one breast hanging pendent into an opening. Quality data can only be obtained if the patient lies very still during the imaging process. Movement may interrupt or corrupt the steady state actuated tissue motion, which may lead to false positive / negative screening results or may require a repeat in screening.

Early feedback from clinical trials indicates that improvements could be made to the top surface of the DIET machine to increase comfort. On occasion, trial participants have adjusted their position during an imaging session due to the uncomfortable surface. To ensure the integrity of the imaging data, it is therefore very important that the ergonomics of the system are improved.

While a majority of women find the DIET machine comfortable to lie on during a clinical trial, 45% of women provided constructive feedback on aspects of the ergonomics that could be adjusted to improve comfort. The main area of discomfort, described in 58% of ergonomic feedback, was defined to be in the ribs area where a rigid bend is located. It is believed that this bend is pushing on some women's rib cages, causing discomfort. Other causes of discomfort included pain in the breast not being examined, awkward positioning of the headrest and overall itchiness. Figure 2.9 shows how a woman would lie on the current DIET machine being used for clinical trials, including the location of the rigid bend causing majority of the discomfort.

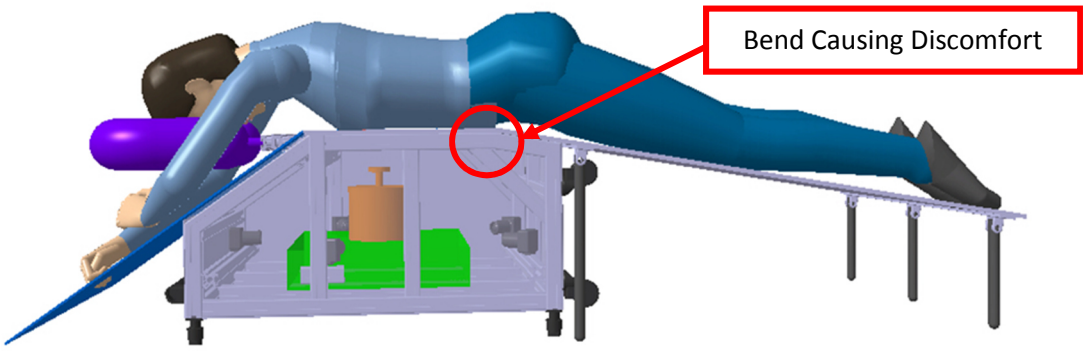

Figure 2.9: Sketch of woman lying on DIET machine (Kashif, 2013)

Anthropomorphic data of women provides guidelines on geometrical limitations of the proposed DIET surface. The design of the ergonomics for the DIET machine is based on providing for up to the 95th percentile sized women. Key anthropometric dimensions found in sources such as NASA reference data and human ergonomic textbooks (Huston, 2009), are summarized in Figure 2.10 and Table 2.4.

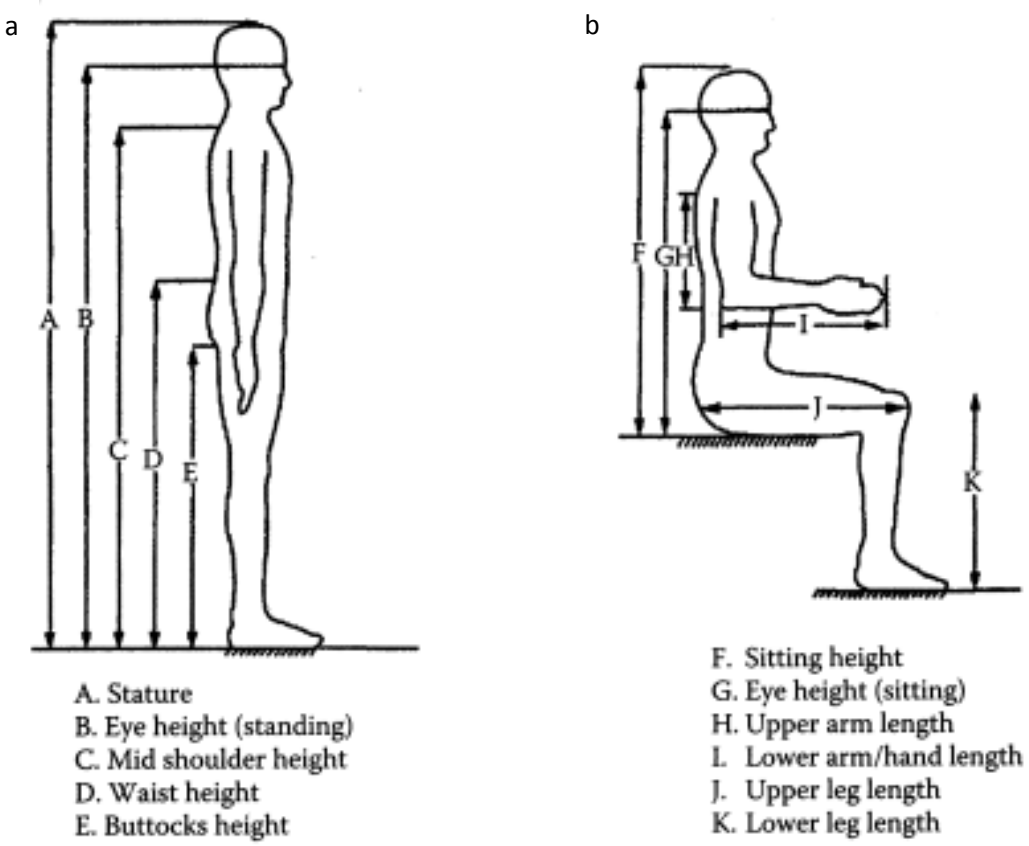

Figure 2.10: Human anthropometric dimensions for (a) Standing dimensions, (b) Sitting dimensions (Huston, 2009)

Table 2.4: Human anthropometric data (in meters), see Figure 7 (Huston, 2009)

		Percentile		
	Name	**5th**	**50th**	**95th**
A	Stature	1.518	1.618	1.724
B	Eye Height	1.427	1.520	1.630
C	Mid Shoulder Height	1.210	1.314	1.441
D	Waist Height	0.907	0.985	1.107
E	Buttocks Height	0.691	0.743	0.832
F	Sitting Height	0.797	0.853	0.911
G	Eye Height (Sitting)	0.692	0.743	0.791
H	Upper Arm Length	0.306	0.332	0.358
I	Upper Arm / Hand Length	0.396	0.428	0.458
J	Upper Leg Length	0.531	0.578	0.628
K	Lower Leg Length	0.461	0.502	0.546

Three DIET surface concepts have been produced. All three designs have been designed to accommodate a wide range of breast shapes and sizes. Due to the mechanical properties of the machine, each surface shall be suitable for a woman to lie prone (face down) with one hole to allow for one breast at a time. Each concept design has been modelled on SolidWorks 2014 (Dassault Systèmes, Velizy-Vallacoublay, France).

2.2.1 Surface Concept 1: Rounded edges

Certain breast cancer detection modalities, such as with MRI, PET and CT, share similarities with the DIET system as they all have women lying face down with a breast hanging pendant into an opening. An investigation of shapes of platforms used in these applications provide inspiration for possible shapes for the DIET system platform. Figure 2.11 shows two current surfaces that provide a curved surface, possessing a similar shape to the existing DIET design. The main difference between these surfaces and the DIET surface is that these examples have no rigid bend, are more curved and have a glossier finish. Replacing the sharp bend with a more curved bend may provide a more ergonomic solution, as the gradual transition would limit the possibility of the surface pressing into a woman's ribcage.

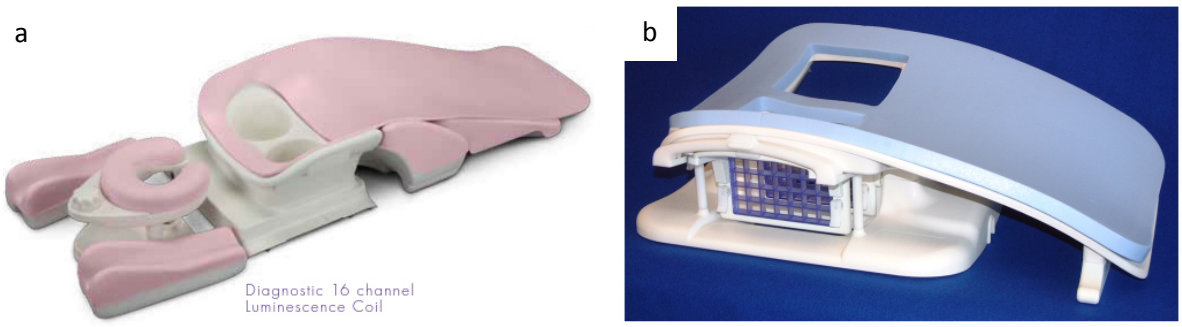

Figure 2.11: Examples of existing curved surfaces used for breast examination: (a) Siemens - Breast Array Coil, and (b) Invivo™ - Biopsy Breast Array Coil

The first concept surface has been designed such that it shares similar qualities to the current device, but has a much more curved surface. The curves of the new surface have been designed based on the size and shape of a 95th percentile woman. Key dimensions taken from the reference data are summarised in Table 2.5.

Table 2.5: Key dimensions used in Surface Concept 1 (Huston, 2009)

Length Location	Dimension (mm)
Shoulder to Hip	471.5
Shoulder to Centre of Breast	234.0
Centre of Breast to Hip	237.5
Hip to Knee	423.5
Knee to Ankle	546.0
Shoulder Breadth	464.0
Chest Depth	277.0

A profile of a 95th percentile sized woman's chest has been used as the basis of the curve on the top part of the surface. Viewed in the transverse plane, the chest has been approximated as an eclipse, as shown in Figure 2.12. The horizontal dimensions for this ellipse were based on the width of the arms when they are at rest which is typically where a woman is the widest.

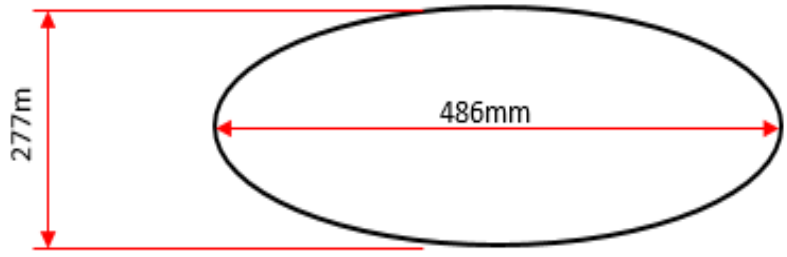

Figure 2.12: Approximation of slice thought 95th Percentile Woman's Shoulders

Figure 2.13 shows the design of the first concept surface, which includes the cuved bends previously mentioned and shows the overall dimesions. The angles of the bends used in the side profile for the

Concept 1 Surface are also shown in Figure 2.13. These angles were chosen based on comfort angles indicated in a previous ergonomic study on the DIET system (Kashif, 2013).

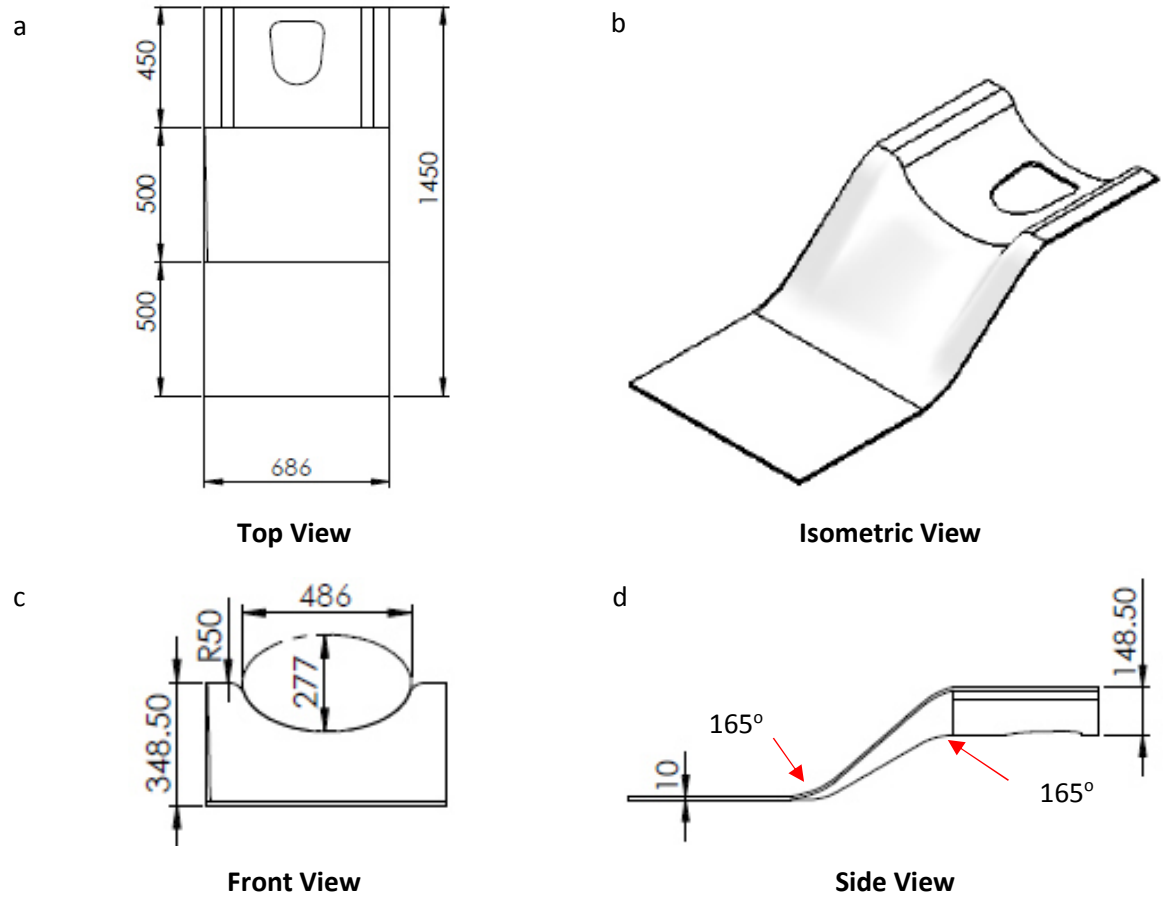

Figure 2.13: Concept 1 Surface views: (a) Top view, (b) Isometric view, (c) Front view, and (d) Side view

2.2.1.1 Prototype Production of Concept 1

The first prototype has a number of curved edges to allow for a comfortable transition at major body joints including the hips and knees. To produce an inexpensive, geometrically accurate prototype a combination of timber, polyurethane foam and fibreglass was used. Additionally, a layer of 5mm soft ethylene-vinyl acetate (EVA) foam was draped over the surface once the final shape was produced. The production of Concept 1 is shown in Figure 2.14.

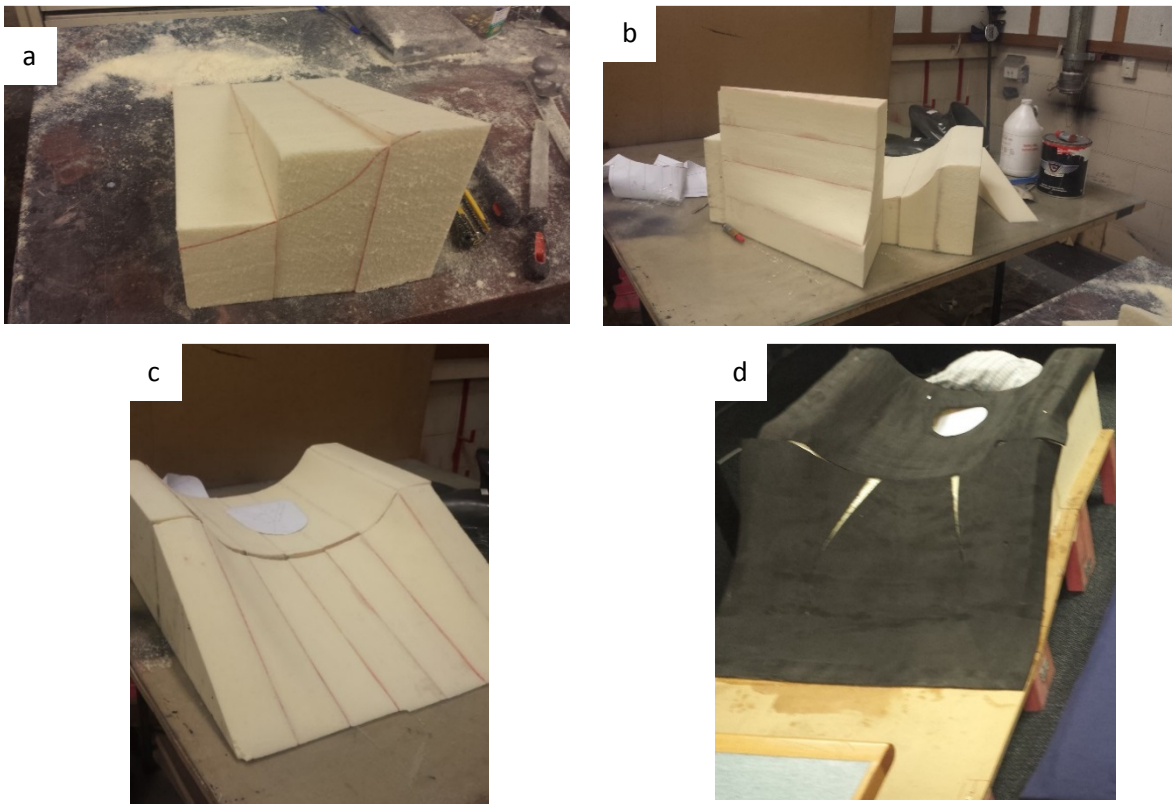

Figure 2.14: Production of Prototype 1: (a) Developing curves of surface on polyurethane, (b) Curved surfaces shaved into polyurethane, (c) Polyurethane base of surface, shaved down to required contours, and (d) Prototype 1 complete with 5mm of soft foam

2.2.2 Surface Concept 2: Flat Surface

The inspiration for the shape of the second surface came from the designs of breast CT machines, as shown in Figure 2.15. Both of these machines work by having x-ray images taken at all orientations about the breast (Huang et al., 2011), (Ning et al., 2010). Thus, the imaging equipment rotates 360° around the breast beneath the surface of the machine. Comparable to the DIET machine, these type of machines also have one opening on the surface to examine one breast at a time.

These surfaces are predominantly flat. However, at the location of the breast hole, both surfaces curve slightly downward. This shape allows a woman to align herself against the profile of the surface and have her whole breast hanging into the machine, shown best in Figure 2.15 (a). The design for the second concept surface is shown in Figure 2.16, which includes an isometric view and overall dimensions of the concept surface.

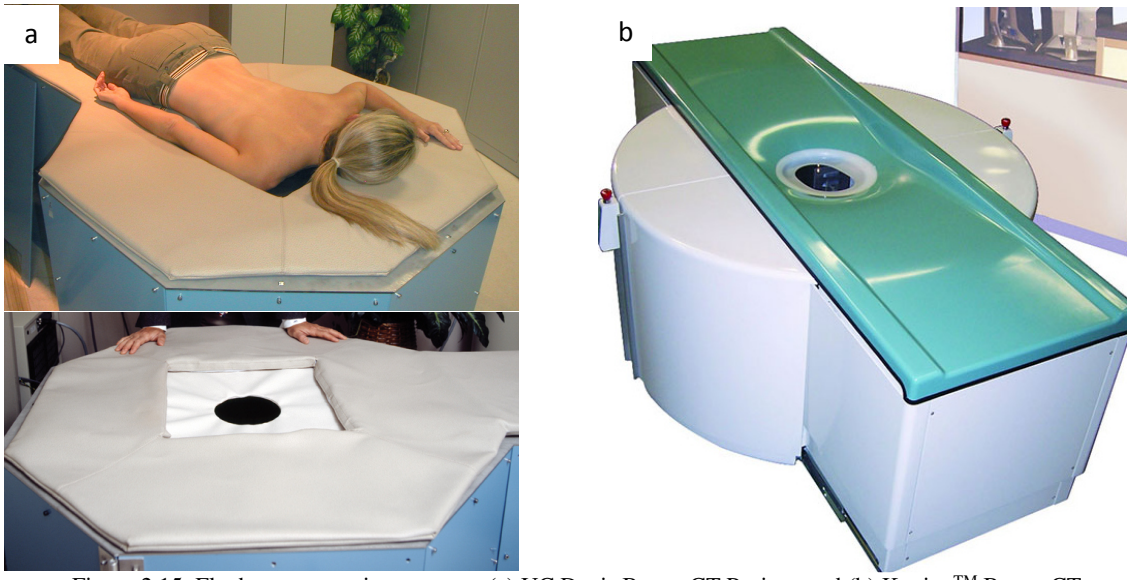

Figure 2.15: Flat breast screening systems: (a) UC Davis Breast CT Project, and (b) Koning™ Breast CT

The breast opening on Concept 2 is located in the centre of the mostly flat surface. Figure 2.17 shows a section through the centre of this concept surface to highlight important dimensions. A drop of 40mm between the top of the surface to the top of the breast opening, as shown in Figure 2.17 (b), was chosen based on visual inspection of existing breast screening systems with flat surface profiles.

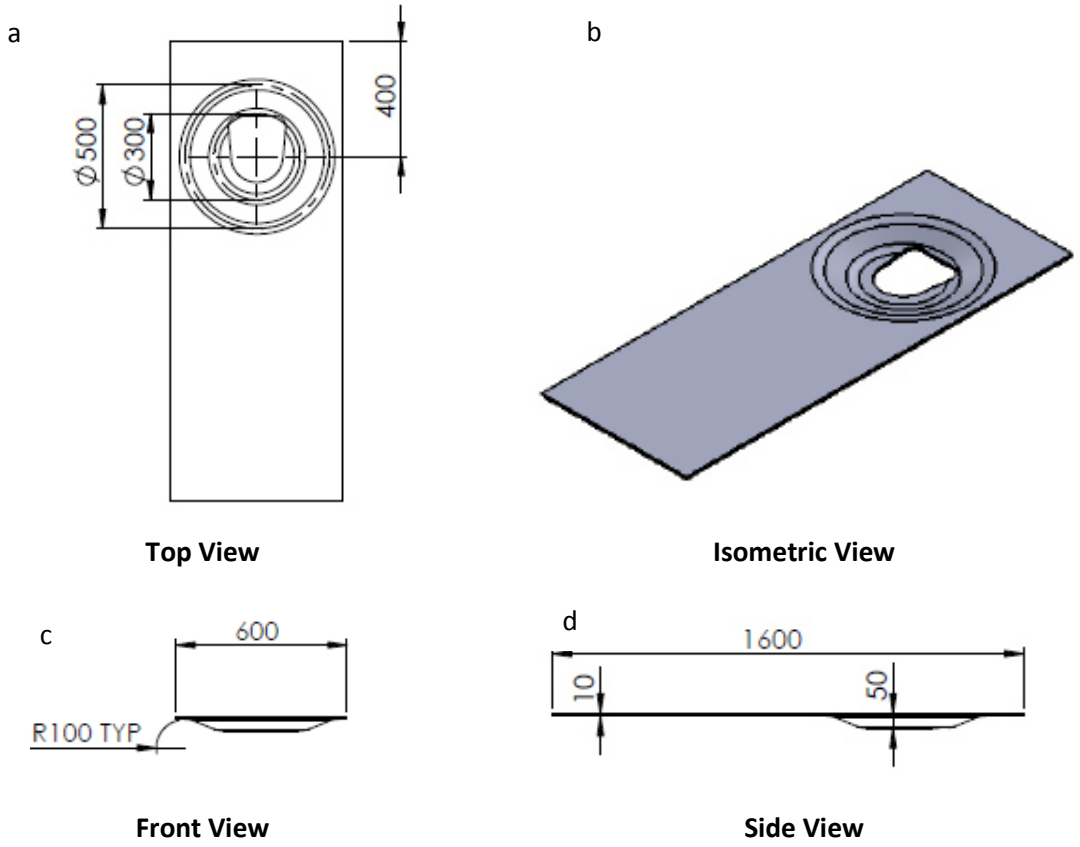

Figure 2.16: Overall dimensions of Concept 2: (a) Top view, (b) Isometric view, (c) Front view), and (d) Side view

Large radius bends (R100mm) were used at all corners to avoid any discomfort. The Ø300mm lower surface was sized such that the majority of the breast opening was on a flat surface. The Ø500mm upper surface was sized to allow for all women's shoulders to within the bowl-shaped surface, a 95th percentile female has a shoulder to shoulder width of just over 350mm (Rong, 2006).

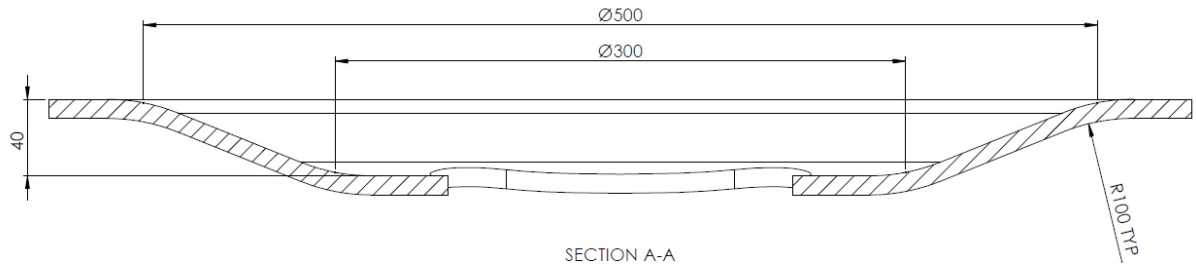

Figure 2.17: Section through Concept Surface 2

2.2.2.1 Prototype Production of Concept 2

Concept 2, much like Concept 1, has a number of curved surfaces to allow for a woman's chest to form around the breast opening. Such forming prevents light leakage by encouraging a good seal. The same materials used for Prototype 1 have been used in Prototype 2. The production of this prototype is shown in Figure 2.18.

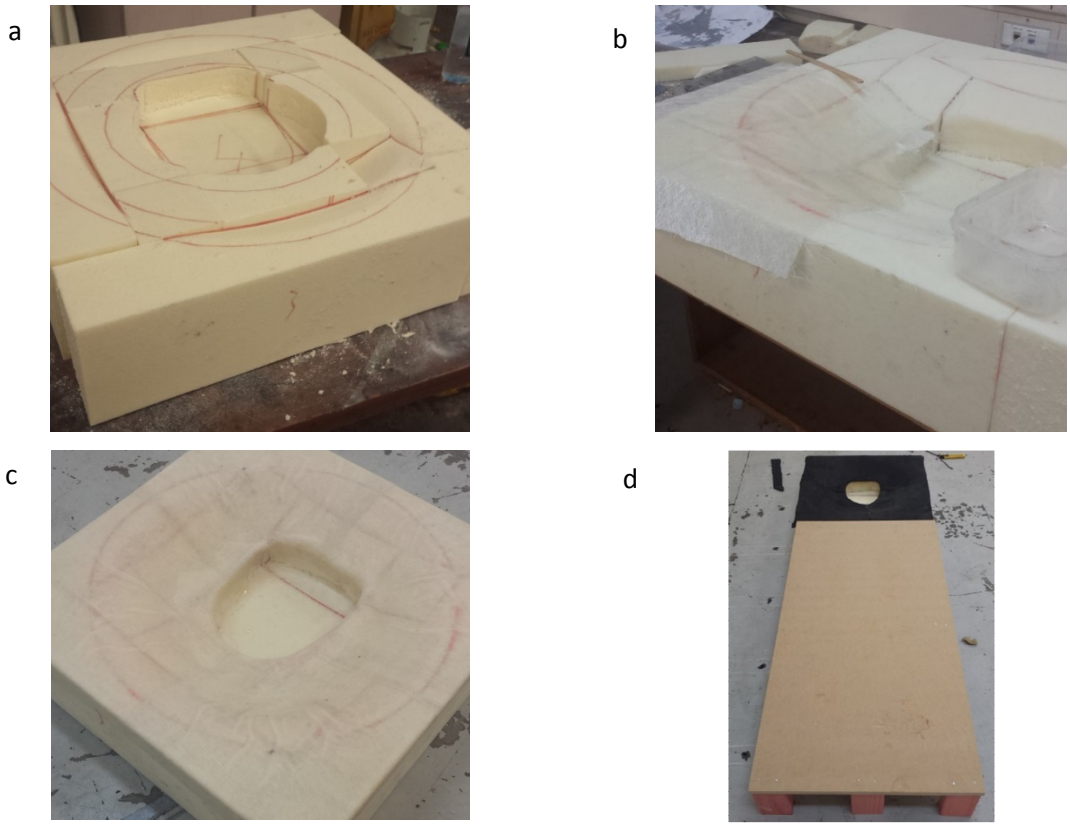

Figure 2.18: Production of Prototype 2 (a) Polyurethane foam cut with contours drawn for sanding back, (b) Applying fibreglass to surface, (c) Fibreglassed surface, and (d) Completed prototype 2 with EVA foam and flat surface for body

2.2.3 Surface Concept 3: Formable Surface

The first two surface concepts assume that the contours of a surface designed for larger women would also be comfortable for a much smaller woman to lie on. While this assumption may be the case, and will be tested in the ergonomic trial, it is beneficial to have a concept that allows contours to be formed for all body types. For this reason, the final concept surface is a simple rectangular surface made from a formable material, shown in Figure 2.19. While there are not necessarily similar existing surfaces for breast examination, there are a number of times formable materials are used in the medical industry.

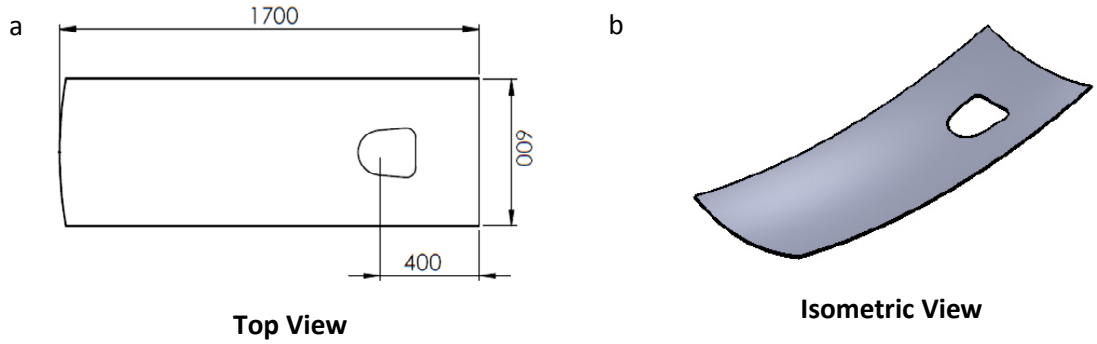

Figure 2.19: Concept Surface 3: (a) Top view, and (b) Isometric view

One similar, simple and common example is the emergency medical stretcher, Figure 2.20 (a), which is specifically designed to carry patients of all body shapes regardless of the patient's weight, shape or injuries. The stretcher is designed to have a body lying face up, rather than face down. However, it still has enough elasticity in the material to form slightly to contours along the back of a body. Such elasticity might also provide better comfort, at lower cost, by its conformity to the body surface. Equally, such conformity is also desirable to prevent light leakage.

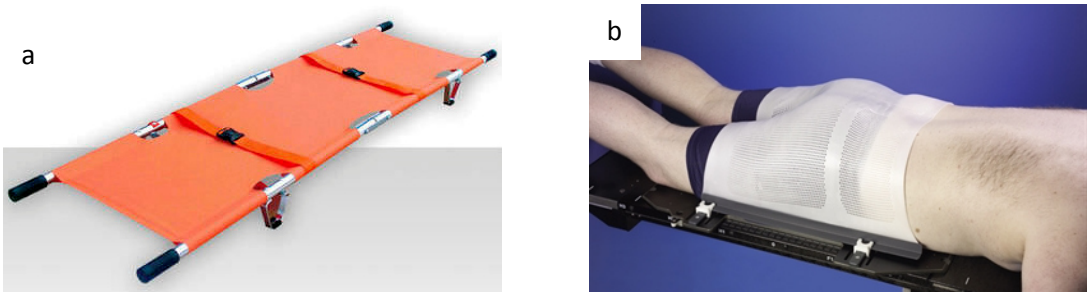

Figure 2.20: Examples of medical devices which use formable material: (a) Emergency Medical Stretcher("XIEHE Medical Apparatus & Instruments," 2010), and (b) Thermoplastic Positioning System ("CIVCO Medical Solutions," 2015)

The second example of formable material used in medical applications is the Thermoplastic Positioning System, shown in Figure 2.20 (b), which is designed to keep a body still during a CAT scan or similar imaging process. This system uses a sheet of thermoplastic to wrap firmly over part of a

body where it forms to the contours of the body. It is then fixed to the base of the machine used for imaging. Before using the thermoplastic positioning system, the plastic sheet is heated to 65°C for at least four minutes("orfit," 2016). This heating allows the sheet to reform over the body part as it cools.

2.2.3.1 Prototype Production of Concept 1

The third prototype is simply flat with a mouldable material such that the surface moulds to any body shape or size. A camping stretcher has been used to produce this prototype, as shown in Figure 2.21, as the size and shape is already designed to fit most body types. Additionally, the material forms to differing bodies. The material is also easy to work with and can easily be cut with a craft knife.

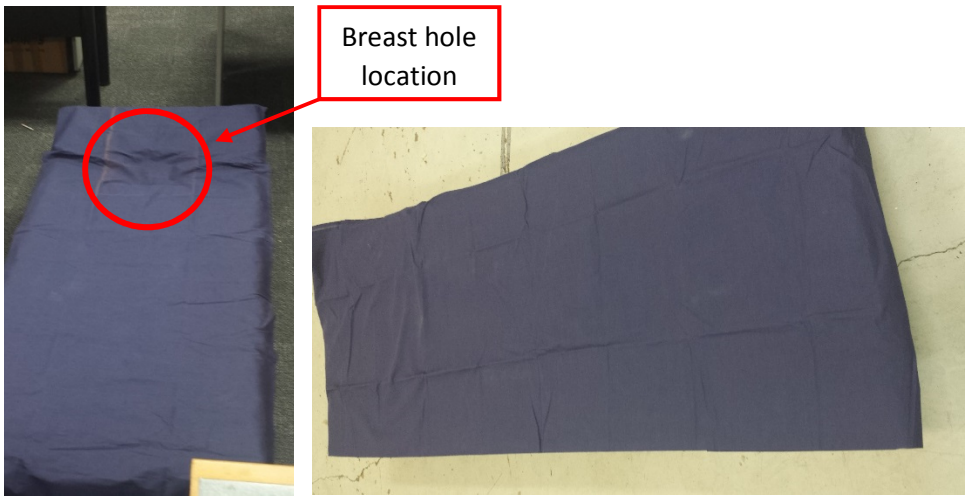

Figure 2.21: Prototype 3 with sheet on top to make comfortable for trial participants.

2.3 Summary

The existing DIET system utilises breast rings to account for differing sized breasts. This causes clinical workflow issues which lead to a "one size fits all" approach being desired. A new breast opening concept has been proposed in this chapter which accounts for the size and shape of women's breasts. The shape and size of the breast opening, Figure 2.8, was chosen based on simplicity of design, scope to capture the Tail of Spence, likelihood of light pollution and the desire to minimise discomfort.

In addition, early feedback from an ongoing clinical trial carried out on the existing DIET system has indicated ergonomic improvements could be made to the surface of the system. This would reduce the chance of a woman wanting to shift their position while being screened which could lead to compromised data. To address this issue, three prototype surfaces have been produced based on the concepts discussed. The surfaces will be used in an ergonomic trial and have been designed such that each surface is significantly different from the other two, yet potentially mitigates the issues raised.

Figure 2.22: Isometric view of each concept surface with approximate location of where a woman would lie (a) Concept 1, (b) Concept 2, (c) Concept 3

Concept 1 is similar to the existing DIET surface but has additional large radii where bends are made. Concept 2 is a flat bench based off surfaces used in breast CT devices. Concept 3 is a formable surface which is capable of forming to the complex curves of the female body. Figure 2.22 summarises the concept benches with the approximate location of where a woman would lie.

3. Ergonomic Trial

All prototype surfaces produced, as discussed in Chapter 2, were used in an ergonomic trial to find which surface provided the most comfortable fit for women of all anthropometric make ups. This trial consisted of women, who varied in age and size, lying prone, fully clothed, on each of the prototype surfaces for up to five minutes at a time. Each participant gave ergonomic feedback after both two and a half minutes, and five minutes, of lying on the surfaces then give general feedback at the end of their trial session.

3.1 Ethics Approval

To carry out any trial including human participants, ethics approval is required. This was sought through the University of Canterbury's Human Ethics Committee (HEC). The trial was recognised as a low risk application because no issues were raised on the low risk checklist provided by the HEC. It was determined that a participant would not encounter any more risk than might be encountered in normal daily life. The trial would not raise any issues of deception, threat, invasion of privacy, mental, physical or cultural risk or stress and does not involve gathering personal information of a sensitive nature about or from trial participants.

The ethics application form, along with advertising material, consent forms and information sheets, were submitted to the HEC on the 30th of October 2015. The application was accepted on the 26th of November 2015 which allowed up to 50 participants to participate in the trial. All forms are included in Appendix A.

3.2 Recruitment of Volunteers

the HEC application allowed up to 50 volunteers to participate in the trial. However, the initial intention was to aim for at least 30 participants. Of the 30 participants, the following variety was sought:

- At least three participants for each dress size group (6-8, 10-12, 14-16, 18+)
- At least three participants for each age group (18 – 35 years, 36 – 50 years, 50+ years)

If the initial response did not have the required variety, additional participants would be sought. Initial recruitment was made via email to contacts already known to the researcher. Members were regularly reminded that they were welcome to pull out of the trial at any point during email correspondence.

Those who expressed interest in participating in the trial had their names and contact details recorded on a spreadsheet located on a password protected external hard drive. Times and dates of each trial were determined individually with each participant to best suit their timetable.

The total number of participants assessed on the prototype surfaces was 27. After the first 16 participants, there were clear, consistent indications for improvement on the initial prototypes. Thus, it was decided to stop the initial trial and have an additional trial with improved surfaces. The breakdown of participant sizes and ages for each trial are described in Table 3.1. The desired variety of having at least three participants from each age and clothes size group was achieved for the initial trial, and at least one participant from each group was present for the secondary trial.

Table 3.1: Breakdown of participants ages and sizes for ergonomic trials

		Ages of Participants (Years)			**Clothing Size of Participants**			
	Number of Participants	**18 – 35**	**36 – 50**	**50+**	**6 – 8**	**10 – 12**	**14 – 16**	**18+**
Initial Trial	16	9	3	4	6	4	3	3
Secondary Trial	11	7	2	2	3	4	3	1
Total	27	16	5	6	9	8	6	4

In addition to the variance of age and dress size, the heights and weights of participants also have a wide variance which is important for obtaining a broad range of data to represent the general population. Figure 3.1 shows the spread of height and weight of participants.

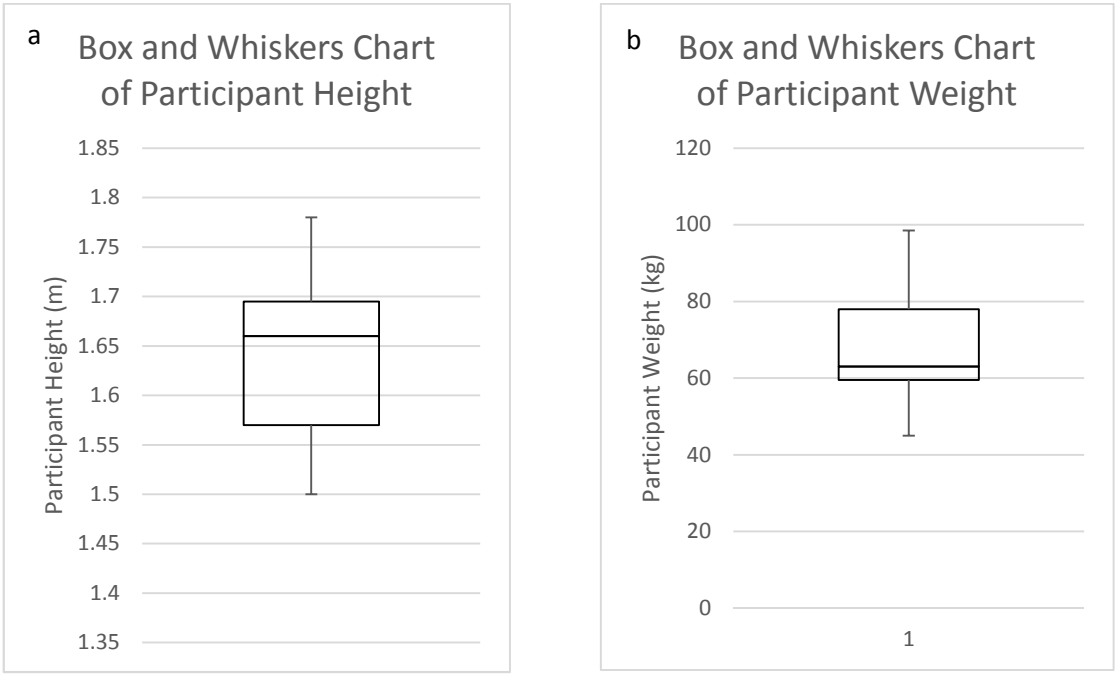

Figure 3.1: Spread of (a) height and (b) weight of participants in initial and secondary ergonomic trials

Table 3.2 shows the mean and standard deviation of the participants' weight and height from the initial trial compared to that of New Zealand women as of 2014 and 2015 (Ministry of Health). It shows that while the average height compared well, the weight and body mass index of the average participants were notably lower than that of the average New Zealand woman. This difference likely occurred due to the recruitment and research being done on a university campus. As a result, the data might not reflect all New Zealand women.

Table 3.2: Comparison of trial participants to the average New Zealand woman

	Mean Value from Initial Trial Participants	**Mean Value from New Zealand Ministry of Health Survey 2014 / 2015**
Height (m)	1.64	1.63
Weight (kg)	66.7	74.4
BMI (kg/m^2)	24.8	28.1

3.3 Trial Method

When participants arrived to the trial they were given hard copies of the information sheet, the consent form and the questions that would be asked during the trial. The details of the trial were then discussed with the participant before the participant signed the information and consent form. This gave the participant an opportunity to withdraw from the study if they felt uncomfortable with the procedure or any questions.

Figure 3.2: Prototype surfaces used in initial ergonomic trial

Once all required forms were signed, the researcher demonstrated how to mount each surface shown in Figure 3.2, including where to position their arms, chest and head. Once a participant was on a

prototype surface, the researcher would start a timer. After two and a half minutes, the researcher would ask about the comfort levels in the neck, chest, waist and then if any discomfort could be felt anywhere else. This process was repeated after five minutes. The participant would then lift themselves from that prototype and trial the next two prototypes in the same manner.

Once all three prototypes had been assessed, the participant would rank all surfaces based on the most and least comfortable. They were then welcome to provide any other feedback related to the ergonomics of the surface. While each participant may have different sensitivity to discomfort or pain, this method is appropriate when comparing surface ergonomics. This method was repeated for the second trial with the improved surfaces.

3.4 Trial Results

The ergonomic trial provided clear indications of where surfaces are more, or less, comfortable. It only required 16 volunteer responses in the initial trial before it was clear that improvements could be made on the original prototype surfaces. At this point, the prototypes were modified to suit the constructive feedback given by trial participants and the improved surfaces were used in a secondary trial. During the secondary trial, fewer participants were required before it was clear which surface was the most preferred.

3.4.1 Initial Trial

The original three prototype surfaces, discussed in Chapter 2, were used in the initial trial which consisted of 16 volunteers of varying age and dress sizes as described in Table 3.1. Figure 3.3 shows that the highest area of discomfort experienced by participants was in the neck. This issue was mostly due to awkward arrangement of the head. Some women indicated that because of the discomfort in their neck, their shoulders also began to feel strained and uncomfortable, which made them uneasy on the prototype surfaces for extended periods of time.

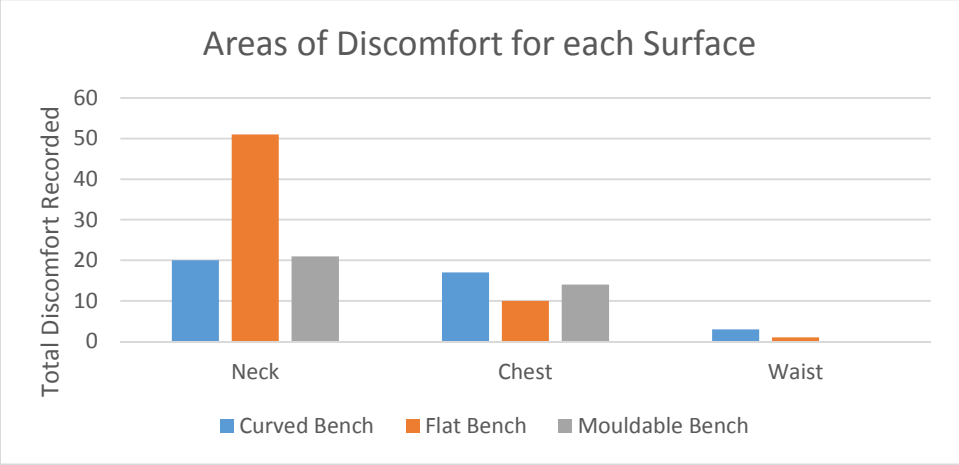

Figure 3.3: Areas of discomfort for each surface determined in initial trial

Concept 2 showed the worst results in the neck, with all participants stating some form of discomfort in the neck while on the flat surface. The neck discomfort was because the participants needed to rest their heads on their side. While one woman indicated that she preferred her head on the side, all women indicated that they would prefer to have the choice of having their head either to the side, or face down. Two volunteers also indicated that they felt claustrophobic with the prototype headrest as it was not fully open below the mouth. This indicated the need for a proper head rest system where women could alter the orientation of her head.

Another area of discomfort in all benches was the chest. A major reason for this discomfort was due to the non-examined breast being pressed into the surface. This discomfort made the participants want to re-arrange their chest area. This issue indicated a need for either a softer surface or a surface that has a cavity for the non-examined breast.

Discomfort in the chest was worst in Concept 1. Three of the participants in the smallest clothing group indicated that they felt claustrophobic in the curved bench around the chest area. The curvature of that bench was designed to accommodate a 95th percentile sized woman which assumed a much larger torso depth than that of a smaller woman. Because a smaller woman has a shallower torso depth, their shoulder width exceeded the width of the surface which caused the discomfort and claustrophobic feeling. Additionally, larger women did not indicate that there was any benefit to having the curved profile. It was thus decided to remove the front view, from Figure 2.13 (c), curvature from the design.

Few women experienced discomfort in their waist during the trial with no recordings of discomfort at the waist for the mouldable surface. The few participants that did indicate discomfort in their waist

said that it was because they felt like their hips were digging into the surface. This feedback mostly came from participants in the smaller two clothing size groups.

Additional feedback was given on the discomfort experienced on the lower back, knees and the discomfort of lowering to the benches to lay on them. Three women, from a range of ages and sizes indicated they experienced lower back discomfort while on Concept 1 and Concept 3. For Concept 1, the main reason for this discomfort was because they felt too hunched over the surface, which strained their back. Those participants suggested a gentler angle for their legs to lay upon. The lower back discomfort experienced on Concept 3 was reportedly due to the perception that their back was being arched backwards. Consequently, it was suggested that the surface might be more comfortable if the fabric was pulled tighter such that it had less give. A number of women, who were in the oldest age bracket, indicated that their knees felt uncomfortable while they lay on Concept 2 and suggested the surface would benefit from being covered in thicker, softer foam. Four women indicated that the height of the surface should be raised, and suggested a height similar to medical benches found in general practice clinics, so that the act of mounting onto the surface is less cumbersome. Table 3.3 summarises the areas for improvements of each surface as determined by the initial ergonomic trial of N = 16 women.

Table 3.3: Summary of suggested improvements to original prototypes

Surface	Area of Improvement
Concept 1	- Addition of clinical headrest - Softer surface or opening for non-examined breast - Removal of chest curvature - Softer surfaces at hips - Surfaces to be raised
Concept 2	- Addition of clinical headrest - Softer surface or opening for non-examined breast - Softer surface, especially at hip and knee location - Surfaces to be raised
Concept 3	- Addition of clinical headrest - Softer surface or opening for non-examined breast - Stiffer surface to reduce chance of back arching - Surfaces to be raised

The most, and least, preferred prototype as determined by the 16 participants in the initial trial are summarised in Figure 3.4. The most preferred surface was the mouldable surface with 9 participants indicating they preferred that prototype. A number of participants described lying on the mouldable surface as being similar to lying on a bed as said they could fall asleep if given the chance. The least preferable surface was the flat bench. However, majority of women indicated that if a different head position was available they might prefer that surface.

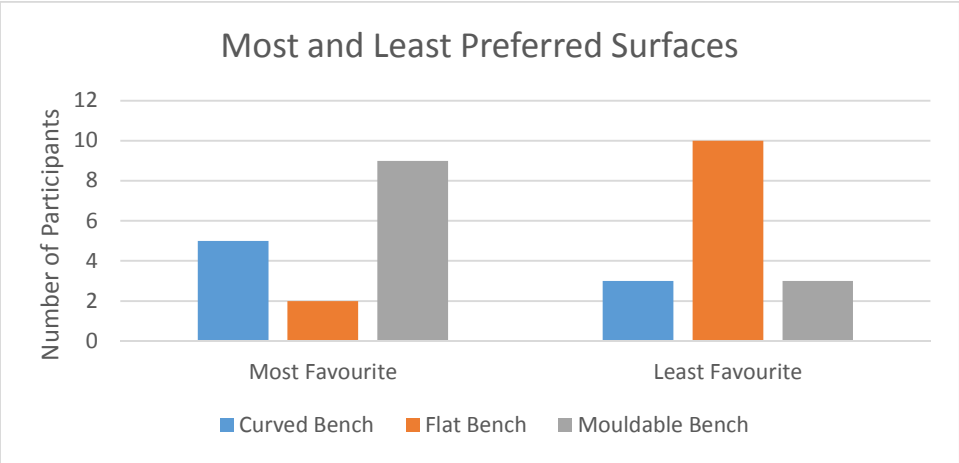

Figure 3.4: Most and least preferred surface determined in initial trial

With only 16 people participating in the initial trial, important improvements to the surfaces were made apparent. Because of this early and clear outcome, changes were made to the prototype surfaces based on the initial trial feedback. Two surfaces were produced that have two removable inserts to change the chest area of the surface, as shown in Figure 3.5. This adaptation allowed for four different combinations of surfaces for the secondary trial.

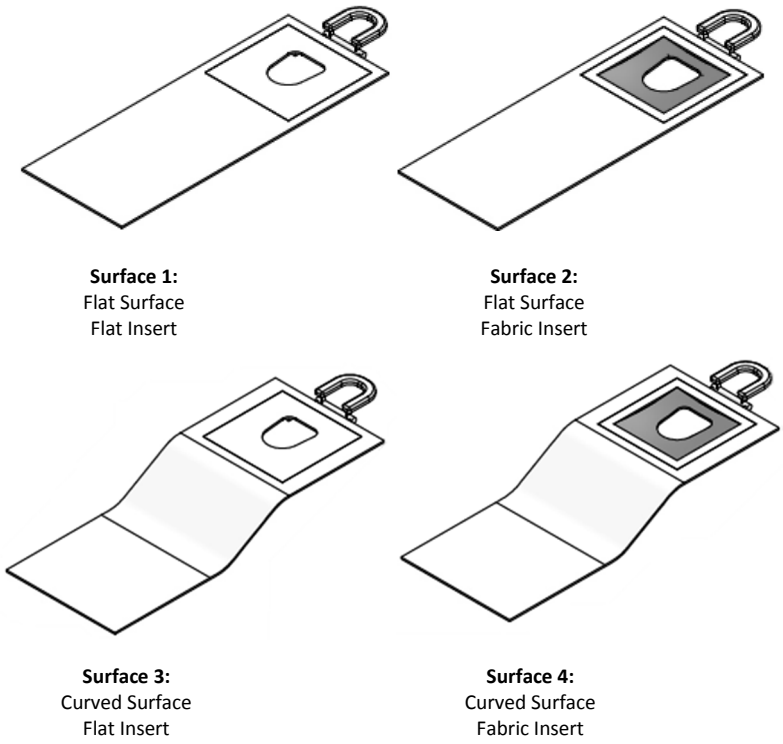

Figure 3.5: Isometric view of improved prototype bench combinations for use in second trial

Figure 3.6 shows the modified surface prototypes for the second trial. Both surfaces and both inserts have 40mm of soft foam on top with fabric holding the foam in place. In addition, the head rest was interchangeable between the two surfaces.

Figure 3.6: Modified prototype surface used in second trial

3.4.2 Secondary Trial

The secondary trial method was similar the first trial. However, additional questions were asked. In particular, discomfort levels in the shoulders and lower back were recorded, participants ranked all surface combinations in order of preference, and participants were asked if they preferred their arms in front, at their sides or if they preferred either option. These additional questions gave a greater insight into the comfort levels on the surfaces. It also gave the participant further prompts to recognise locations of discomfort.

Eleven participants took part in the second trial with a range of ages and dress sizes, as described in, Table 3.1. Figure 3.7 shows where the discomfort was experienced for each of the modified surfaces. The two most common locations of discomfort were the chest and the lower back. There were two reasons for the discomfort in the chest area: **1)** The non-examined breast pressing into the surface; and **2)** The outer edges of the opening hole digging into the chest. The chest discomfort was felt worst on the flat surface and participants indicated that possibly the different angle on the curved surface removed most of the chest discomfort. In contrast, the lower back discomfort was felt worst on the curved surface. Many of the participants indicated they felt awkward lying on the curved surface and that they generally felt more natural lying face down on the flat surface.

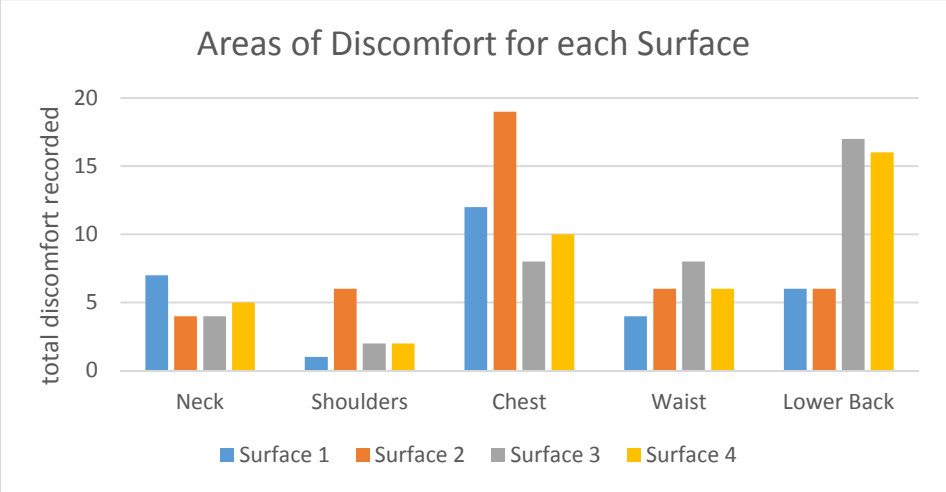

Figure 3.7: Areas of discomfort recorded for each surface in the secondary trial where the surfaces 1 – 4 are: 1) Flat surface – flat insert, 2) Flat surface – fabric insert, 3) Curved surface – flat insert, and 4) Curved surface – fabric insert

Participants were asked if they preferred their arms either in front of them, shown in Figure 3.8, at their sides or the option to have either. All participants in the secondary trial indicated they preferred the option of either, while nine out of the eleven participants placed their hands in front of them during the trial. The two who had their arms at their side indicated higher levels of discomfort in their shoulders compared to participants who chose to have their arms in front. When asked to give additional commentary on the ergonomics of the surface, most women said that an additional focus on the arm rest would be beneficial.

Figure 3.8: Trial participant lying on curved surface with arms in front (photo taken with consent)

The surface preferences were weighted, as described in Table 3.4, and summarised in Figure 3.9. Additionally, total discomfort recorded on each surface. Figure 3.9 shows the least discomfort was experienced on Surface 1, which also had the highest rank weighting.

Table 3.4: Weighting of rankings

Ranking	Weighting
1st	3
2nd	2
3rd	1
4th	0

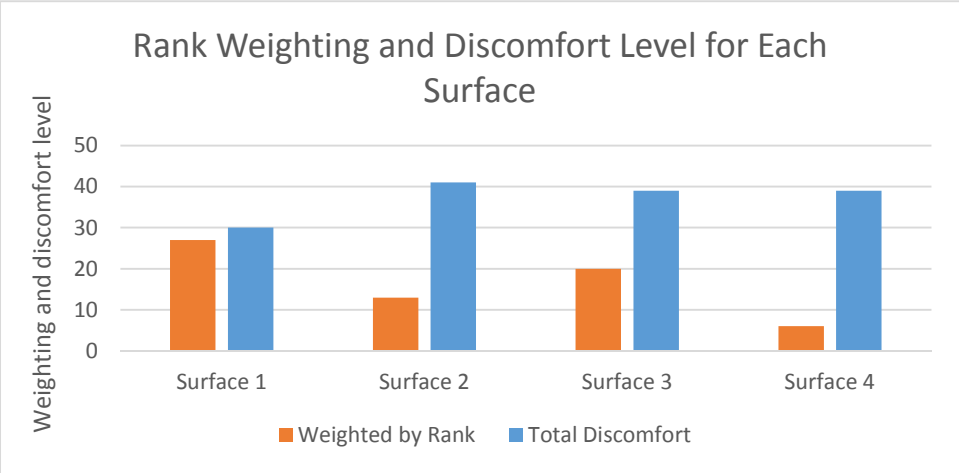

Figure 3.9: Results of weighted rankings and total discomfort levels for each surface prototype

Many women in this trial indicated that they preferred Surface 1 because it is similar to a bed, which they are used to lying on. Of those who did not prefer the curved surface, their main criticism was that the angle of the curve did not match their specific dimensions and indicated that if it were to work, they would prefer it to be adjustable.

Other comments made during this trial related to the head rest and the height of the surface. Two women felt like the head rest opening was too narrow and that their faces felt squeezed. Both participants indicated that different sizes of headrest could be provided. As with the first trial, participants indicated that the height of the surface should be raised so that they are not so cumbersome to climb onto.

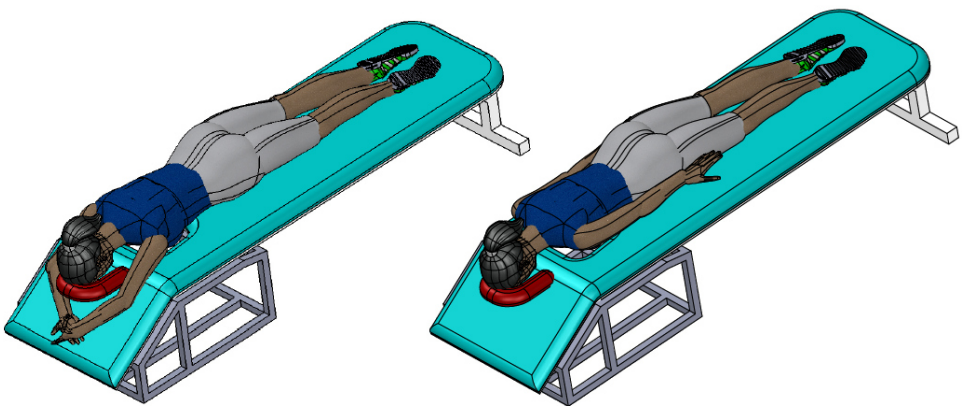

Figure 3.10: Proposed DIET surface showing both arm rest positions

All information from the trials were used to produce the final concept, which will be used to manufacture a surface. This final surface will eventually be used on the DIET machine for clinical trials. Figure 3.10 shows this final concept, which is very similar to Surface 1 used in the second trial. The main difference between the two surfaces is the addition of the angled arm rest. Further development of this surface is discussed in Chapter 6.

3.5 Summary

An ergonomic trial was performed to determine what kind of surface would be suitable for the DIET system. Ethics approval was granted from the University of Canterbury Human Ethics Committee under a low risk application. A total of 27 participants took part in the ergonomic trials and these participants had a wide range of ages, clothing sizes, heights and weights.

An initial trial consisted of participants providing feedback on three different surfaces. Key ergonomic feedback was sound during this initial trial, however there was no obvious preference for either surface. For this reason, an additional trial was performed with modified surfaces. During the secondary trial, it was made clear that there was a preference for a simplified surface which felt more natural for women to lie on. The flatter surface was the clear winner of the four options. Additionally, important details were made apparent including the need for an arm rest in front of a patient's head and the preference for a wider, or interchangeable, headrests. The flat surface will be developed further and will be manufactured, which is discussed in Chapter 6.

4. Phantom Breasts

4.1 Background

Phantom breasts are a useful tool used in the development of the DIET system. They allow for testing of new ideas and developments without the immediate need for human trials. Phantoms thus aid rapid development and reduce risk before clinical testing.

With the current DIET machine, only the cup of the breast is exposed in images with a completely black background due to the shape of the opening and the use of breast rings. When only the cup of the breast is exposed, an edge can be easily detected using segmentation methods which provide the basis for analysing the vibrational response along the breast surface (Botterill et al., 2014). Therefore, the detection of stiffer cancerous tissue can proceed only for this region.

It is proposed to change the opening hole on the surface of the machine to a larger, unique shape, as discussed in Chapter 2. This change will likely expose a portion of the patient's chest wall in the background of the images. This exposure, in turn, may require new methods for detecting edges of the breast. For this reason, phantom breasts have been produced with the same outer shape as the proposed breast opening.

Along with testing edge detection methods the phantom breasts have also been used to determine the impact on the imaging software. Finally, for the phantom breast to accurately represent a real breast, the shape, size, colour and material properties should be as close as possible to human breast tissue.

4.2 Phantom Breast Material

Previous work on the DIET system used phantom breasts made out of silicone material. This work showed that these phantoms mimic human breast tissue properties well (Linda, 2012). In particular, the silicone material can be varied in stiffness by altering the mixture ratios. This adaptability enables stiffer silicone tissue to be produced to represent cancerous tissue (Peters, Chase, & Van Houten, 2008) and allows for different compositions of silicone to represent the skin and adipose portions of the breast. Moreover, silicone material is easy to source and does not require complex methods to create a phantom. For this reason, silicone, as in Figure 4.1, was chosen as the material to use in for the phantom breasts.

Figure 4.1: Materials used to produce the phantom breasts: (a) Silicone Soft Gel A-341 Parts A and B (Factor II, Arizona, USA), (b) Silicone oil (Dow Corning Silicone Fluid; Dow Corning, Michigan, USA)

Table 4.1 shows the proportions of each material used in each portion of the phantom breast tissue. These proportions were determined based on previous phantom breast production for the DIET system (Kashif, 2013). Stiffer incisions were not produced for these assessments so are not included in the table.

Table 4.1: Proportion of matierials used to make phantom breasts

	Percentage of Mixture		
	A-341-A	**A-341-B**	**DC-200**
Skin	90%	10%	-
Adipose	40%	4%	56%

4.3 Phantom Breast Size

Phantom breast size is based on the anthropometric data in Section 2.1.4. Dimension Y, from Figure 2.7, has been used to determine the depth of the breast with the values of these dimensions summarised in Table 2.3. The data used to obtain these values were from a study of 456 Chinese women who were between 20 and 39 years of age (Rong, 2006). To account for differing breast sizes between ethnicities and to allow for the growing population, a 10% increase in breast depth has been made. This choice was compared to ongoing, New Zealand based, DIET clinical trial data carried out on women, and matched well. As the main purpose of these phantoms is to determine if the machine is capable of detecting the location of the edge of the breast, the smaller, 5th percentile, breast dimensions is used. The smaller breast would show more of the chest background compared to a larger breast, and is thus a worst case scenario.

To produce phantom breasts out of silicone, a mould was produced. Figure 4.2 shows the dimensions of the mould. Detailed drawings of these parts, including drawings required to produce a 50th and 95th percentile breast mould, have been included in Appendix B.

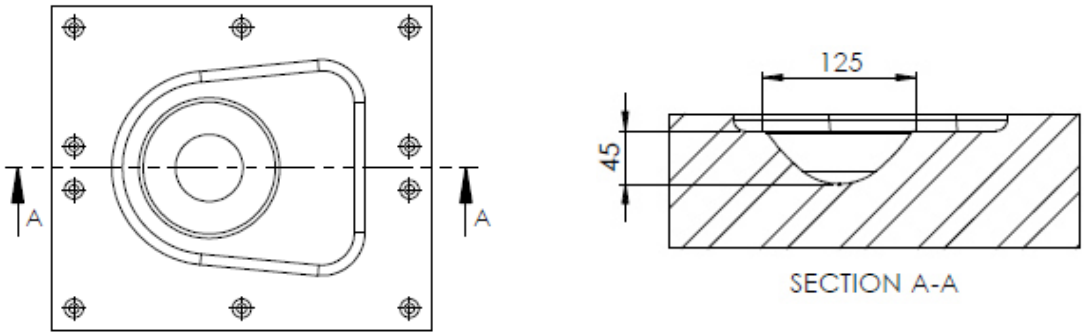

Figure 4.2: Design of Phantom Breast Mould

The mould is made out of modelling board and was CNC machined to accurately produce the complex curves of the cup of the breast. A support plate was produced out of Perspex plastic. This plate was laser cut and served the function of supporting the phantom, roughly simulating the rib cage. The plate has a number of 10mm diameter holes to allow pouring of the liquid silicone. In addition, two top plates were laser cut out of Perspex plastic to hold the support plate in place and allow up to 10mm of silicone to set above the support plates. Table 4.2 summarises the parts used to form the phantom breast moulding assembly.

Table 4.2: Materials used to produce the phantom breast moulding assembly

Part #	Part Name	Material Used
1	Mould	Modelling Board
2	Support Plate	5mm Perspex
3	Top Plates	25mm Perspex

4.4 Phantom Production Methods

Methods used to produce the phantom breasts were based on previous phantom production for the DIET system (Linda, 2012) and modified for the different geometry. The silicone material, Section 4.2, was used in conjunction with the moulding assembly, Section 4.3. Demoulding agents were also used in the production of the silicone phantoms. A combination of CRC Silicone Demoulding Agent and Mould Release Wax was used. When both release agents were used, the silicone would peel off Part #1 with little issue. Figure 4.3 shows the moulding assembly and mould release agents used to produce the phantom breasts. The steps required to produce the phantom breasts have been outlined in Table 4.3.

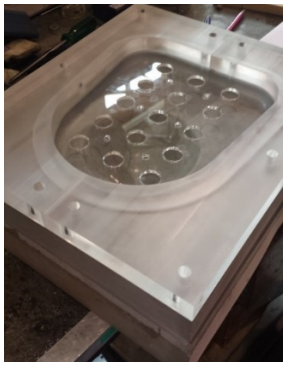

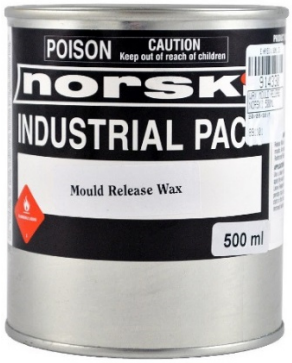

Figure 4.3: Materials used to produce the phantom breasts: (a) Moulding assembly including parts 1, 2 and 3, (b) CRC demoulding agent (CRC, Manukau, NZ), and (c) Norski mould release wax (Norski, Wellington, NZ)

Table 4.3: Methods used to produce silicone phantom breasts

Step	Method	Photos (if applicable)
1	Clean all surfaces of Part #1, #2 and #3.	NA
2	Smear the mould release wax on the surface of Part #1 and Part #3. Apply an even, smooth coating (approx. 1mm). Place Part #1 in the oven (70°C) for 30 minutes to allow wax to dry.	NA
3	Remove from oven and spray Part #1 and Part #3 with CRC-808.	
4	Prepare skin mixture and add a small amount of colouring agent. For the smaller breast size, 200g of skin mixture is required.	
5	After Part #1 has been pre-heated for 30 minutes in the 70°C oven, pour half the skin mixture into mould. Manually rotate mould to achieve an even coating. Allow for some of the mixture to harden while rotating, particularly at the very edges of the mould, and place into oven for up to 3 minutes.	NA

Step	Method	Photos (if applicable)
6	Pour remaining skin mixture into the mould and rotate to get even thickness. The thickness of the skin should be approximately 5mm at this stage. Place mixture back into oven for another 10 minutes.	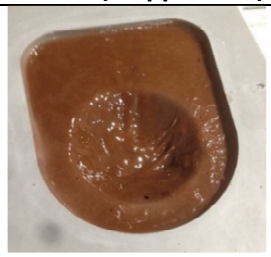
7	Prepare adipose mixture. For smaller breast size, 1.2kg of adipose mixture is required. Add a small amount of skin pigmentation if the brown phantom is being produced; this will prevent the skin portion from appearing transparent. Assemble Part #1, #2 and #3 and pour the adipose mixture into the mould.	
8	Ensure that 10mm of mixture is above Part #2 before placing into the 70°C oven for 3 hours	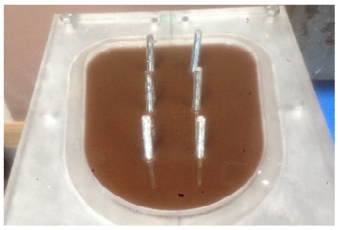
9	While the whole assembly is still warm, demould the phantom breast. Note that the adipose portion of the phantom may detach from the skin at this stage, however this will not alter the shape of the final phantom. If this does occur, carefully peel the skin off Part 1 in one piece and immediately drape over the adipose	

4.5 Human skin colour

Extensive testing has previously been carried out on the DIET system with phantoms that have "Flesh" coloured skin or, much earlier, yellow coloured phantoms (Kashif, Lotz, McGarry, Pattison, & Chase, 2013). The yellow colour was used very early in the development of the DIET system and was not intended to accurately represent human skin colour. The Flesh colour represents the skin tone of a relatively small portion of the female population which can generally be described as a Mediterranean type skin (Visscher, 2010). The aim for the DIET system is to be capable of screening women of all ethnicities and thus all skin colours. For this reason, phantom breasts have been produced with a

variety of skin colours, which represent either extreme of the human skin spectrum, as well as one from the centre of the spectrum.

4.5.1 RGB Colour Scale

A colour image can be numerically represented in MATLAB by an NxMx3 matrix, where N and M are the height and width of an image in pixels respectively. Each NxM matrix layer represents the irradiance values of the image for each of the three colours; red, green, and blue. The combination of the colour values for each pixel then yields the actual colour of that pixel, commonly known as an RGB value. Conversely, a grayscale image is represented by just one NxM matrix. This NxM matrix expresses the irradiance of each pixel on a scale, usually from zero to one, representing black to white. Figure 4.4 shows how an image is made up of each RGB colour and compares it to the grayscale image.

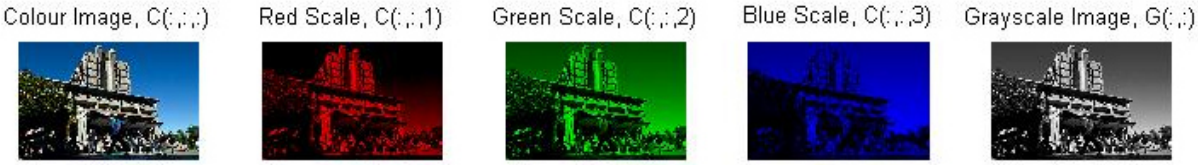

Figure 4.4: Images in a) Colour (RGB), b) Red Scale, c) Green Scale, d) Blue Scale, and e) Grayscale (image: http://www.canterbury.ac.nz/)

4.5.2 Skin Colour Detection

4.5.2.1 Fitzpatrick Skin Colour

The Fitzpatrick classification method is a subjective way of determining the reaction of skin to solar stimuli and has become the standard for determining human skin phototypes (González, Martínez-Escanamé, Muñoz, Torres-Álvarez, & Moncada, 2010). The scale is useful for assessing risk factors of melanoma and non-melanoma skin cancer, as well as estimates for UV, PUVA, and laser treatment doses (Astner & Anderson, 2004). To classify skin using the Fitzpatrick skin scale, a questionnaire, including questions about a person's tendency to burn and ability to tan, is completed (Ravnbak, 2010). The results of the questionnaire give a person one of six possible skin types, which are summarised in Table 4.4. The RGB and Colour Intensity values have been numerically determined in MATLAB.

Table 4.4: Fitzpatrick skin types with associated RGB and colour intensity values (Ravnbak, 2010)

Type	Description	Colour Image	RGB Value	Grayscale Image	Colour Intensity*
1	Pale white skin. Always burns, does not tan		[244,208,176]		0.84
2	Fair skin. Burns easily, tans poorly.		[232,180,143]		0.75
3	Darker white skin. Tans after initial burn.		[211,158,124]		0.67
4	Light brown skin. Burns minimally, tans easily.		[187,119,80]		0.53
5	Brown skin. Rarely burns, tans darkly easily.		[165,93,42]		0.43
6	Dark brown or black skin. Never burns, always tans darkly.		[60,32,29]		0.16

*Colour intensity normalised (White = 1, Black = 0)

The Fitzpatrick Skin Colour Scale has limitations, including subjective diagnosing methods. However, the main limitation is that this scale is known to correlate well for pale skin, but does not correlate well for darker skin types (Sachdeva, 2009). This issue occurs because there is not enough variation for darker pigmented skin, as can be seen in the Colour Intensity row in Table 4.4. Hence, another skin type scale, the von Luschan Chromatic Scale (Swiatoniowski, Quillen, Shriver, & Jablonski, 2013), has been used for analysis of the darker pigmented skins.

4.5.2.2 von Luschan Skin Colour Scale

Until the 1950s, the only method for determining skin types was based on visual matching with standardized colours on strips of paper or glass tiles. The most widely used were the coloured glass developed by Austrian anthropologist, Felix von Luschan (Swiatoniowski et al., 2013). The von Luschan scale uses a series of 36 opaque glass tiles, as shown in Figure 4.5, which are used to characterize skin colour. Different tiles can be compared to a part of skin, which is not normally exposed to the sun, to classify the skin (Tedeschi-Oliveira, Melani, de Almeida, & de Paiva, 2009). While this method is crude, it has historically been given a guide for skin colour characterisation(Bois, Luschan, & Reform, 2016).

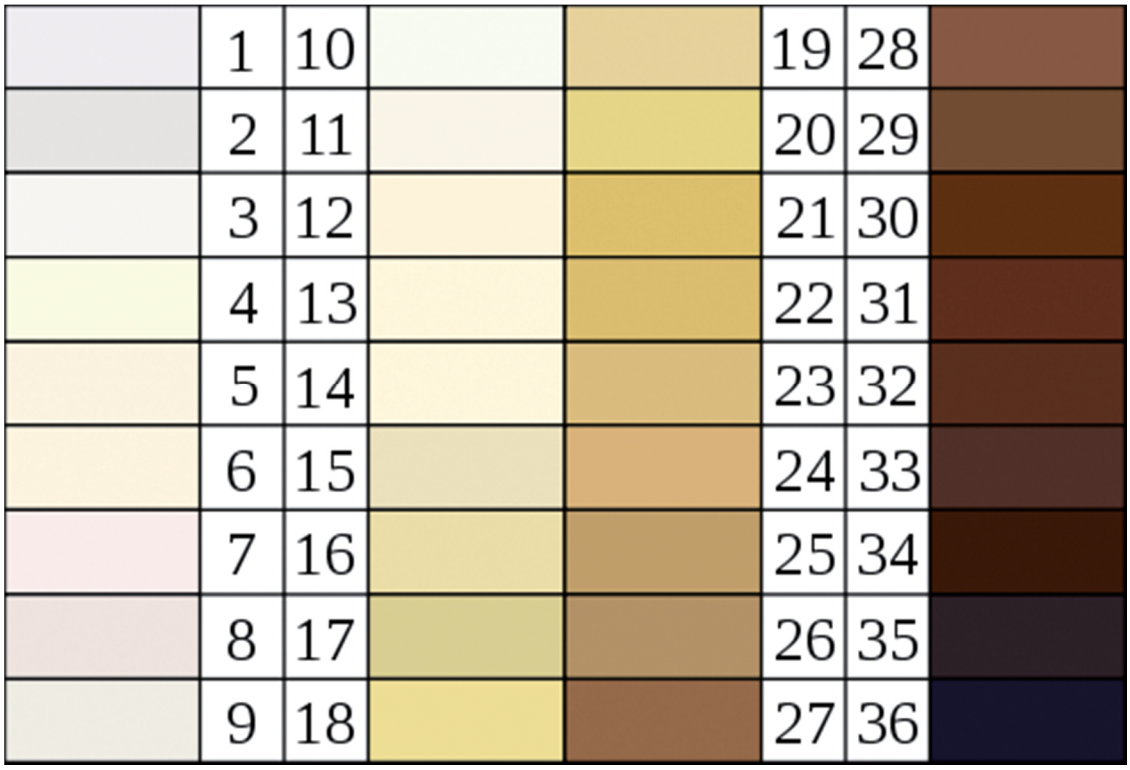

Figure 4.5: von Luschan Skin Colour Chart (Visscher, 2010)

Similar to the Fitzpatrick Skin Colour Scale, the majority of variation in the von Luschan Scale represents lighter skin tones. However, this scale does give more variation for the darker skin tones than the Fitzpatrick Scale, and is thus used to classify darker skin tones. The correlation between the von Luschan Colours and the FitzPatrick Scale is summarised in Table 4.5.

Table 4.5: Correlation between von Luschan colour scale and Fitzpatrick Types (Visscher, 2010)

Fitzpatrick Type	von Luschan Colour	Description (von Luschan's Description)
I	1 – 5	Pale, fair, freckles (Very light)
II	6 – 10	Fair (Light)
III	11 – 15	Light brown (Intermediate)
IV	16 – 21	Olive brown (Mediterranean)
V	22 – 28	Brown (Dark or brown)
VI	29 – 36	Black (Very dark or back)

4.5.2.3 Other skin colour detection methods

Another common method of skin colour detection is the use of a narrowband reflectance spectrometer, as shown in Figure 4.6. This device measures the reflectance of green and red light emitting diodes (LEDs). The LEDs illuminate the surface and record the intensity of the reflected light(Clarys, Alewaeters, Lambrecht, & Barel, 2000).

Figure 4.6: Mexameter Narrowband Reflectance Spectrometer (GmbH, 2016)

Skin colour evaluation using a skin colour scale chart has shown a high correlation with skin colour evaluation done by a narrowband reflectance spectrophotometer (Haghir, Mokhber, Azarpazhooh, Haghighi, & Radmard, 2013). For this reason, skin colour classification in this study will be achieved using both the Fitzpatrick and von Luschan scales, rather than the more expensive option of the narrowband reflectance spectrometer. This choice is pragmatic and does not create limitations due to the good correlation noted.

4.5.2.4 Comparing Digital and Photographed Scales

Classifying skin colour using the Fitzpatrick and von Luschan scales is subjective, as it relies on visually comparing colours. Thus, the classification is limited to what colours the human eye can detect. To provide a repeatable, non-subjective classification method, photographs of each colour have been taken and the red, green, blue and grayscale values of these colours are compared to the two colour scales. All photos were taken in natural lighting on the same day to provide a consistent approach.

This method was first tested with a printed version of the von Luschan skin colour scale, shown in Figure 4.7. The colour composition of the digital and printed versions of the scale were analysed in MATLAB to obtain RGB values. While the digital and printed colour intensity plots, shown in Figure 4.8, do not match perfectly, they follow a similar trend and will be useful for comparative assessments.

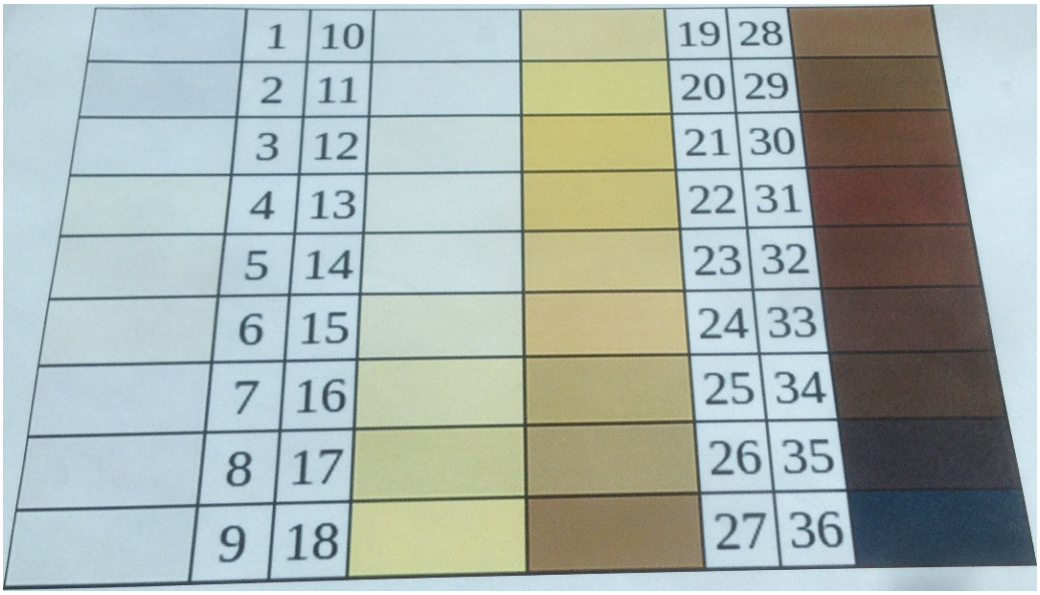

Figure 4.7: Printed von Luschan Scale used for comparison

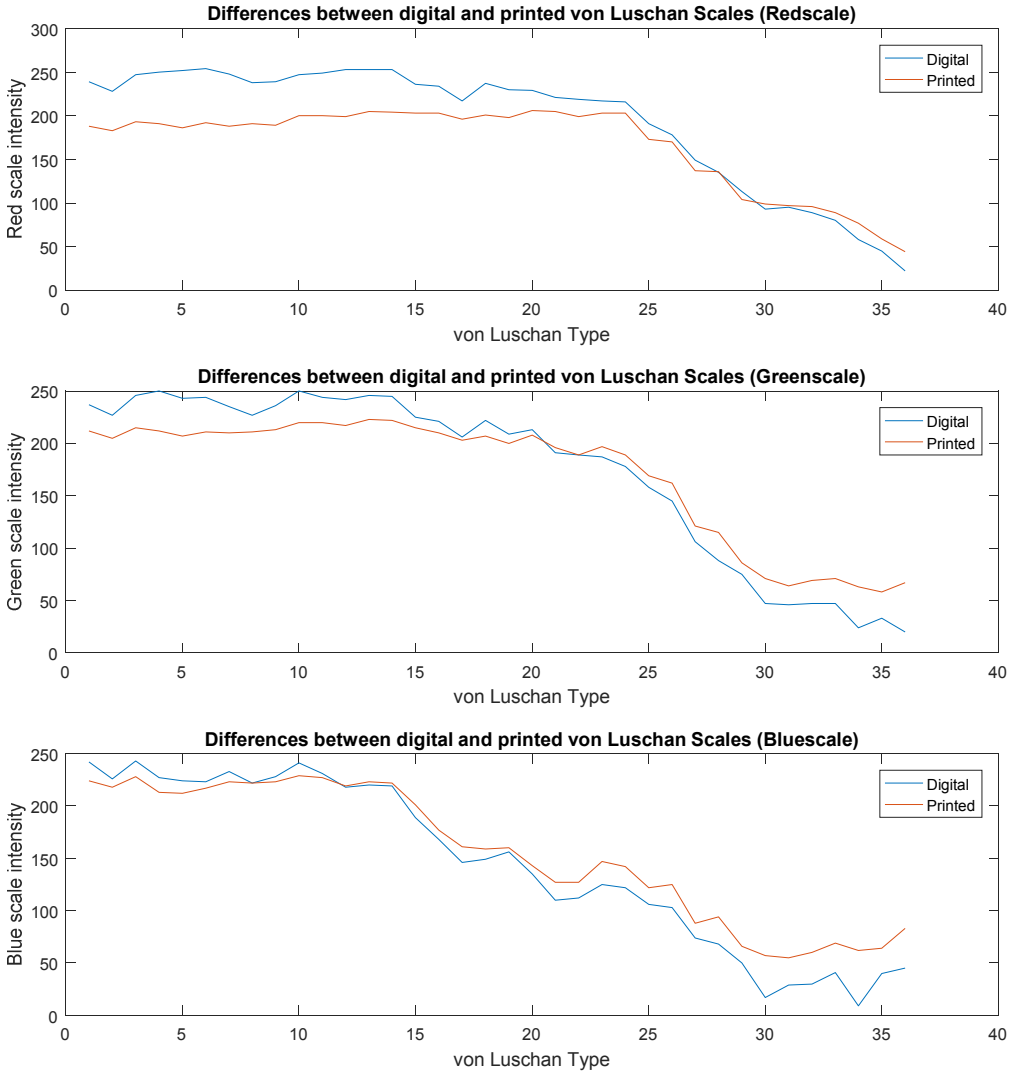

Figure 4.8: Differences between digital and printed von Luschan scales (Red, Green and Blue)

4.5.3 Silicone Skin Pigments

Silicone material is naturally pellucid. However, silicone pigments can be added to a mixture to make it opaque and to add colour. Silc Pig silicone pigment from Smooth-On (East Texas, PA, USA), as shown in Figure 4.9, has been used to alter the colour and opaqueness of the phantom skin layer of the phantom breast. A number of different combinations of colours have been produced in test pots to compare the silicone colour against the von Luschan scale, for dark skin types, and the Fitzpatrick scale, for light skin, types. All colours from both scales were printed and up to 5 colours that were visually similar were placed on the test colours. This method of skin colour detection is similar to that proposed by Felix von Luschan whereby his coloured tiles were placed next to human skin tissue and each colour was visually compared.

Figure 4.9: Smooth-On Silicone Pigment (Shop, 2016)

The closest match by visual inspection was used to describe the skin colour of the patient. While this method is simple, it will show if the phantom skin colour is similar to human skin colour. In addition to the visual inspection, photographs have been analysed to determine more exact RGB components of the picture to confirm the closest colour. The pigment combinations tested, along with the von Luschan and Fitzpatrick skin types, are summarised in Table 4.6.

Table 4.6: Skin colour tests with colour chart samples

Test colours and Classification	Photo	Test colours and Classification	Photo
Test Colours: White and Flesh **Classification:** Fitzpatrick II	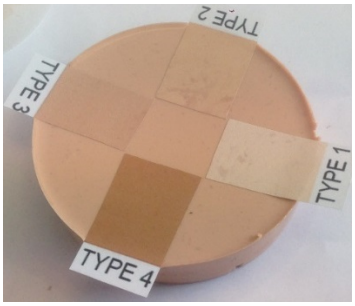	**Test Colours:** Flesh **Classification:** Fitzpatrick IV	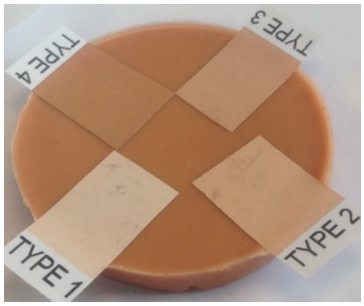
Test Colours: Flesh and Brown **Classification:** von Luschan 30	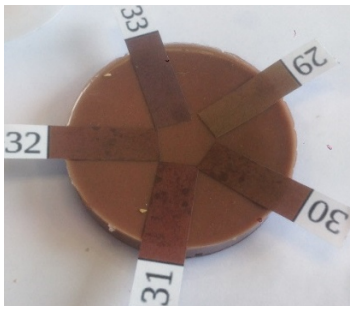	**Test Colours:** Brown **Classification:** von Luschan 31	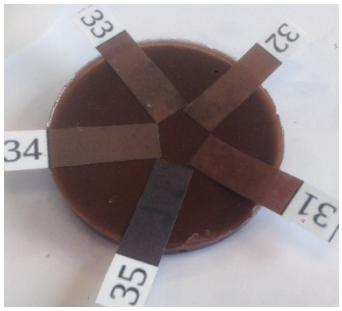
Test Colours: Brown and Red **Classification:** von Luschan 30	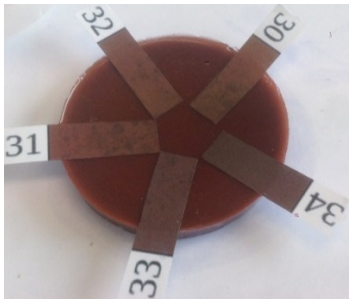	**Test Colours:** Flesh, Red and Brown **Classification:** von Luschan 30	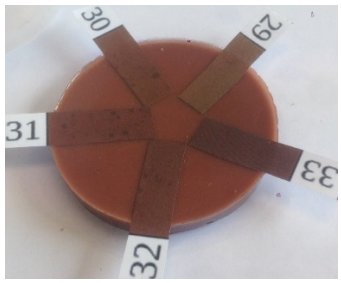

4.5.3.1 Human Skin Optics in RGB Colour Space

Relationships between the ratios of red, green and blue colours within pixels can be used in pixel based skin detection. It has been found that if a pixel has specific ratios of RGB components, there is a high likelihood that the pixel represents skin (Brand & Mason, 2000). Specifically, if:

$$\frac{R}{G} > 1 \qquad \text{(Equation 4.1)}$$

$$\frac{R}{B} > 1 \qquad \text{(Equation 4.2)}$$

$$\frac{G}{B} > 1 \qquad \text{(Equation 4.3)}$$

This concept can be utilised to confirm whether the silicone pigment is capable of representing skin colour.

The colour ratios of the test colours, and the two skin colour scale types, have been plotted, as shown in Figure 4.10. This figure shows that all phantom skin is likely to represent a real skin colour. It also shows that most test colours are within the band of possible skin types present in the Fitzpatrick and von Luschan skin colour scales.

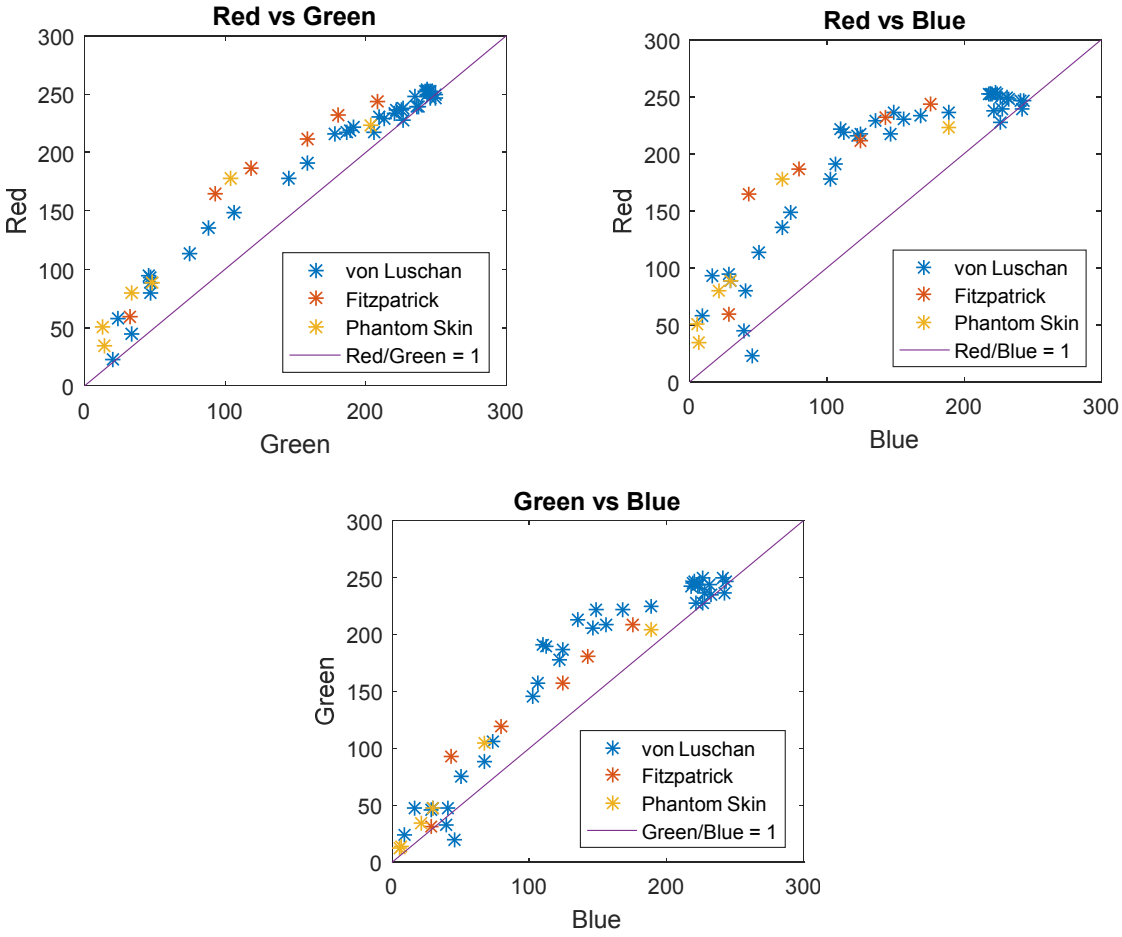

Figure 4.10: Comparison of RGB colours for von Luschan, Fitzpatrick and phantom skin

4.5.3.2 Grayscale Analysis

While it is important to be able to represent skin colour in the phantom breasts, the DIET system currently uses grayscale images in the analysis of images for computational ease. For this reason, analysis of the grayscale values of the phantom test colours has also been carried out. Figure 4.11 shows that the "Brown" test colour has the lowest irradiance value, which is close to the irradiance value of the darkest von Luschan type. Additionally, the highest irradiance value is present in the

"White and Flesh" test colours, which are also similar to the lightest Fitzpatrick type. The "Flesh" test colour is approximately in the middle of the irradiance spectrum.

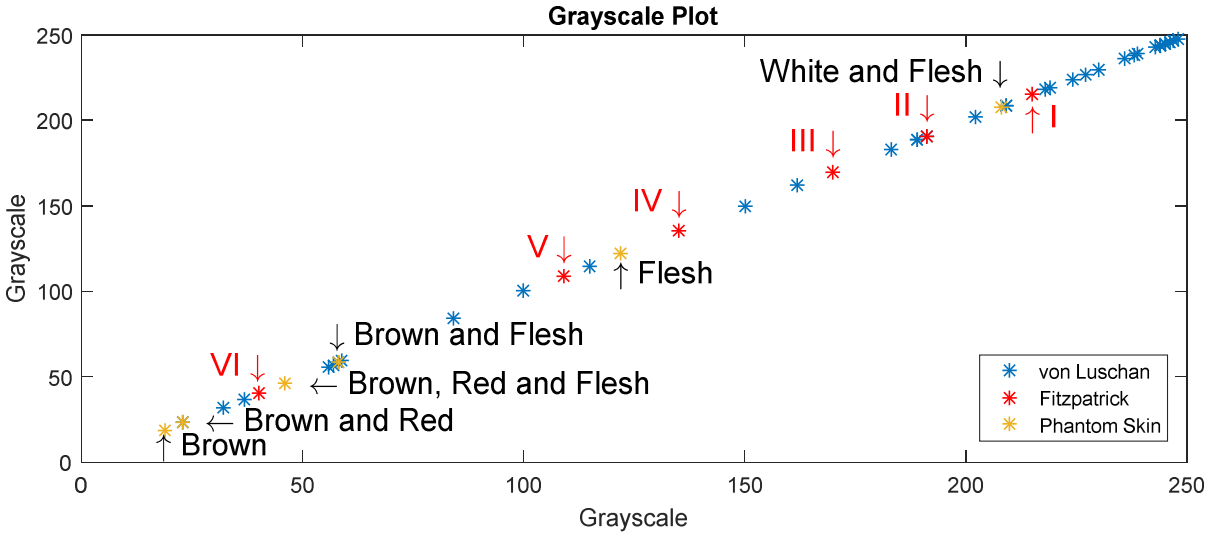

Figure 4.11: Grayscale values of von Luschan types, Fitzpatrick types and phantom test colours

To represent a range of skin colours found in the human population, three skin colours will be used in the production of phantom breasts: 1) "White and Flesh" which represents pale white, or fair skin; 2) "Flesh" which represents olive brown, or Mediterranean, skin; and 3) "Brown" which represents very dark, or black, skin. Each of the skin colours produced as phantom skin are shown in Figure 4.12.

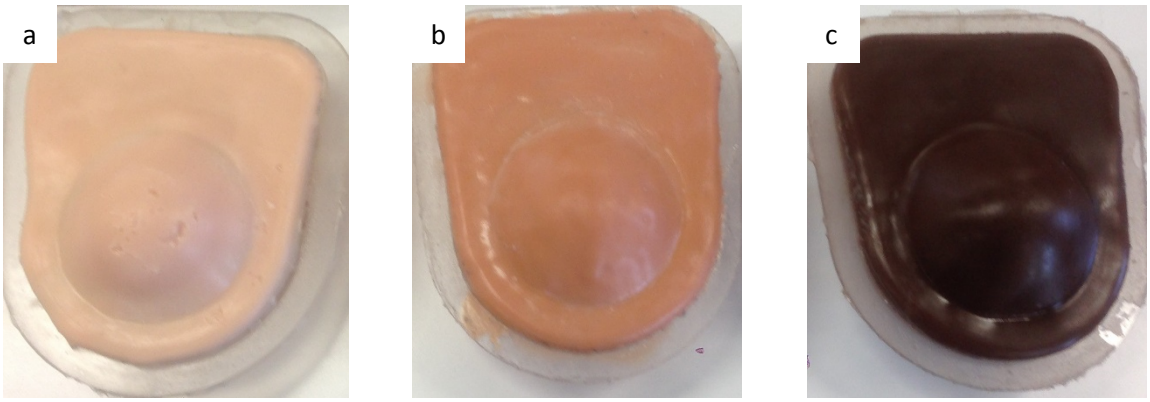

Figure 4.12: Phantom breasts with varying skin colour: (a) Pale white skin, (b) Mediterranean skin, and (c) Dark brown skin

4.6 Summary

Proposed changes to the surface of the DIET system, in particular changing the size and shape of the breast opening, may cause changes to the system. In particular, the edge detection algorithm, which detects the location of the breast surface and its motion, may no longer work efficiently if the chest

wall is exposed. To explore how changing the shape and size of the breast opening will affect the functionality of the DIET system, phantom breasts have been created.

Phantom breasts have been produced out of silicone, which has been used extensively during the development of the DIET system. Silicone has been shown to exhibit similar mechanical properties to that of human breast tissue. Moreover, it is an ideal material because silicone is inexpensive, easy to source and does not require complicated manufacturing methods.

The size of the phantom breasts were determined from anthropometric data. In particular, a study of 456 Chinese women gave key dimensions for the phantom mould design. A smaller breast would expose more of the chest wall, which could lead to ineffective edge detection. Thus, the 5^{th} percentile anthropometric data was used. The methods used to produce the phantoms have been outlined in this chapter; including details on the preparation of the mould parts as well as mixture composition of the silicone, setting temperatures and duration.

Finally, previous studies have only examined one flesh colour on the phantom breasts, and the chest wall was not exposed in images. It has been predicted that the contrast in light intensity between the cup of the breast and the chest wall may vary significantly depending on skin colour, which is likely to effect the method required for detecting the surface of the breast. For this reason, three different colours have been used to represent the skin of the phantom breasts: 1) Pale white; 2) Mediterranean; and 3) Dark brown. These three colours give a wide spectrum of the possible colours exhibited in human worldwide. The colours used in the phantoms skins compared well with human skin colour described in the Fitzpatrick Skin Colour Types and von Luschan Skin Colour Scale.

5. Impact of Changing Breast Opening

5.1 Background

In the existing DIET system, breast surfaces are detected using common edge detection methods (Botterill et al., 2014). Currently, the use of breast rings ensures only the cup of the breast is exposed against a black background, providing a significant change in light intensity between the breast surface and the matte black background. If a portion of the chest wall is exposed, as expected with the shape and size of the proposed new breast opening, a clear distinction between the chest wall and the breast surface may not be achieved with the current algorithm.

The phantom breasts produced, as described in Chapter 4, have the same outer shape as the proposed new breast opening, and thus have a chest wall and breast cup. Three colours of phantom breast were produced: pale white, Mediterranean and dark brown. The phantoms have been tested in trial runs to determine what impact the new shape has on the existing imaging software. Images from these trials are evaluated in MATLAB. Segmentation methods are explored to determine how to detect the edge of the surface of the breast and whether it is possible to isolate the edge of the breast from the remainder of the image.

5.2 Temporary Modifications to Existing DIET Machine

Phantom breasts are to be used in trials with the original DIET machine. Thus, a temporary surface was required to attach the phantoms to the original frames. Figure 5.1 and Figure 5.2 show the dimensions of the existing DIET screening machine. Adjustable screw holes, Figure 5.1, are used to fix any surface to the machine. Figure 5.2 shows the centre of the actuator is 100mm from the lower bar of the existing DIET machine's shell. The centre of the actuator is required to align vertically with the centre of the breast to provide an even vibration input. In addition, all cameras are set up to capture breast surface motion around this central point.

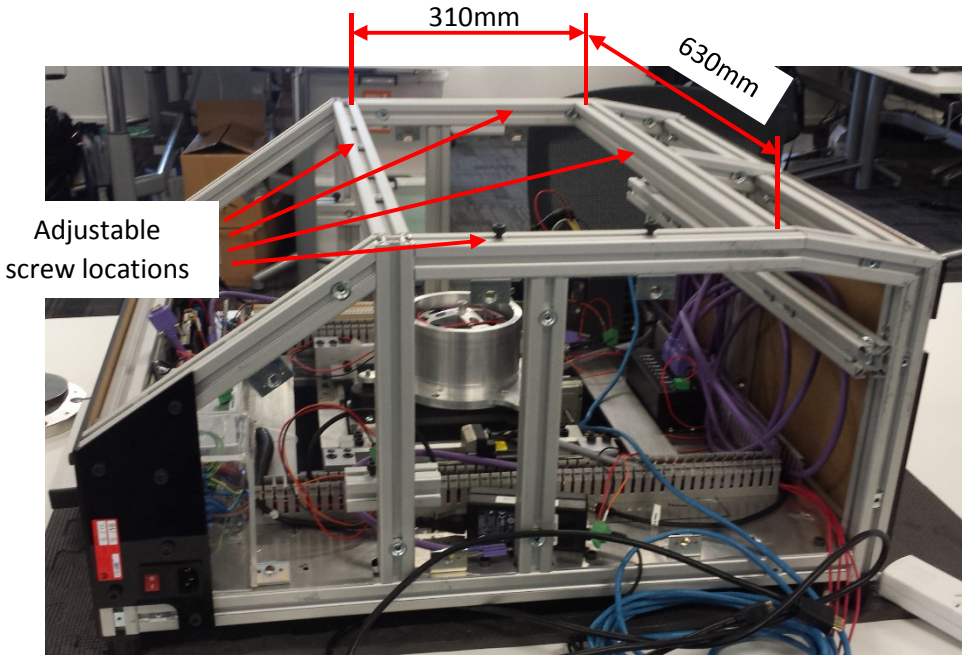

Figure 5.1: Existing machine with key dimensions showing where screws can be attached.

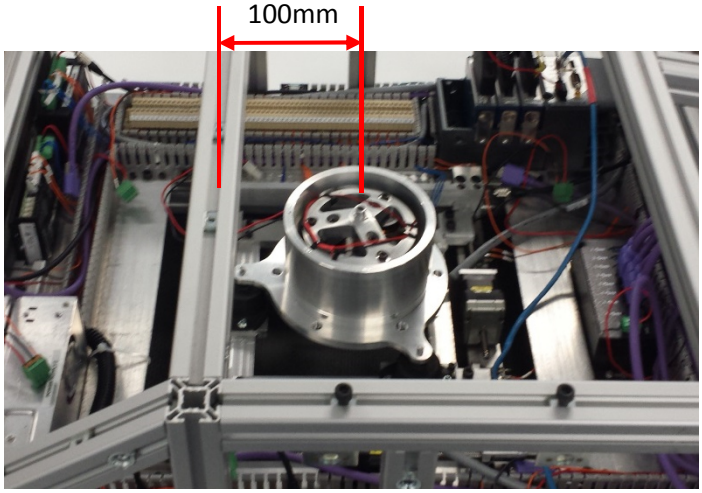

Figure 5.2: Distance between lower bar and centre of actuator on the existing DIET machine shell.

A modified surface has been produced, Figure 5.3, and used on the machine. This surface was spray painted black on the side that faces the internal components of the DIET machine. This colour provides a matte black finish, which reduces reflections and glare within the machine. In addition, to prevent light pollution, the exposed sides of the machine were temporarily blacked out with paper.

Figure 5.3: Modified surface on DIET System with dark brown phantom breast

5.3 Impact of Changing Breast Opening

The existing DIET system automatically aligns the actuator to sit directly below the centre of the breast. This approach works well with the circular breast rings as and phantoms because the upper plane is defined by the location of the circle. In addition, edges of the breast were also used to position the actuator. As the shape of the hole has been changed for this test, manual actuator positioning was required.

In addition to changing the actuator positioning settings, the number of frequencies at which the actuator was vibrated was also changed. Ordinarily, the actuator sweeps frequencies between 16 Hz and 50 Hz in 2 Hz intervals. Because the DIET technology is in early stages of development, a wide range of frequencies is tested to determine the most useful frequency band, and different frequencies have been shown to detect tumours more accurately than others.

However, for this phantom breast screening, vibration analysis is not immediately required. The main focus of these tests are to determine if, and how, the edge of the breast can be detected. Thus, only four frequencies were tested: 20 Hz, 30 Hz, 40 Hz, and 50 Hz. The preload applied to the breast was 300grams.

Ten photos from each of the five camera views were produced for each frequency range. Figure 5.4 shows images taken from Camera 1, for each of the three phantom breasts used. The pale

white phantom, shown in Figure 5.4 (c), required additional cardboard support to hold the phantom skin in place because the pigment used in the pale white skin reduces the adhesiveness of the phantom skin and caused the skin to peel off the adipose portion of the phantom when it was held upside down. As the images are used to detect an edge between the cup of the breast in the foreground and the phantom chest in the background, this additional support structure does not affect the overall results of the test.

Figure 5.4: Images of camera view 1 during motion of (a) dark brown phantom, (b) Medditerrenean phantom, and (c) pale white phantoms with additional cardboard structure

Upon visual inspection of the images in Figure 5.4 (a – c), it appears that an edge is well defined in the lighter skin colours. This observation suggests that edge detection of these images may be more straightforward than edge detection of the dark brown phantom. This hypothesis will be further examined numerically in MATLAB.

5.4 Examination of Images

MATLAB has been used to examine edge detection and segmentation options from the images obtained. The purpose was to determine the extent at which the cup of the breast could be isolated from the remainder of the image and the chest wall portion of the phantom. If the cup of the breast could be extracted from the image, similar algorithms could be used as are already present in the DIET system for 3-D representation of the breast and vibration analysis. Figure 5.5 shows the three edges of the breast that can be detected from a single view. However, the two edges required to form the 3-D representation of the breast are the left breast profile and the right breast profile (Botterill et al., 2014). These edges need to be separated from the chest wall in the background. Therefore, the focus of the edge detection will be on the left and right breast profiles.

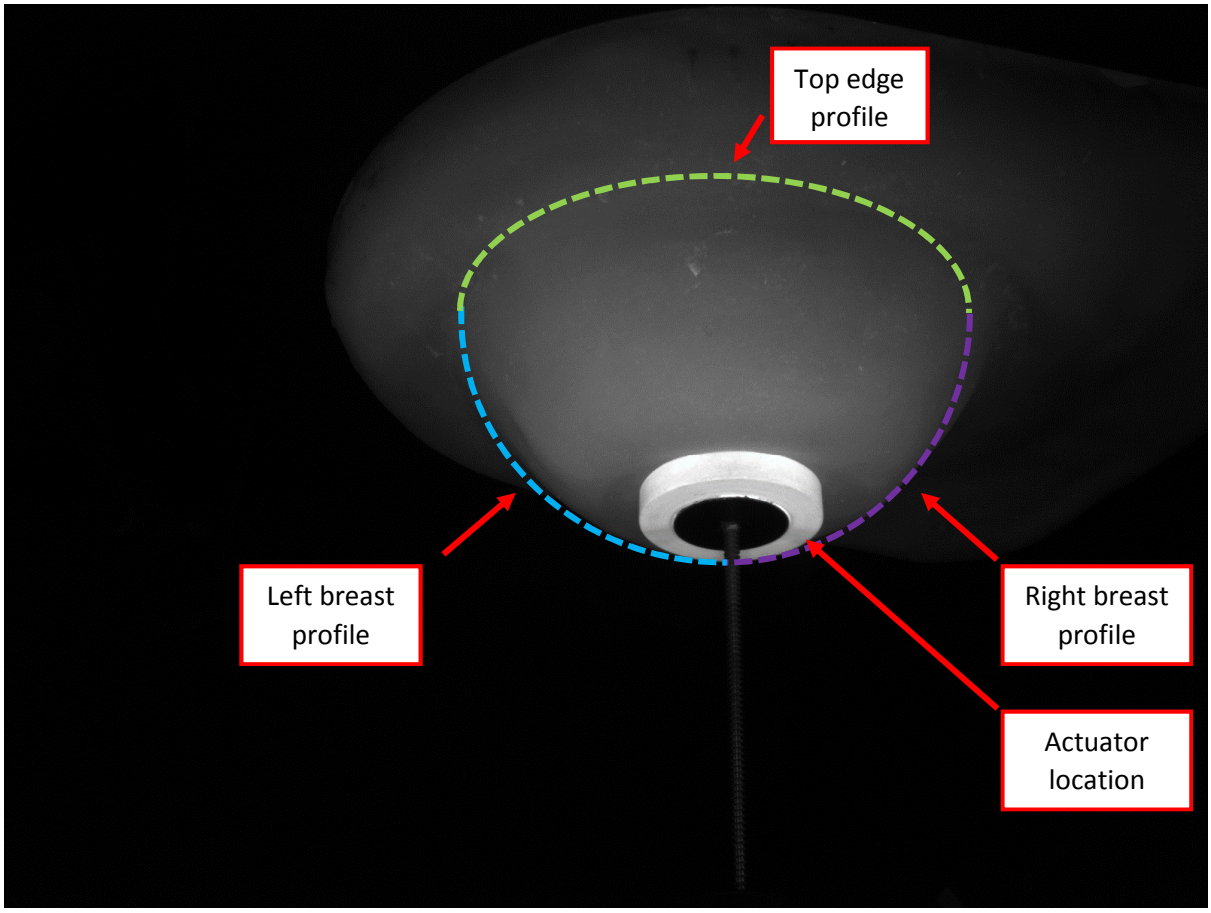

Figure 5.5: Camera 1 view of Mediterranean phantom with edges of breast cup illustrated

5.4.1 Properties of Images

Before edge detection methods were applied to the image, each image was examined mathematically. All images obtained from the DIET machine are captured in grayscale. Thus, each image is represented by a single two dimensional matrix of pixel values. All images were captured from the same type of camera, and all images have the same dimensions: 1600 pixels wide and 1200 pixels high. Each pixel value represents the intensity of the pixel on a scale from 0 to 255, where 0 represents a completely black pixel and 255 represents a completely white pixel.

Figure 5.6 shows the histograms of each phantom breast for View 1, as in Figure 5.4. The cluster of pixels at the dark end of the spectrum, with intensity values less than five, represents the background of the images, which is the matte black interior of the DIET machine. All other portions of the spectrum represent the phantom breasts. These portions of the histograms vary significantly for each phantom colour, as expected.

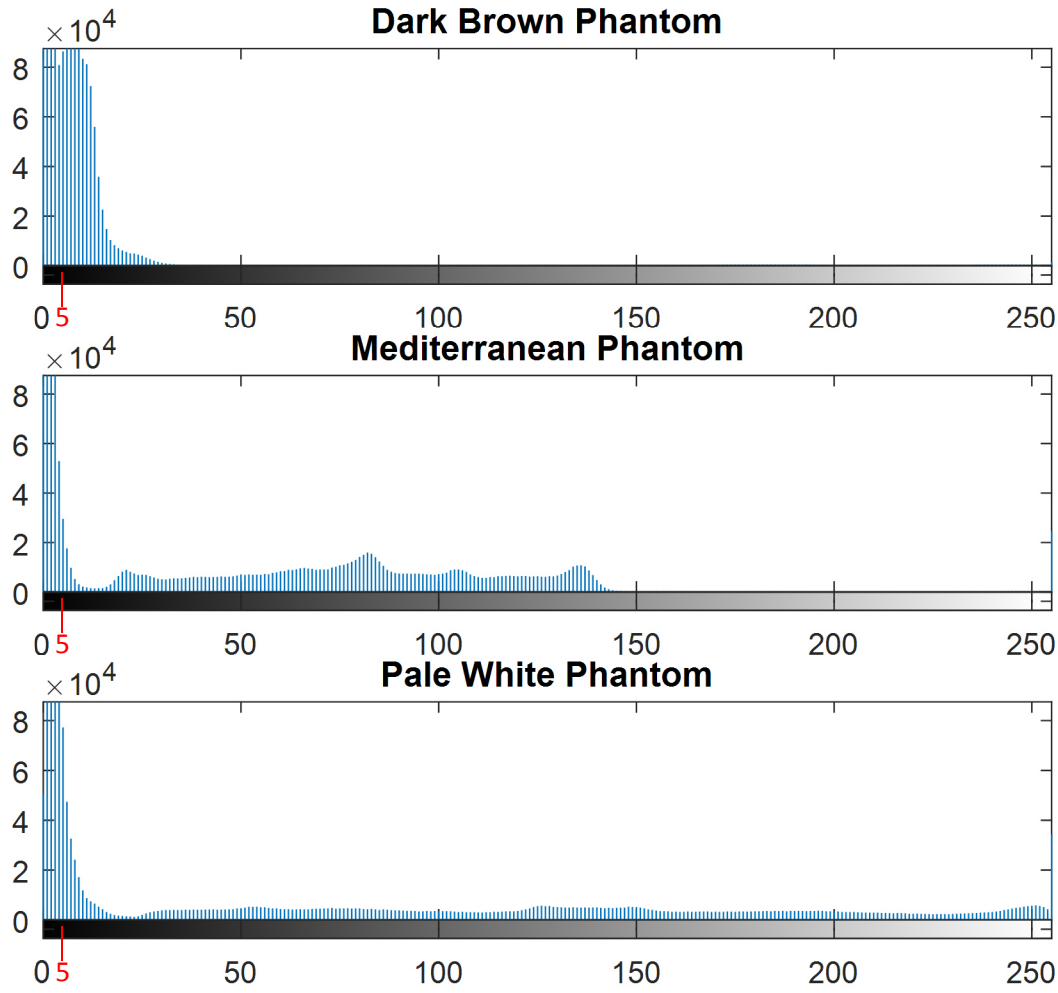

Figure 5.6: Histograms of image intensity values of pixels in View 1 for all three phantoms. Left of the red line, at intensity = 5, represents pixels that make up the matte black background of the DIET system.

The locations where the image intensity changed were also examined for all images. The distribution of the image intensity values have been plotted on a three dimensional surface, as shown in Figure 5.7. These surfaces show that the colour intensity of the actuator is significantly different from the colour of the Mediterranean and Brown phantom breasts, but is similar to the pale white phantom. It is, thus, expected that distinguishing between the pale white phantom and the actuator will be difficult. Figure 5.7 also shows that changes in pixel intensity of the brown phantom are minimal in comparison to the Mediterranean and pale white phantoms. These lesser changes might make edge detection of the brown phantoms more computationally expensive. The intensity values of the actuator remain the same regardless of phantom colour, as expected, because lighting conditions within the machine remain constant.

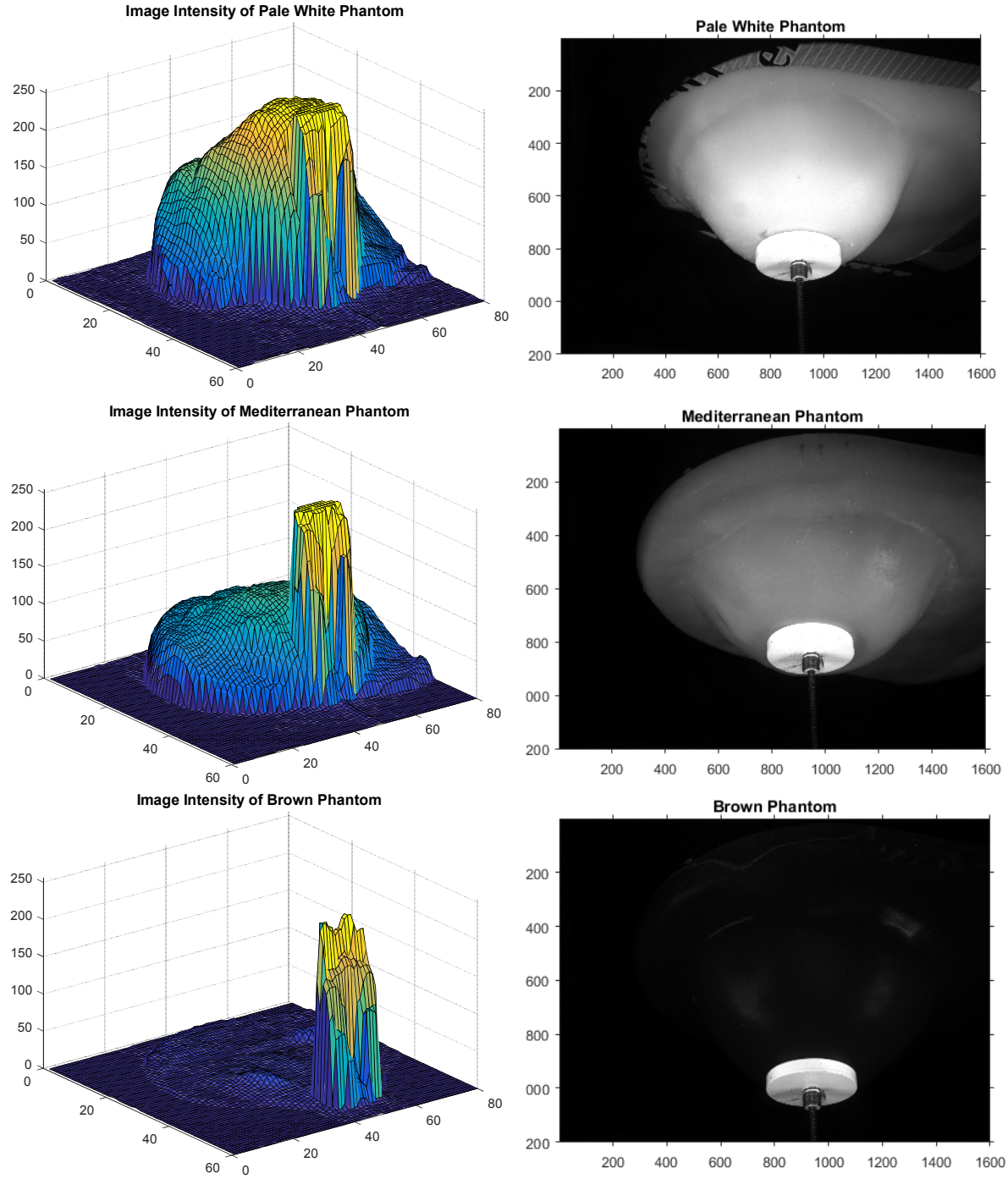

Figure 5.7: Left: Image intensities of each phantom breast, at 20 pixel intervals. Right: Images of each phantom breast.

5.4.2 Image Filtering

Before edge detection was carried out on the phantom breast images, a blurring function was applied to each image. Blurring the images reduces the chance of noise, or imperfections, being detected as edges and is essentially an averaging or low pass filter process. This approach ultimately results in a smoother, and more accurate, edge being detected. A simple five-pixel wide disk point spread function (PSF) was filtered with each image. This type of PSF was chosen as it provides non-directional

smoothing of an image. However, a Gaussian filter would also achieve a similar result. The resulting filtered image looks slightly out of focus due to the smoothing, as can be seen in Figure 5.8.

Figure 5.8: Filtered images with disk filter used

5.4.3 Image Segmentation

Image segmentation is a tool used to subdivide an image into regions or objects. This tool is useful for isolating a portion of an image, such as the cup of the breast, from the remainder of the image. Segmentation algorithms for grayscale images are generally based on two properties of image intensity values: **1)** discontinuity, and **2)** similarity (Gonzalez, Woods, & Eddins, 2004). A discontinuity in an image may represent an edge whereas a region of similar intensity values, a similarity, may represent an object.

5.4.4 Edge Detection

There are three main types of image discontinuities: **1)** points, **2)** lines, and **3)** edges(Gonzalez et al., 2004). For the case of edge detection, first and second order derivatives are used to determine locations of discontinuity(Gonzalez et al., 2004). Under this approach, an edge can be located at either of the following:

1. Where the first derivative of the intensity of greater in magnitude than a specific threshold.
2. Where the second derivative of the intensity has a zero crossing.

A number of edge detection methods can be used which rely on these two principles. MATLAB has an built-in function, `edge`, which uses both of these methods. Within the function are image post processing steps, such as line thinning and smoothing. This function has been used to compare common edge detection methods.

Sobel Method

The Sobel method uses the masks to approximate the first derivatives, G_x and G_y, as defined:

Sobel Mask (x-direction, G_x)

-1	-2	-1
0	0	0
1	2	1

Sobel Mask (y-direction, G_y)

-1	0	1
-2	0	2
-1	0	1

$$G_x = (z_7 + 2z_8 + z_9) - (z_1 + 2z_2 + z_3) \quad \text{(Eq. 5.1)}$$

$$G_y = (z_3 + 2z_6 + z_9) - (z_1 + 2z_4 + z_7) \quad \text{(Eq. 5.2)}$$

The gradient, g, at the centre point of a neighbourhood is computed:

$$g = \left[G_x^2 + G_y^2\right]^{\frac{1}{2}}$$
$$g = \{ [(z_7 + 2z_8 + z_9) - (z_1 + 2z_2 + z_3)]^2 + [(z_3 + 2z_6 + z_9) - (z_1 + 2z_4 + z_7)]^2 \}^{\frac{1}{2}} \quad \text{(Eq. 5.3)}$$

From this value, an edge is identified as the gradient value greater than a given threshold value where T is a user defined value:

$$g \geq T \quad \text{(Eq. 5.4)}$$

Thresholding values are further discussed in Section 5.4.5. The method described was applied in MATLAB with default threshold values for images of all three phantoms taken from Camera View 1. Figure 5.9 displays resulting images from the edge detection process. The images display a zoomed in portion of the phantoms including the actuator and right hand side of the breast cup. This portion of the breast is shown for clarity and will be used throughout for comparison purposes.

The images in Figure 5.9 show the Sobel edge detection method accurately displays the location of the edge of the breast cup for two of the three phantom colours, where the dark brown phantom breast edge was not detected. The reason the dark brown edge was not detected is because the edge is considered a weak edge. The change in image intensity between the cup of the breast and the

background in the Brown phantom does not vary greatly, as was displayed in Figure 5.7. The default thresholds can be altered to find weaker edges, which will be further explored in Section 5.4.5.

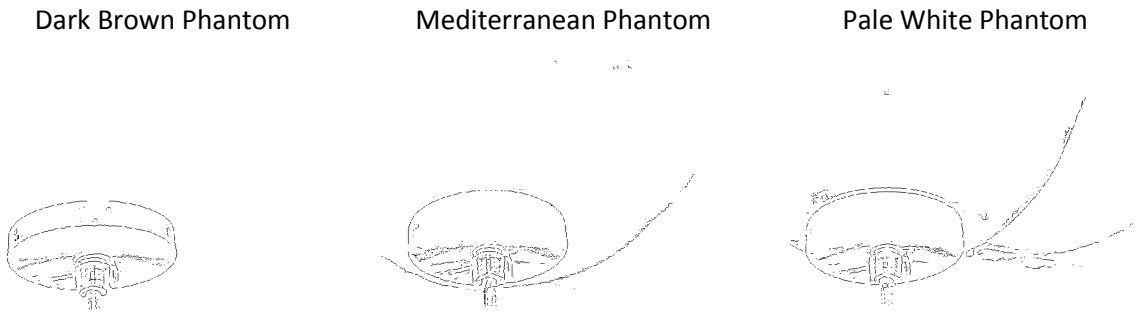

Figure 5.9: Sobel edge detection method using basic principles on all phantom breasts in View 1.

Figure 5.9 also shows the edge of the actuator was detected in all images. Image pixels representing the actuator have significantly different image intensity values than the surrounding pixels in the image, as could be seen in Figure 5.7. This difference results in a strong edge, which is able to be detected with the default thresholding values. A final observation about Figure 5.9 is that a large amount of noise is present within the image, where false edges were detected.

Prewitt Method

The Prewitt edge detection method is similar to the Sobel method but with different masks, as defined:

Prewitt Mask (x-direction, G_x)

-1	-1	-1
0	0	0
1	1	1

Prewitt Mask (y-direction, G_y)

-1	0	1
-1	0	1
-1	0	1

$$G_x = (z_7 + z_8 + z_9) - (z_1 + z_2 + z_3) \quad \text{(Eq. 5.5)}$$

$$G_y = (z_3 + z_6 + z_9) - (z_1 + z_4 + z_7) \quad \text{(Eq. 5.6)}$$

Computationally, the Prewitt method is similar to the Sobel method. However, it is known to produce noisier results because the coefficient with value 2, in the Sobel detector, provides smoothing the Prewitt detector lacks. Images from edge detection using the Prewitt method are displayed in Figure

5.10. These images show that, like the Sobel method, edges could be detected for the Mediterranean and pale white phantoms in View 1, but not for the dark brown phantom. Similar to the Sobel mothed, these results show the actuator edges were detected for all phantom breasts.

Dark Brown Phantom | Mediterranean Phantom | Pale White Phantom

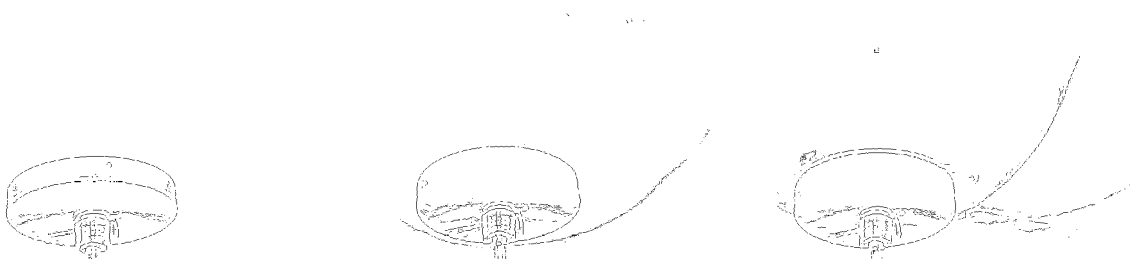

Figure 5.10: Prewitt edge detection method using basic principles on all phantom breasts in View 1

Roberts Method

The Roberts edge detection method also works in a similar way to the Sobel method with different masks, defined:

Roberts Mask (x-direction, G_x)

-1	0
0	1

Roberts Mask (y-direction, G_y)

0	-1
1	0

$$G_x = z_9 - z_5 \quad \text{(Eq. 5.7)}$$

$$G_y = z_8 - z_6 \quad \text{(Eq. 5.8)}$$

The Roberts method is the simplest of all edge detection methods, but is used considerably less often due to its limited functionality. The Roberts method is asymmetric, unlike other methods, and cannot be generalised to detect edges, which are in multiples of 45°. However, the Roberts method is used in applications where speed and simplicity are dominant factors.

When the Roberts method was examined in MATLAB, edges were detected for two of the three phantom breasts. Figure 5.11 shows a definitive edge could not be found in the dark brown phantom, but could be found in the Mediterranean and pale white phantoms. Noise issues were present in the resulting images, as were present in the Sobel and Prewitt methods.

Dark Brown Phantom Mediterranean Phantom Pale White Phantom

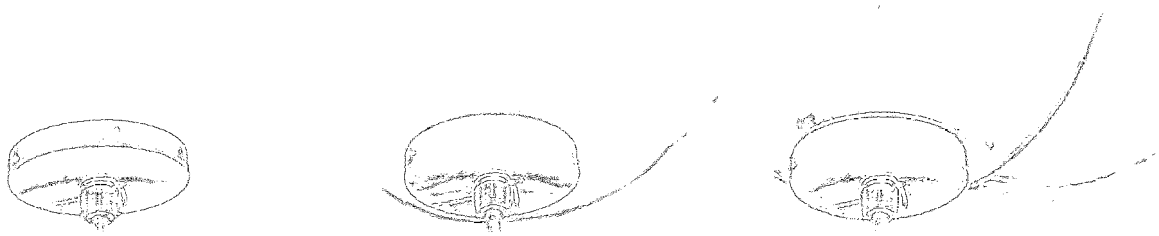

Figure 5.11: Roberts edge detection method using basic principles on all phantom breasts in View 1

Canny Method

The Canny Method is the most powerful edge detector in MATLAB. The edge detector employs four steps:

1. An image is smoothed using a Gaussian filter
2. Local gradients and edge directions are commuted at each point using either the Sobel, Prewitt or Roberts method.
3. The edge detected is smoothed to give a thin line edge. The gradient function is then refined using two thresholds, T1 and T2, where T1<T2. Gradients with values greater than T2 are considered strong edges and gradients with values between T1 and T2 are considered weak.
4. Edge linking is performed, linking weak and strong edges.

While the Canny method is the most powerful edge detector, it is also the most computationally complex. By having two thresholds, the Canny method is less likely than other methods to be influenced by noise, as was seen in Figure 5.9, Figure 5.10 and Figure 5.11. As a result, the Canny method is more likely to detect true weak edges, which should aid in edge detection for the dark brown phantom. The Canny method would be used when accuracy outweighs cost and time of computation. Figure 5.12 shows that when the Canny method is used, edges are detected for all phantom colours. In particular, weaker edges, which are present in the Brown phantom, could be detected as well as the stronger edges detected by other methods. While noise is present in these images, thresholding methods can be used to reduce the amount of noise.

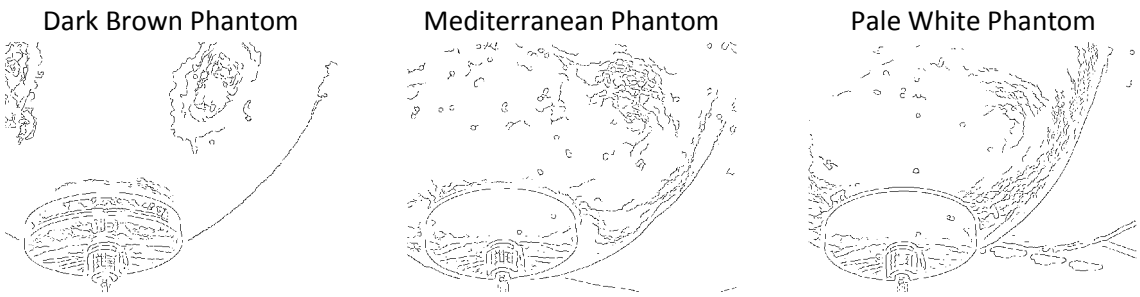

Figure 5.12: Canny edge detection method using basic principles on all phantom breasts in View 1

Other Edge Detectors

Two other built-in edge detection methods exist, but were not analysed; The LOG and Zero-Crossing detectors. The LOG, or Laplacian of a Gaussian, detector locates edge by finding zero crossing between double edges after an image has been smoothed with a Gaussian filter and a Laplacian has been performed on it. The Zero-Crossing detector works in a similar way to the LOG method. However, any smoothing filter can be used. These two methods were not examined as early use with these methods showed poor results for this application.

Results of Initial Test

In the previous section, one typical edge was examined from one camera view. For use with the existing DIET software, all 10 edges will need to be detected from all five camera views. Figure 5.13 shows all five camera views within the DIET system. All five images, for each phantom breast, have been analysed with the four edge detection methods using the edge function with default settings. The summary of the edge detection test on all images, detailed in Table 5.1, shows the Canny method is a robust edge detection method and is capable of detecting most edges regardless of phantom breast skin tone.

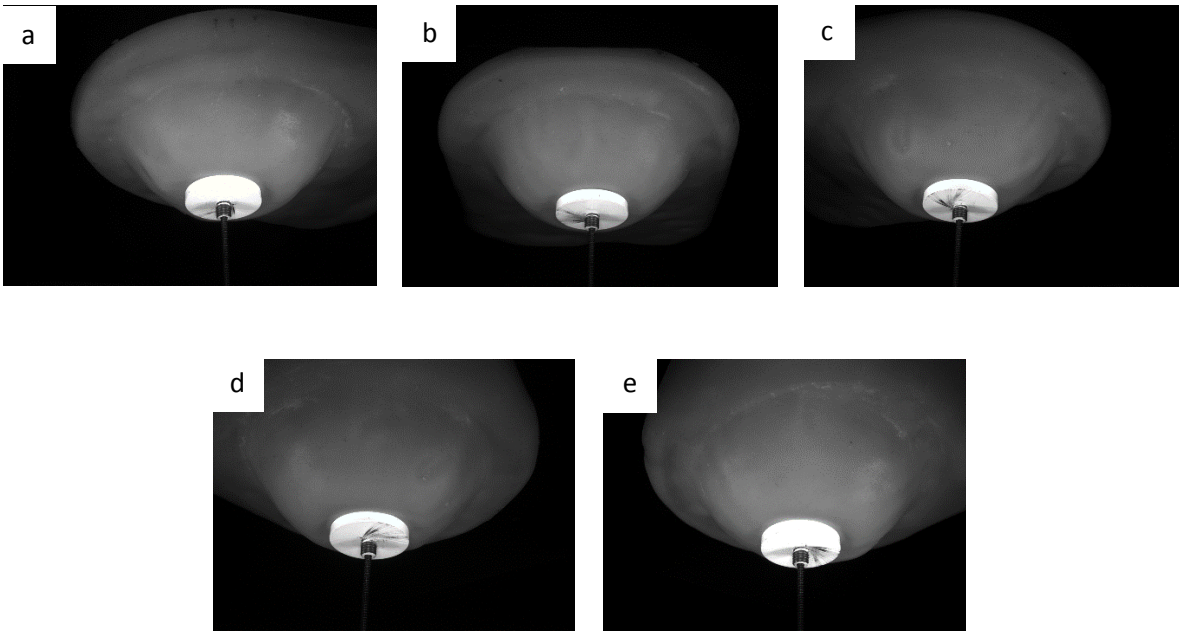

Figure 5.13: View of Mediterranean phantom breast taken from: (a) Camera 1, (b) Camera 2, (c) Camera 3, (d) Camera 4, and (e) Camera 5

Table 5.1: Outcome of edge detection test using default settings with four methods, with green cells representing a successful edge detection of both edges within each image

Method	View	Edge Detected		
		Dark Brown	Mediterranean	Pale White
Canny	View 1	Yes	Yes	Yes
	View 2	No	Yes	Yes
	View 3	Yes	Yes	Yes
	View 4	Yes	Yes	Yes
	View 5	Yes	Yes	Yes
Prewitt	View 1	No	No	Yes
	View 2	No	Yes	Yes
	View 3	No	No	Yes
	View 4	No	No	Yes
	View 5	No	No	Yes
Roberts	View 1	No	No	Yes
	View 2	No	No	Yes
	View 3	No	No	Yes
	View 4	No	No	Yes
	View 5	No	No	Yes
Sobel	View 1	No	No	Yes
	View 2	No	Yes	Yes
	View 3	No	No	Yes
	View 4	No	No	Yes
	View 5	No	No	Yes

Table 5.1 also shows the pale white Skin tone edges were detected by all four edge detection methods. While successfully detecting the edges of the breast in one skin tone may be beneficial for a portion of the female population, it is important to have a detection method which works well for all skin tones, and therefore all women. Thresholding methods will be looked into to determine how to refine the edge detection methods and methods.

5.4.5 Thresholding

In Section 5.4.4, one of the four edge detection methods discussed accurately detected and isolated the both edges of the cup of the breast for all colours of phantoms. Thresholding can be used to refine the edge detection algorithm. Thresholding is a fundamental approach applied to image segmentation, and is commonly used when speed or accuracy is an important factor. With the four methods discussed, it works by determining whether a gradient value, $g(x, y)$, is above or below a given threshold value and then assigning a binary value, as defined:

$$f(x,y) = \begin{cases} 1 \; if \; g(x,y) \geq T \\ 0 \; if \; g(x,y) < T \end{cases} \quad \text{(Eq. 5.9)}$$

For the Canny edge detection method, two threshold values are used, T1 and T2. For any gradient value above T2, the edge function would be defined as 1. If weak gradients, defined as values between T1 and T2, are found to connect with strong gradients, defined as values greater than T2, the edge function will also be defined as 1. For all other gradient values, the edge function is defined as 0.

When using the `edge` function within MATLAB, a threshold can be input manually. If a threshold value is not defined, MATLAB chooses a default threshold heuristically, depending on the input data. The default threshold value is a function of the magnitude of the gradient function, g, defined:

$$Threshold_{default} = \sqrt{s * average(g)} \quad \text{(Eq. 5.10)}$$

Where s is a scale unique to each edge detection method. While this method is likely to give good results in some cases, a more specific approach might be required for images with poorly defined edges. Threshold values can be determined by looking at the values of the gradient function at the location of edges, as shown in Figure 5.14. This approach is time consuming, as each image has to be examined manually, and relies on a visual assessment of where an edge is located. However, this approach would give a more accurate threshold value, and thus improved edge detection.

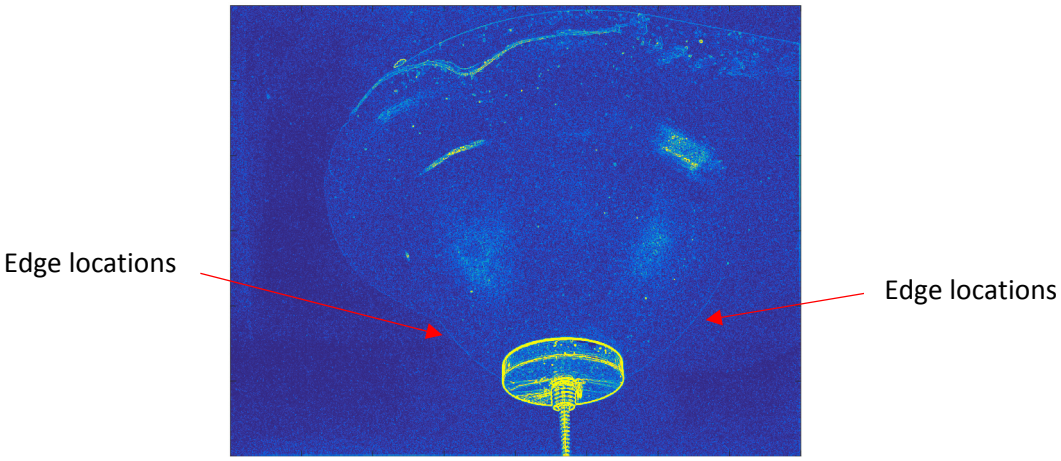

Figure 5.14: Representation of gradient function brown phantom breast after being passed with a Sobel filter. Image shown in colour for clarity

Figure 5.15 shows the results of edge detection after threshold values have been changed iteratively to an optimum value. The threshold was found to be a trade-off between an accurate edge detection and a reduction in resulting noise. Figure 5.15 shows an image with slightly less noise than was seen in Figure 5.12. However, a large amount of noise is still present in the image, and the cup of the breast has not been isolated, with this method. This result occurs largely because there is not a strong change in the gradient function for there to be a well-defined edge. An edge detection method should instead be used in combination with other segmentation methods to accurately isolate the breast cup.

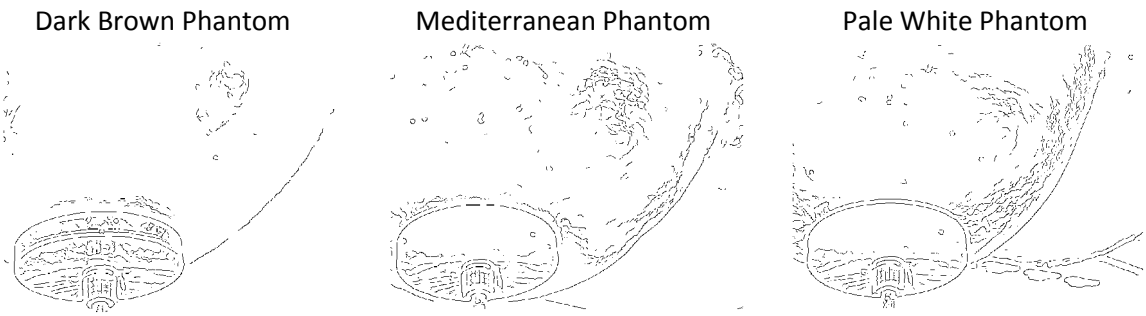

Figure 5.15: Canny edge detection method with altered threshold values on all phantom breasts in View 1

5.4.6 Region Detection

The edge detection functions, discussed in Section 5.4.4, relied on examining changes within an image to identify an object. Another way to identify objects within images is to look for where pixel values are similar and to group these similar pixels together (similarity methods). This grouping is achieved by applying a threshold to each pixel value. This type of thresholding is similar to that discussed in Section 5.4.5. However, the image intensity values are examined, rather than the gradient function, as defined:

$$f(x,y) = \begin{cases} 1 \; if \; I(x,y) \geq T \\ 0 \; if \; I(x,y) < T \end{cases} \qquad \text{(Eq. 5.11)}$$

Where f is the resulting segmented image, I is the original image and T is a scalar threshold value. An appropriate threshold value needs to be determined for this method to give accurate results. This threshold value can be determined by looking at the pixel values within an image.

Intensity values within any grayscale image range from 0, which represents black pixels, to 255, which represents white pixels. For analysis of the phantom breast images produced in the DIET system, the intensity scale has been broken up into 6 zones. Figure 5.16 shows these zones within each image.

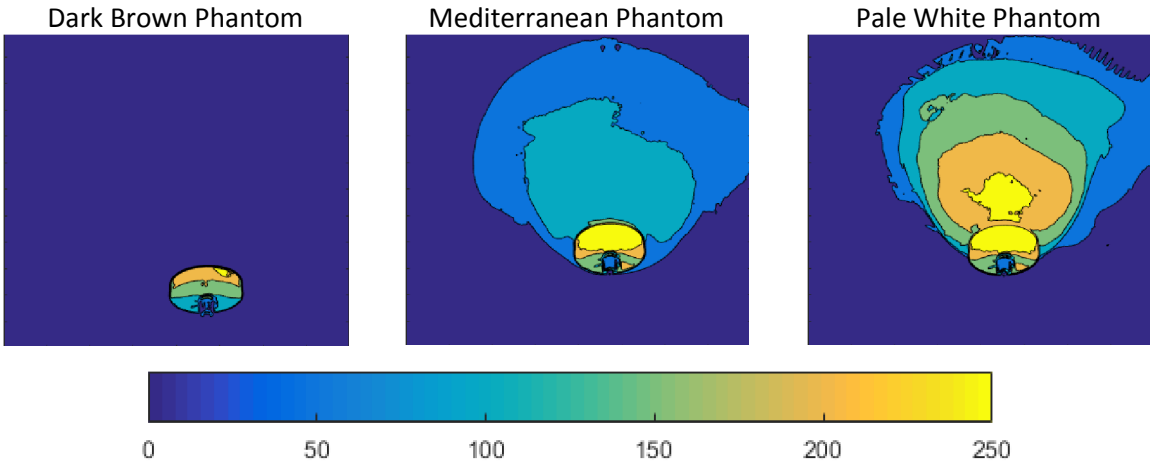

Figure 5.16: Phantom breasts with pixel values grouped into zones, shown in colour for clarity

It is clear to see that the pixel value of the cup of both the Mediterranean and pale white phantom breasts are different to the pixel values of the surrounding image. The same is true for the pixels located at the actuator. However, with the dark brown phantom breast, only the actuator can be distinguished from its surroundings. This result clearly shows all pixels of the brown phantom breast and the background have intensity values that fall within the lowest zone. Thus, a low threshold value would need to be applied to this image before the breast cup was detected.

Threshold values were chosen iteratively, as a starting point, for each image. These values were found to be 6, 57 and 100 for the dark brown, Mediterranean and pale white phantoms, respectively. Figure 5.17 shows the segmented image of each phantom breast. The cup of the breasts, at the location of the left breast profile and right breast profile, has clearly been isolated from the background in each case. However, the actuator has been included within the cup of the breast.

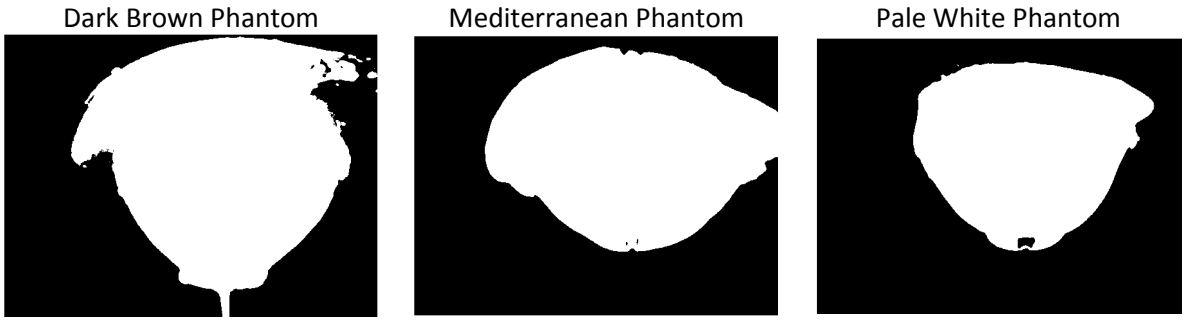

Figure 5.17: Segmented images with threshold values manually chosen

The segmented image in Figure 5.17 yields a strong edge between the breast cup and the surrounding image. Thus, any edge detection method, from Section5.4.4, can be applied to give a distinct edge. Figure 5.18 shows that clear edges have been produced for all phantom breasts.

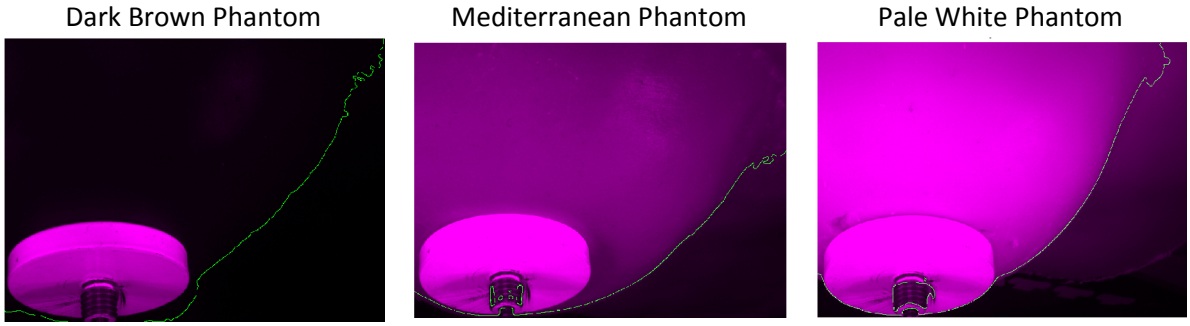

Figure 5.18: Resulting edges from segmented image overlaid on original images

Otsu's Method

While manually picking thresholding values gives accurate approximations of edge locations, this method requires user input for each tone of breast colour and reduces automation of the DIET system. Otsu's method can be utilized to determine threshold values methodologically. This histogram based method determines an optimum threshold value that maximizes the variance within an image intensity matrix. Otsu's method relies on the image histogram, explored in Section 5.4.1, exhibiting a bimodal pattern.

A built-in function in MATLAB, `graythresh`, takes an image as an input and gives an appropriate threshold value using Otsu's method. Using this function, threshold values were determined, as shown in Table 5.2, and compared against those found manually. The results show that the thresholds for the Mediterranean and pale white phantoms were the same, or similar, for both methods. The thresholds found for the Brown phantom was found to be considerably different. This is because the strongest bimodal relationship within the dark brown phantom image separates the actuator, rather than the cup of the breast, from the remainder of the image. If the actuator did not display such contrasting intensity, Otsu's method is likely to work for all images with more similar thresholds.

Table 5.2: Threshold values determined manually and with Otsu's method

	Brown	**Mediterranean**	**Pale White**
Iterative Method	6	57	100
Otsu's Method	91	57	98

One simple way to reduce the contrast between the breast cup and the actuator is to change the colour of the actuator. The internal walls of the DIET machine are matte black and early edge segmentation work showed that this background could be isolated from the phantom breast. Colouring the actuator matte black is likely to have a similar result. This theory has been examined by artificially changing the actuator colour, as shown in Figure 5.19. The actuators in the images have identical image intensities as the matte black background, as would occur with a matte black actuator.

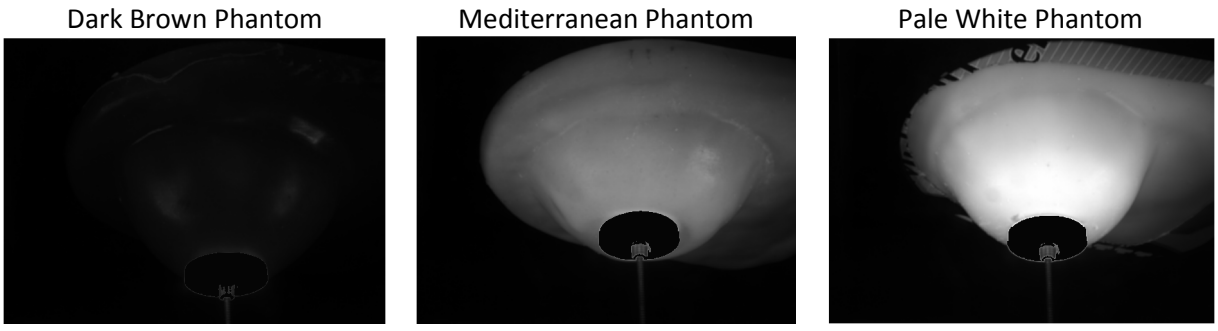

Figure 5.19: Images segmented after actuator colour artificially changed to black

Repeating Otsu's method on the images from Figure 5.19 gives the threshold values displayed in Table 5.3. These thresholds are much closer to the threshold values found iteratively, in comparison to when a white actuator was present. Using these threshold values gave clear indications of the edges, as can be seen in Figure 5.20.

Table 5.3: Threshold values determined manually and with Otsu's method after blackening the actuator

	Brown	Mediterranean	Pale White
Iterative Method	6	57	100
Otsu's Method	6	50	94

Figure 5.20: Resulting edges from segmented image overlaid on original images

Table 5.4: Outcome of edge detection test after blackening actuators and using Otsu's method, with green cells representing a successful edge detection of both edges within each image

View	Edge Detected		
	Dark Brown	Mediterranean	Pale White
View 1	Yes	Yes	Yes
View 2	Yes	Yes	Yes
View 3	Yes	Yes	Yes
View 4	Yes	Yes	Yes
View 5	Yes	Yes	Yes

This thresholding method, with blackened actuators, was carried out on all camera views with the results shown in Table 5.4. In all cases, the edges of the cup of the breasts were detected. By changing the DIET machine actuator colour to matte black and utilizing Otsu's method, the edges of the breasts can be detected without the need for manually thresholding each image. However, if it is not desirable to change the colour of the actuator, either the actuator colour could be artificially changed after detecting the actuator edge, or localised image segmentation could be implemented.

Localised Image Segmentation

All edge detection methods examined so far have examined the whole image. However, as was have discovered with the dark brown phantom, the colour of the actuator has a large impact on the colour intensity distribution across an image. One way to counter this is to change the colour of the actuator to the same colour as the internal structure of the DIET machine, matte black. However, this approach

may not be desirable, as it would be more difficult to locate it within the machine, which is especially important while manually adjusting the actuator location.

Another way to reduce the impact of the actuator is to analyse only portions of the image which do not have the actuator in it. This outcome can be achieved by cropping an image into three, as shown in Figure 5.21. This approach allows edge detection of the left and right breast profiles without needing to account for the image intensity of the actuator.

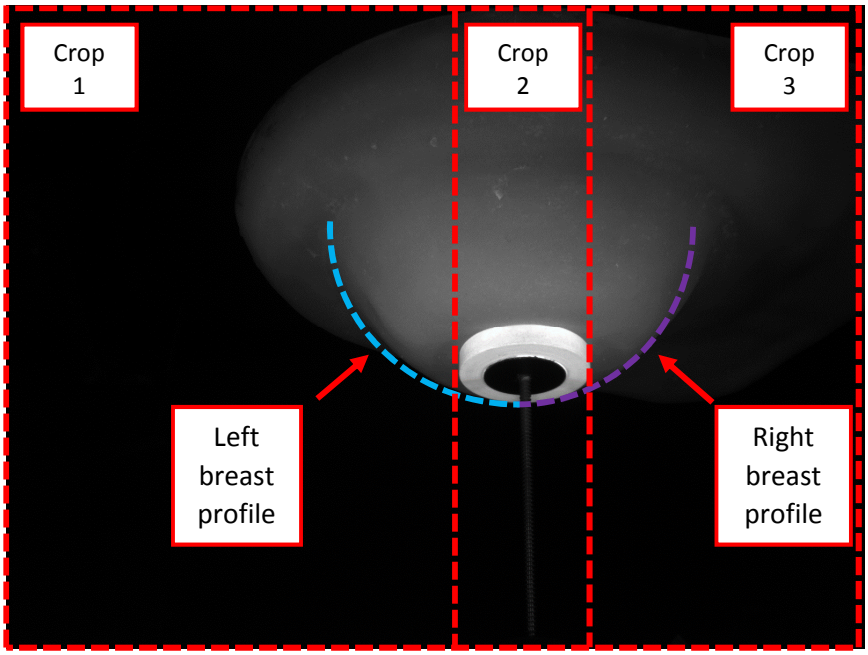

Figure 5.21: Camera 1 view of Mediterranean phantom broken into three images

Local image segmentation methods are more computationally expensive than previous segmentation methods. However, they give good segmentation results, while removing the need for user input. The first step required is to determine where the actuator is and to find the horizontal extents of the actuator. This task could be done manually, or with the use of markers. Second, the image must be cropped into the three regions from Figure 5.21. Following this step, threshold values of both the left and right cropped images will be determined using Otsu's method. Edges can then be detected using the MATLAB function `edge`. Finally, the cropped images can be overlaid onto the original image to determine whether an accurate image was detected. Figure 5.22 shows that this localised segmentation method has similar results to those found with manual thresholding and after blackening the actuator.

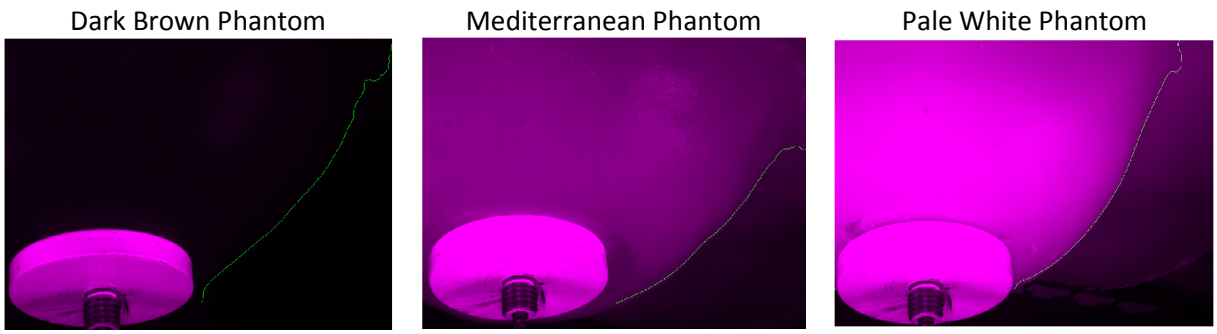

Figure 5.22: Results of localized image segmentation, with edge overlaid on original image

5.5 Limitations of Analysis

A number of methods discussed in this chapter accurately isolated the cup of the breast within an image. Edge detection could then be carried out which gave the left and right breast profile required to compute a 3-D model of the breast for vibration analysis. While these edges could be detected, the extent of the edge, which truly represents the cup of the breast, varied for each phantom colour. For each image, regardless of camera view or phantom colour, the exact location where the breast cup connects with the chest wall was not clearly defined. At this location, a shadow or imperfection is present. This shadow causes the segmentation of the image to not accurately represent the exact edge of the cup of the breast, as can be seen clearly in Figure 5.23 and is typical for all phantom colours. As this imperfection appears to be located at the limits of the cup of the breast, it is expected it will have little effect on the computational analysis of the images. However, this portion of edge will need to be removed, or interpolated and smoothed, before analysis takes place.

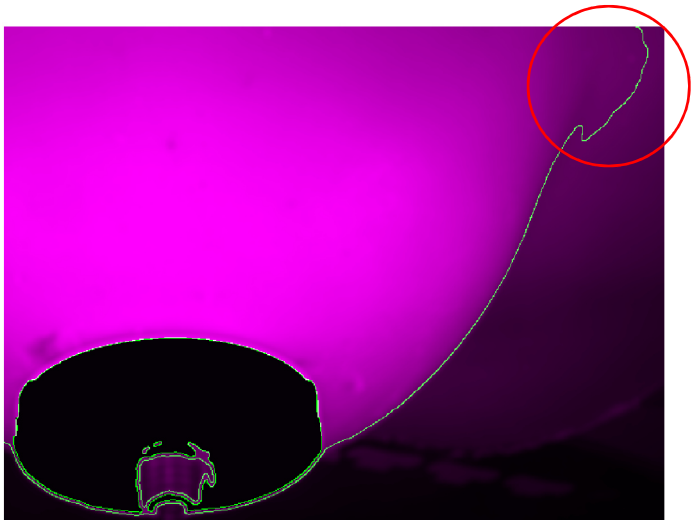

Figure 5.23: Pale white phantom with extent of edge shown. The red circle highlights where the detected edge no longer represents the true edge of the breast cup

The colour of the actuator was discussed throughout this chapter. The existing actuator is white, which is on the extreme end of the image intensity histogram. In cases, particularly with the dark brown skin, bimodal analysis of the images segmented the actuator, rather than the cup of the breast, from the remainder of the image. This outcome required a computationally expensive localised segmentation method before accurate edges could be determined. It has been recommended that the actuator colour be changed to matte black, to match the internal walls of the DIET system. This choice will result in a computationally simpler segmentation method.

During clinical trials on the DIET system, a woman pats talcum powers on the skin of her breast. This reduces the chance of reflection or glare being picked up on the image, which might occur due to reflections from natural moisture occurring on the skin. Talcum powder was also applied to phantom breasts prior to being tested in the DIET machine. This practice is important as glare in an image may be picked up as a false edge. However, care must be taken in evenly applying powder to the whole surface of the breast and chest that would be visible in screening.

The skin colour used for each phantom had very little change in colour across the surface of the breast. This similarity may not be the case on a human breasts due to moles, freckles or other skin imperfections that may be present. If this situation occurs, the segmentation methods discussed may incorrectly identify one of these skin imperfections as the edge of the breast. Filtering images prior to segmentation does reduce the chance of imperfections effecting the process. However, if large imperfections are present it may be necessary to take steps to reduce the impact they might have on the imaging software. These steps could include localised filtering around the location of the imperfection. Another method would be to reduce the visibility of the imperfection prior to screening.

The phantom breast colours chosen were based on the human skin tone spectrum, as discussed in Chapter 4. The three colours chosen was to represent skin at either end of the spectrum and one in the centre of the spectrum. As was experienced with the dark brown phantom, there was very little difference in image intensity between the edges of the cup of the breast and the matte black walls of the DIET machine. In some cases this made it difficult to accurately segment the image. If a breast was any darker than the dark brown phantom, it is likely that the segmentation methods discussed in this chapter would not work. This outcome is also expected if women who have skin lighter than the pale white phantom used the DIET machine. However, the issue would arise when segmenting the breast cup from the actuator. In these cases, it may be necessary to artificially lighten or darken the breast skin, with use of cosmetics, so that segmentation could occur. Equally, the interior colouring of the

DIET machine might be changed for different skin colours. This step may be required in the case of extremely dark or extremely light skin tones.

5.6 Summary

The opening hole of the DIET system has been changed to a shape that includes portions of a patient's chest wall as well as the cup of their breast. Phantom breasts have been produced, as described in Chapter 4, which represent the portion of chest expected to fit within the new opening. These phantom breasts were used in the existing machine and images obtained were analysed to determine the extent at which the cup of the breast could be isolated from the rest of the image.

Image segmentation methods were explored including edge detection methods and thresholding. Edge detection methods alone were not accurate in isolating the cup of the breast from the remainder of the image. However, when these methods were used in combination with region detection, clear and accurate edges could be determined.

Otsu's method was found to be useful when automating the segmentation process, which is desirable for processing many different images. However, the colour of the actuator meant that this method did not work with the dark brown phantom. Artificially changing the actuator to black, or analysing localised images of the breast edges, negated this issue. Thus, it is recommended that the actuator colour be changed to a matte black to reduce computational expense.

Other limitations discovered include the extent at which the breast cup ends was not well defined and image imperfections were found at these locations. In addition, natural skin imperfections and camera glare may result in false edges being detected. These issues could both be mitigated with the even application of powder to the skin prior to image testing. Finally, while care was taken to choose phantom breast colours which represented the extreme of human skin tones, there is a chance the DIET machine will be used by women with lighter or darker skin tones. These cases may require artificial lightening or darkening of the skin with use of cosmetics.

6. Manufacture

6.1 Introduction

Results from ergonomic trials, detailed in Chapter 3, indicate the most comfortable surface for the DIET system is the surface shown in Figure 6.1. This chapter explores the detailed design of the surface including exact dimensions, mechanical analysis of loading and material selection. Finally, a design specification with detailed drawings has been included so the surface can be manufactured when required.

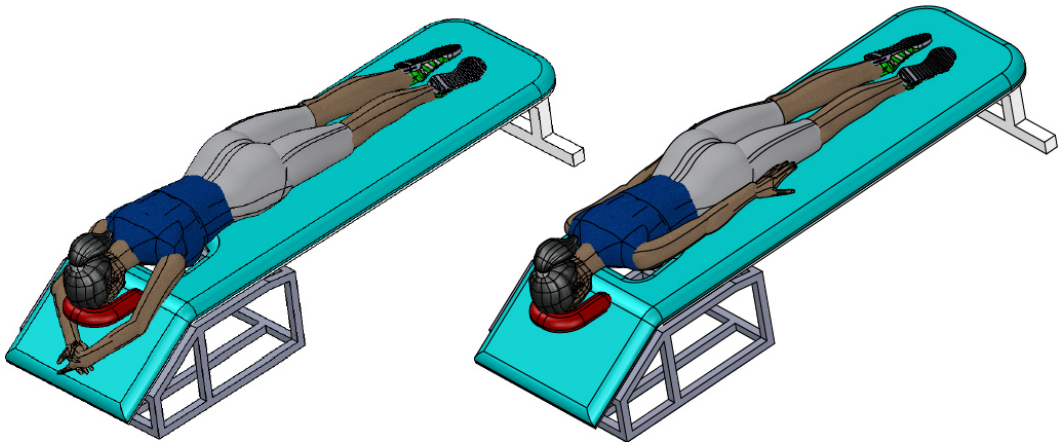

Figure 6.1: Proposed DIET surface showing both arm rest positions

6.2 Dimensions

6.2.1 Modular Design

Two designs have been examined: **1)** A modular design shown in Figure 6.2 that can be packed when not in use; and **2)** A simple surface that does not collapse, as shown in Figure 6.3. The obvious benefit of the modular surface is it will be simpler to store when not in use, and the system will thus be portable and more easily accessible. However, a modular design is it is more expensive to manufacture due to the additional parts needed for connection. Additionally, portability could have the unintended consequence of damaging the expensive internal components within the DIET shell, thus requiring more robust internal componentry.

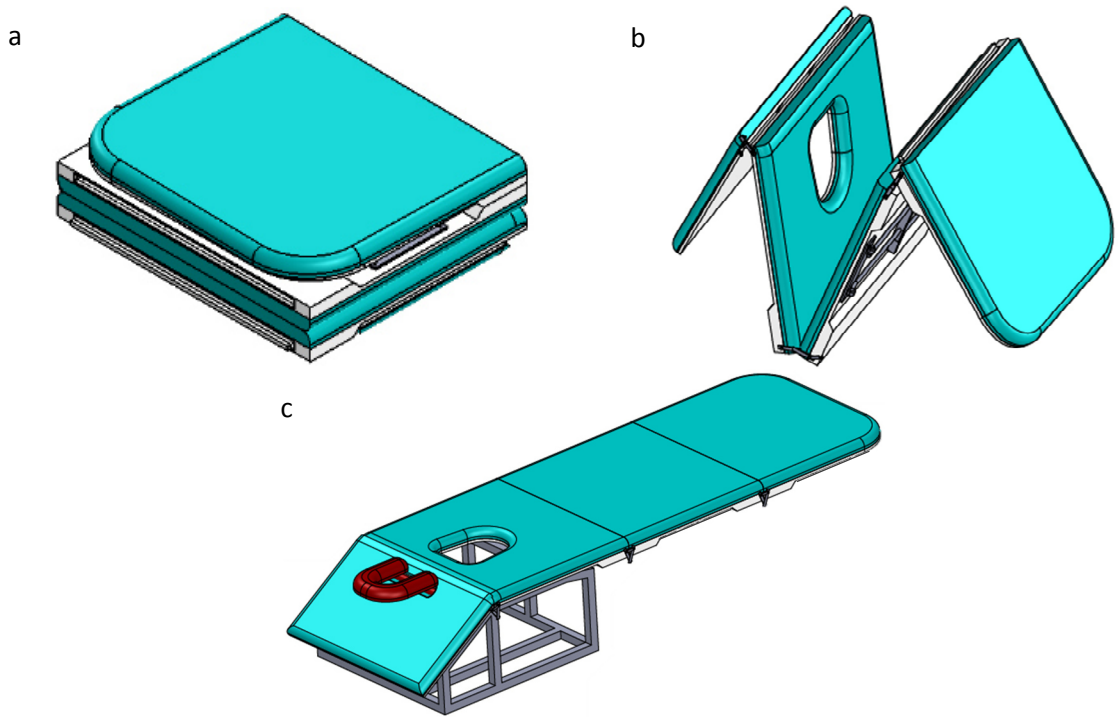

Figure 6.2: Modular surface design: a) Collapsed, b) Assembly step, and c) Assembled surface with DIET machine shell and head rest (legs of surface not shown)

A benefit of the simple, fixed surface in Figure 6.3, is there are no folding grooves along the surface, as there are in the modular surface, which may cause unintended discomfort. These grooves are necessary as folding the surface across its length, as in Figure 6.2, enables a small enough table to be carried. Data collected from the ergonomic trial indicated any gap in a surface may cause discomfort to a user. Thus, at this stage, the simple surface will be developed further. However, a modular option could be reviewed later in the development of the machine if this option becomes desired.

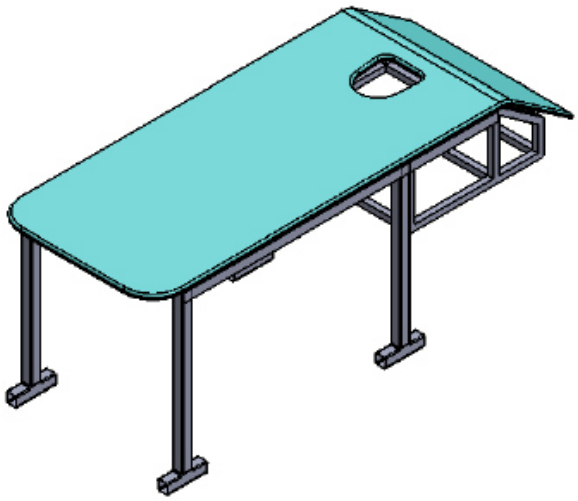

Figure 6.3: Simple surface which cannot collapse

6.2.2 Overall Dimensions

The dimensions of the surface of the DIET system must be large enough to accommodate up to a 95th percentile female, while also allowing the surface to be transported through hospital facilities without requiring complicated disassembly. Existing medical surfaces, where people lie either prone or supine, have been examined. The dimensions of each of these surfaces are shown in Table 6.1.

Table 6.1: Examples of medical surfaces with dimensions (Brewer, 2016; Inc., 2016; Lift, 2016; Oakworks Medical, 2016; Stryker, 2009)

Name	Photo	Dimensions (mm) Length	Width	Height
Howard Wright - M7 Examination Couch General purpose treatment and minor procedures (supine position)		2000	650	850
Stryker - Performance-PRO XT Transportation of patients into / out of emergency vehicles.		1970	560	330 – 1000*
Clinton Industries Inc - Treatment table General purpose treatment and minor procedures (supine position)		1830	700	800

Name	Photo	Dimensions (mm) Length	Width	Height
Brewer Element - Treatment Table General purpose treatment and minor procedures (supine position)		1880	700	800
Oakworks - DTPM300 Imagine Table Used for diagnostic imaging. Table top is electronically height adjustable		1980	610	610 – 1020*
Bailey Manufacturing Company - Space Saver Medical Examination Table General purpose treatment and minor procedures (supine position)		1320 – 1830*	610	770

Name	Photo	Dimensions (mm) Length	Width	Height
Hausnamm Industries - Econo-Line Power Clinic Examination Table General purpose treatment and minor procedures (supine position)		1420 – 1880*	690	610 – 890*
OakWorks Medical - PX100 Series Exam Table General purpose treatment and minor procedures (supine position)		1850	790	460 – 890*
Adapta - Summit 3 – Section Treatment Platform General purpose treatment and minor procedures (prone position)		2010	710	460 – 940*

*Changes dimensions depending on use

Table 6.2 summarises the surface dimensions examined and is used as a guide for finalising the dimensions of the DIET surface. In addition, the width of the existing DIET machine is constrained to a minimum of 800mm to allow for the internal components. Figure 6.4 shows the overall dimensions chosen for the DIET surface.

Table 6.2: Range of dimensions for examined medical surfaces

	Length (mm)	Width (mm)	Height (mm)
Minimum	1320	560	330
Maximum	2010	790	1020
Average	1815	670	745

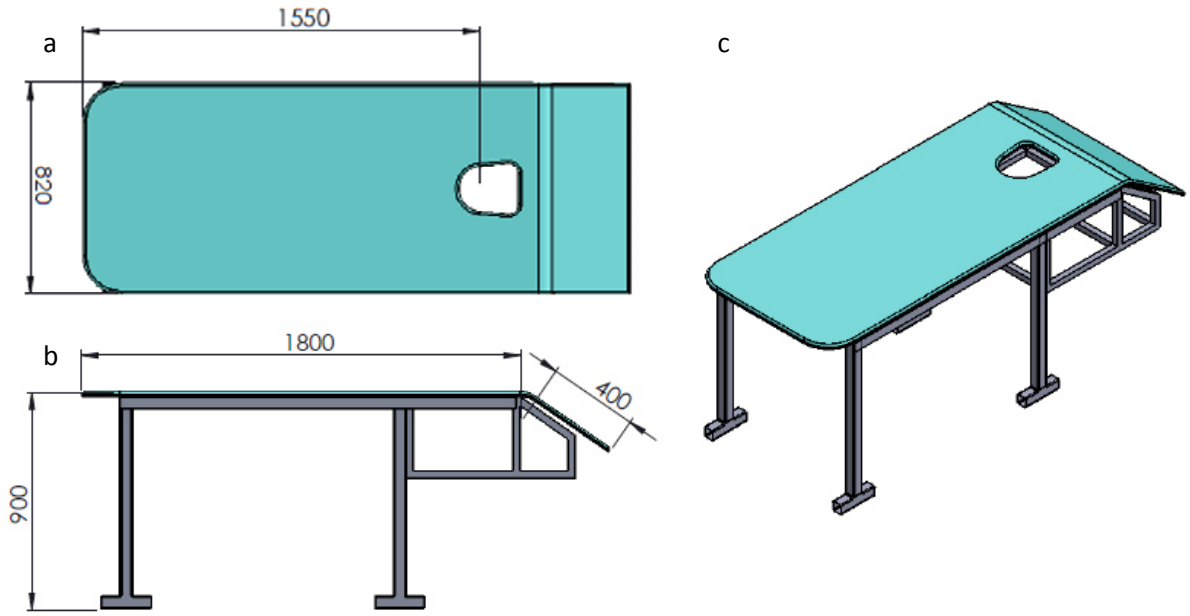

Figure 6.4: Overall dimensions of DIET surface: a) Top View, b) Side View, and c) Isometric View

6.3 Material Selection

A depiction of the proposed DIET surface is shown in Figure 6.5, with all parts labelled. A material has been chosen for each portion of the surface, aside from the DIET shell and internal components, following a mechanical loading analysis. A price comparison has also been carried out for each material.

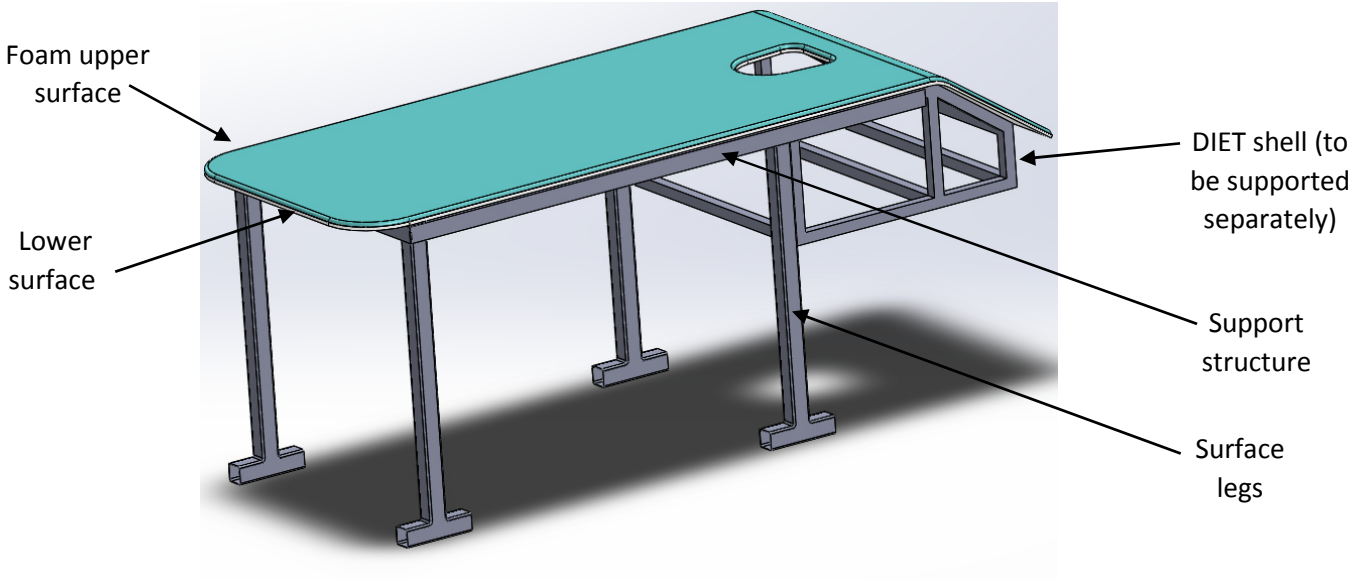

Figure 6.5: Proposed DIET Surface

6.3.1 Mechanical Load Analysis

A shear force and bending moment analysis calculates the maximum forces and moments expected to be experienced on the surface of the DIET machine. A worst case loading situation is used in this study. A simplified free body diagram (FBD) of the system is depicted in Figure 6.6.

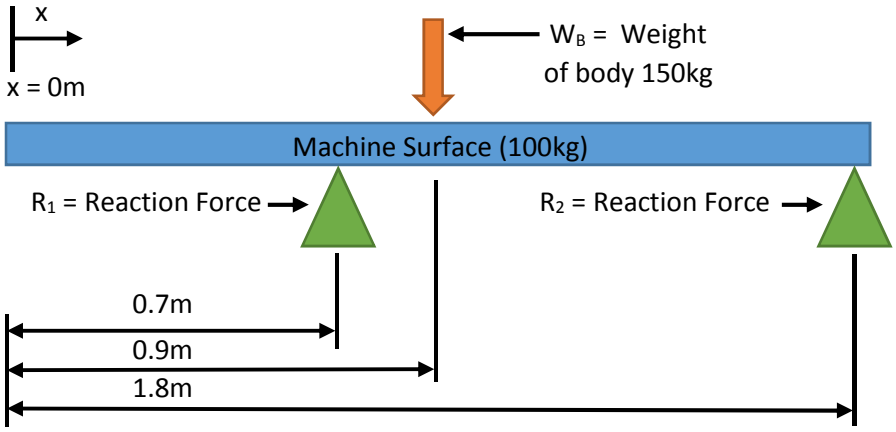

Figure 6.6: Free body diagram of DIET surface

Seven main assumptions have been made for this analysis. All assumptions are designed for the loading case to give a conservative estimate of the loading conditions. The specific assumptions are defined:

- **Assumption 1:** The weight of the body is represented as a point load in the centre (lengthwise) of the surface. Ordinarily, a woman would lie face down and her weight would be relatively evenly distributed along the length of her body. However, this FBD represents a worst case analysis. Such a point load may occur if a woman were to sit / stand on the surface or press into the surface while mounting / dismounting.
- **Assumption 2:** The weight of the body, 150kg, has been chosen as this represents a worst case loading situation. The average weight of women in New Zealand is 74.4 kg ("nzhs-2014-adults-health-status-behaviours-risk-factors-dec10," n.d.), and that figure is increasing annually (The Ministry of Health, 2009). Approximately 6% of the female population is classified as being extremely obese, with a body mass index (BMI) greater than 40kg/m^2 (Sharpe & Bradburuy, 2015). This BMI would correspond to a weight of approximately 110kg, based on an average height of 1.625m ("nzhs-2014-adults-health-status-behaviours-risk-factors-dec10," n.d.). Thus, a weight double that of the average, and much greater than 110kg, was chosen to represent a worst case loading situation.

- **Assumption 3:** The weight of the machine is not taken into account in this analysis. The machine will not be supported by the surface due to the expensive equipment inside and because the machine components require a solid base to absorb machine vibrations.
- **Assumption 4:** The legs of the surface are the only reaction forces. In reality, the machine's support base is likely to take a portion of the load. This worst case analysis examines a case when a woman lies / sits / presses onto the surface when the machine is not located directly below the surface. This case is likely to occur if further ergonomic testing on the surface is carried out.
- **Assumption 5:** The weight of the surface of the machine has been over-estimated to be 100kg. The materials of the surface have not yet been decided. This value gives a worst case condition as it is expected that the true surface weight should not exceed 50kg.
- **Assumption 6:** The arm ramp / head rest has not been analysed as there are no major loading forces acting in these locations.
- **Assumption 7:** The worst case loading situation is in the lengthwise direction. This assumption is justified as the distance between the support legs in the x-direction is greater than the width of the DIET surface and thus bending moments would be greater in the x-direction.

Figure 6.7 shows the shear force and bending moment diagram for the loading case of the DIET surface. Table 6.3 summarizes key parameters from the findings. The values from Table 6.3 have been used when assessing different geometries and materials for varying parts of the surface.

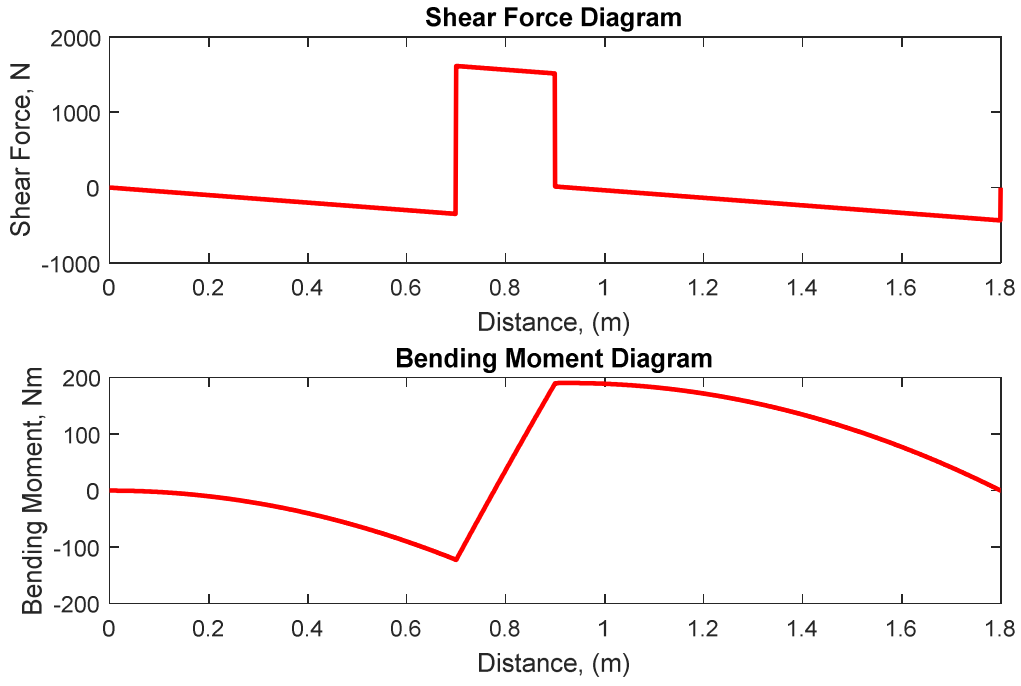

Figure 6.7: Shear force (above) and bending moment diagram (below) for DIET surface

Table 6.3: Summary of shear and bending moment analysis

Parameter	Value	Unit
Reaction force (R_1)	1,964	N
Reaction force (R_2)	436	N
Maximum Shear Force	1,614	N
Maximum Bending Moment	190	Nm

Four materials have been examined in the analysis of the stresses experienced on the DIET surface: 1) Acrylic; 2) Aluminium; 3) Steel; and 4) Stainless Steel. Materials have been assessed for the following three portions of the DIET surface: 1) The flat support surface; 2) The support structure; and 3) The support legs. A summary of the relevant material properties of each of the materials is listed in Table 6.4.

Table 6.4: Properties of Materials Analysed (CYRO, n.d.) (Kaysons, n.d.) (Beer, Johnston, DeWolf, & Mazurek, 2012)

Material	Fatigue Limit [MPa]	Elastic Modulus [GPa]	Density [kg/m^3]
Acrylic	10.4$^+$	3.2	1160
Aluminium	130	69	2800
Steel	270*	200	7800
Stainless Steel	290*	180	8000*

*Values chosen conservatively as heat treatment or other processes can improve the material properties of steel.
$^+$Recommended stress limit due to stress crazing (CYRO, n.d.).

6.3.2 Flat Surface Stresses

Three materials have been analysed to determine the most appropriate for use as the flat surface shown in Figure 6.8. A requirement for the flat surface is for the material to be lightweight, and easy to manufacture and clean. In addition, the bottom surface of the flat surface cannot be glossy as it will affect the optics of the system. Finally, the flat surface should be as thin as practically possible to optimise the scope of breast capture during imaging.

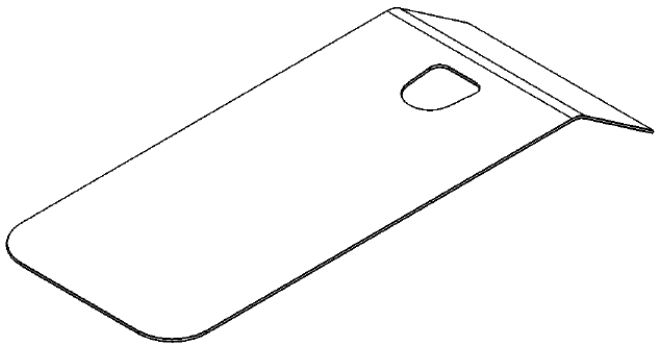

Figure 6.8: Flat surface

The three materials analysed for the flat surface are described:

- **Acrylic:** The existing DIET machine and surface uses a black acrylic surface. The material is low-cost, easy to source and manufacture, and lightweight. In addition, acrylic sheets can be ordered in matte finish, which removes the material's reflectivity. Acrylic material is less strong and more brittle than the other materials.
- **Aluminium:** Sheet aluminium is easy to source and manufacture. It is heavier than acrylic, but much lighter than steel. The material has ideal strength to weight ratios and exhibits elastic material properties. Aluminium sheet can be anodised to give a matte finish.
- **Stainless Steel:** Sheet stainless steel is the heaviest material, but also the strongest. The material is also easy to source and manufacture. Steel can be heat treated to give a matte finish(Cochrane & Henzel, 2005).

A simple shear and bending stress calculation is defined:

$$\sigma_{bending} = \frac{M * y}{I} \quad \text{(Eq. 6.1)}$$

$$y = \frac{thickness}{2} \quad \text{(Eq. 6.2)}$$

$$I = \frac{width * thickness^3}{12} \quad \text{(Eq. 6.3)}$$

Where M is the maximum bending moment, $\sigma_{bending}$ is the maximum bending stress, y is the distance from the centroid to the outer fibre and I is the moment of inertia of the cross section of the surface. Factors of safety, FOS, have been determined:

$$FOS = \frac{\sigma_{bending}}{\sigma_F} \quad \text{(Eq. 6.4)}$$

Where σ_F is the fatigue limit of the materials as per Table 6.4. Materials were assessed at varying thicknesses and all results are summarised in Table 6.5. Weight values exceeding 50kg have been highlighted, along with materials without factors or safety greater than 1.0. These highlighted materials are not appropriate for use at that thickness.

Table 6.5: Summary of Analysis of Surface Support

Thickness [mm]	Material	Weight [kg]	Factor of Safety
15	Acrylic	25.7	1.7
	Aluminium	62.0	21.0
	Stainless Steel	177.1	46.8
10	Acrylic	17.2	0.8
	Aluminium	41.3	9.3
	Stainless Steel	118.1	20.8
8	Acrylic	13.7	0.48
	Aluminium	33.1	6.0
	Stainless Steel	94.5	13.3
6	Acrylic	10.3	0.27
	Aluminium	24.8	3.4
	Stainless Steel	70.8	7.5
4	Acrylic	6.9	0.1
	Aluminium	16.5	1.5
	Stainless Steel	47.2	3.3

Local suppliers and manufacturers have been approached to provide quotes on the materials analysed. Table 6.6 lists the cost of each material from a range of suppliers. At least two companies have been approached for each material.

Table 6.6: Material cost for flat surface

Material (thickness)	Company[+]	Quote [NZD exc. GST]
Acrylic (15mm)	BNT Plastics	$265*
	Mulford Plastics	$490
	Award Plastics	$510
Aluminium (5mm)	Ullrich Aluminium	$307
	Autobend	$261.23
Stainless Steel (4mm)	HI-TECH Sheetmetals	$688.00
	Autobend	$563.52

[+]All companies are located in Christchurch, New Zealand
*Excludes machining costs

Following a mechanical and cost analysis of the flat surface, 5mm aluminium sheet is recommended as the material of choice. The acrylic material needs to be 15mm thick before it can be considered safe enough to withstand a worst case load. This thickness is considered too thick and risks restricting the imaging depth of the breast. The 4mm stainless steel flat surface is almost 50 kg, which would make moving the surface around difficult. For these reasons, a 5mm aluminium surface is recommended.

6.3.3 Support Structure Stresses

Two metals have been analysed to determine which material shall be used for the support structure, as shown in Figure 6.9. The support structure needs to be strong and lightweight as it will take the majority of the load, while supporting the flat surface and the patient. Finally, the support structure needs to have materials easy to source and machine. Extruded angles, shown in Figure 6.9 (b), have been chosen as the type of bar to be used for the structure. This choice of shape optimises the rigidity to weight ratio in comparison to a rectangular hollow section. In addition, connections between extruded sections are simpler than connections between I-beams or channels. Plates are used to connect the extruded angles and fixed with M8 bolts. These bolts have a minimum breaking load of 8kN (Shank, n.d.), giving a factor of safety of 5.0.

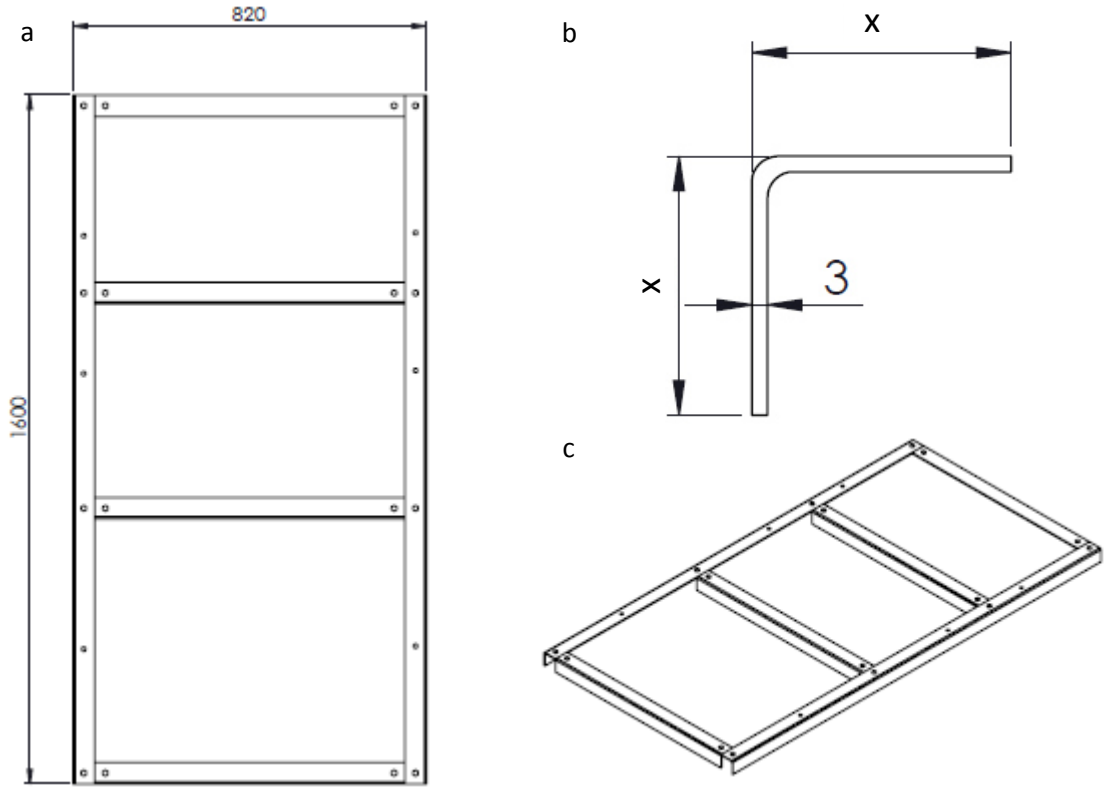

Figure 6.9: Support structure: a) Top View with overall dimensions, b) Section View of extruded angle with x representing the length of the side, and c) Isometric View

Due to holes being drilled into the extruded angles, stress concentrations must be considered when assessing mechanical suitability of the materials. The major stresses acting on the support structure are due to bending moments. The appropriate stress concentration factor for this case is for a central single circular hole with a finite-width plate, as shown in Figure 6.10 (Young & Budynas, 2002). While

the structure is made from extruded angle, rather than a flat plate, the factor for a plate is suitable to apply. The stress concentration factor, K_t, can be calculated:

$$K_t = \left[1.793 + \frac{0.131}{\frac{d}{h}} + \frac{2.052}{\left(\frac{d}{h}\right)^2} - \frac{1.019}{\left(\frac{d}{h}\right)^3}\right] * \left[1 - 1.04\left(\frac{d}{b}\right) + 1.22\left(\frac{d}{b}\right)^2\right] \quad \text{(Eq. 6.5)}$$

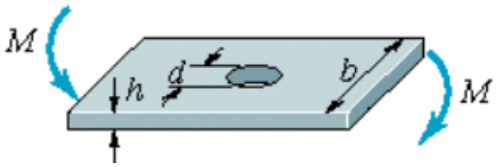

Figure 6.10: Transverse bending for a plate with a hole (Young & Budynas, 2002)

A detailed diagram of the cross sectional area of the extruded angle is depicted in Figure 6.11. Because of the more complicated cross section, the cross section has been divided into two areas, A1 and A2. The moment of inertia has been calculated using the parallel axis theorem, where y_1 and y_2 are the distance for the centroid of A1 and A2, respectively, from the origin, in Figure 6.11. The moments of inertia can be calculated:

$$A1 = h * (b - d) \quad \text{(Eq. 6.6)}$$

$$A2 = h * (b - h) \quad \text{(Eq. 6.7)}$$

$$y_1 = \frac{h}{2} \quad \text{(Eq. 6.8)}$$

$$y_2 = \frac{(b - h)}{2} + h \quad \text{(Eq. 6.9)}$$

$$y = \frac{y_1 + y_2}{A1 + A2} \quad \text{(Eq. 6.10)}$$

$$y_{max} = b - y \quad \text{(Eq. 6.11)}$$

$$I_1 = \frac{(b - d) * h^3}{12} + A1 * y_1^2 \quad \text{(Eq. 6.12)}$$

$$I_2 = \frac{h * (b - h)^3}{12} + A2 * y_2^2 \quad \text{(Eq. 6.13)}$$

$$I = I_1 + I_2 \quad \text{(Eq. 6.14)}$$

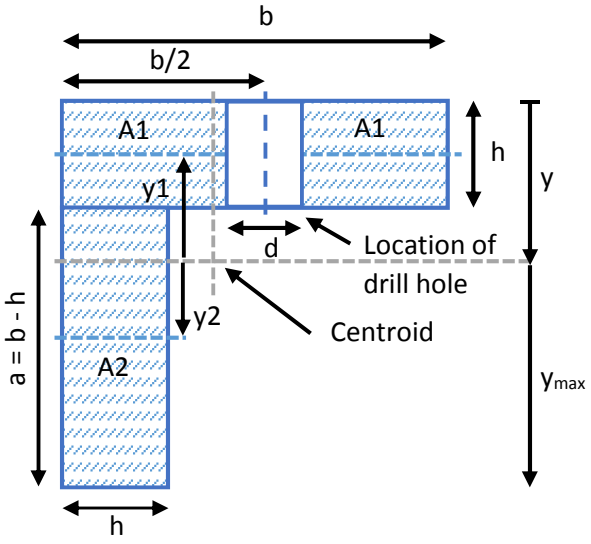

Figure 6.11: Cross section of extruded angle

Shear stresses, due to bending have been determined:

$$\sigma_{bending} = \frac{\left(\frac{M * y_{max}}{I}\right)}{2} \quad \text{(Eq. 6.15)}$$

$$\sigma_{max} = K_t * \sigma_{bending} \quad \text{(Eq. 6.16)}$$

$$FOS = \frac{\sigma_{max}}{\sigma_F} \quad \text{(Eq. 6.17)}$$

Where M is the maximum bending moment, $\sigma_{bending}$ is the maximum bending stress, y is the distance from the centroid to the outer fibre and I is the moment of inertia of the cross section of the surface. Factors of safety have been determined, where σ_F is the fatigue limit of the materials as per Table 6.4.

Materials were assessed at varying width, *b*, and all results are summarised in Table 6.7. Materials without factors or safety greater than 1.0 have been highlighted, as they are considered not suitable. All parts had a reasonable weight suitable for moving the surface around.

Table 6.7: Summary of Analysis of Support Structure

Size of b [mm]	Material	Weight [kg]	Factor of Safety
50	Aluminium	5.5	2.7
	Steel	15.4	5.6
40	Aluminium	4.4	1.8
	Steel	12.3	3.8
30	Aluminium	3.3	1.1
	Steel	9.1	2.3
20	Aluminium	2.1	0.5
	Steel	5.9	1.1

Local suppliers have been approached for quotes on the support structure. Table 6.8 summarises the costs expected for the support structure. These costs include materials only, and do not include any machining required, such as the inclusion of drill holes. Machining and assembly would add cost.

Table 6.8: Material cost for support structure

Material (width)	Company[+]	Quote [NZD exc. GST]
Aluminium (50mm)	Inex Metals	$132.09
	Wakefield Metals	$148.39
Steel (50mm)	Wakefield Metals	$209.00
	Steel & Tube	$219.00

[+]All companies are located in Christchurch, New Zealand
*Excludes machining costs

The mechanical analysis of the support structure showed both aluminium and steel angled extrusions are capable of supporting worst case loading conditions providing the extrusions are large enough. As the price of the material does not significantly vary, the 50mm aluminium extrusions are recommended for this portion of the surface. These extrusions give an appropriate factor of safety with a weight a third that of steel.

6.3.4 Leg Stresses

Two materials have been analysed to determine which material should be used for the support legs of the surface, as shown in Figure 6.12. The support legs need to be strong and resist buckling from compressive loads. In addition, the support structure needs to have materials easy to source and machine. Square hollow sections have been chosen for this application as they have good strength to weight ratios and are easy to work with in combination with extruded angles. The square hollow sections connect to the support structure via M8 bolts.

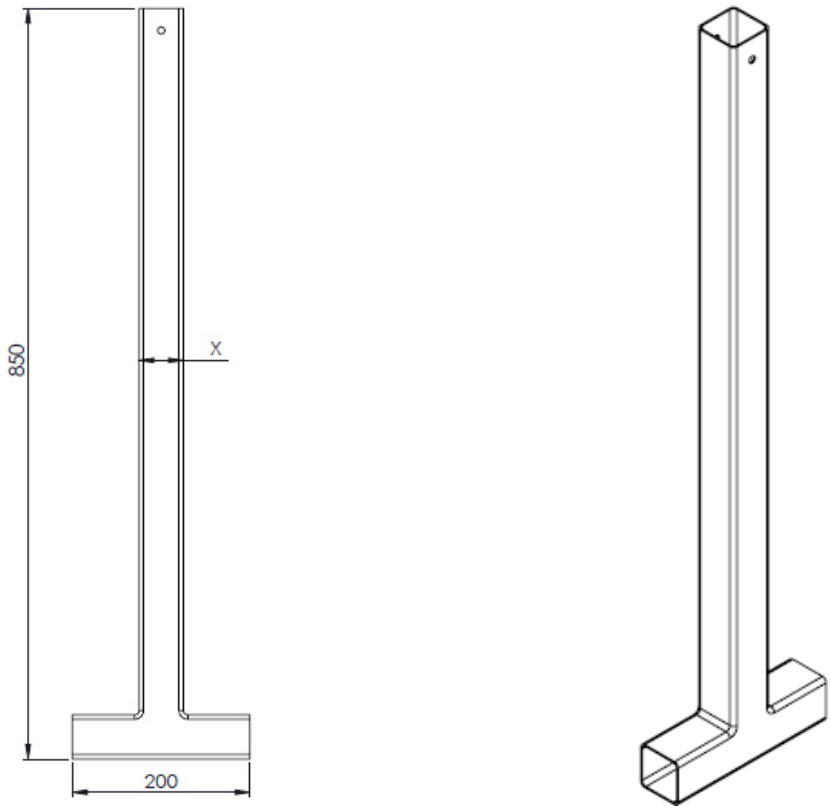

Figure 6.12: Support legs: a) Side View with dimensions, where x represents the width of the square hollow section, and b) Isometric View

Stress concentrations must also be determined for the mechanical analysis of the support legs, due to the holes drilled in for connections. The major stress acting on the legs is axial stress from compression and bending stressed caused by the bending moment indicated in Table 6.3. The stress concentration factor appropriate for the buckling case is a central single circular hole in finite-width plate, as shown in Figure 6.13. The stress concentration, K_a, required for the bending moment is identical to that used in the analysis of the support structure, and is defined:

$$K_a = 3 - 3.14\left(\frac{d}{b}\right) + 3.667\left(\frac{d}{b}\right)^2 - 1.527\left(\frac{d}{b}\right)^3 \quad \text{(Eq. 6.18)}$$

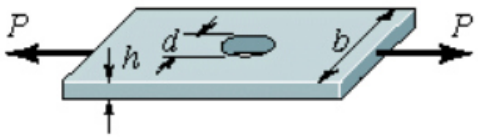

Figure 6.13: Central single circular hole in finite-width plate

The cross sectional area of the square hollow section is depicted in Figure 6.14, which includes key dimensions. The cross section has been broken into two sections for calculation of the second moment of inertia, I, calculated using the parallel axis theorem. Since the shape is vertically symmetric about the center of the drill holes, the moment of inertia has been calculated once for the top half and then doubled, for simplicity, where y_1 and y_2 are the distance for the centroid of A1 and A2, respectively, from the line of symmetry. These values are thus calculated:

$$c = \frac{b-d}{2} - h \quad \text{(Eq. 6.19)}$$

$$A1 = h * c \quad \text{(Eq. 6.20)}$$

$$A2 = h * b \quad \text{(Eq. 6.21)}$$

$$y_1 = \frac{c+d}{2} \quad \text{(Eq. 6.22)}$$

$$y_2 = \frac{b-h}{2} \quad \text{(Eq. 6.23)}$$

$$I_1 = \frac{2 * h * c^3}{12} + A1 * y_1^2 \quad \text{(Eq. 6.24)}$$

$$I_2 = \frac{b * h^3}{12} + A2 * y_2^2 \quad \text{(Eq. 6.25)}$$

$$I = 2 * (I_1 + I_2) \quad \text{(Eq. 6.26)}$$

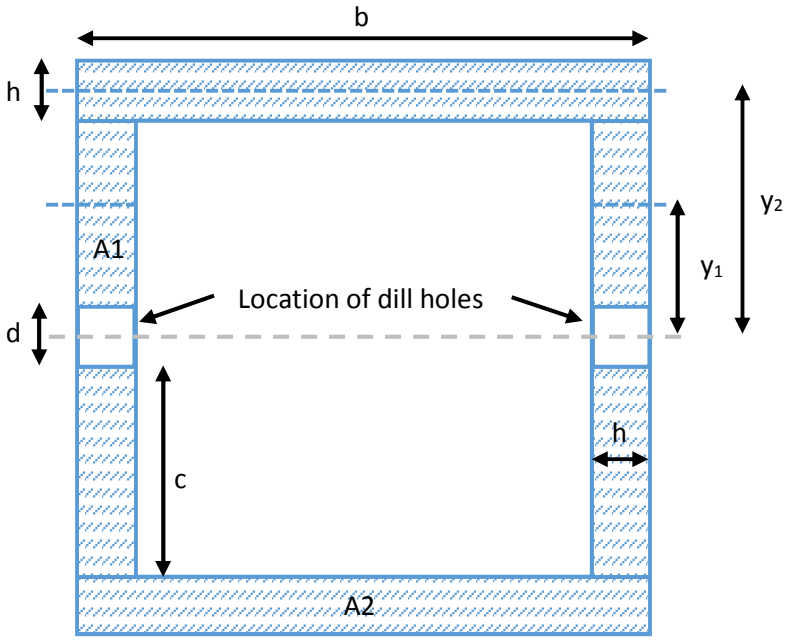

Figure 6.14: Cross section of square hollow section with key dimensions

Critical buckling forces, due to weight loading, have been determined:

$$F_C = \frac{\pi^2 * E * I}{(K * L)^2} \quad \text{(Eq. 6.27)}$$

$$F_{max} = K_a * \frac{R_{max}}{2} \quad \text{(Eq. 6.28)}$$

$$FOS_{buckling} = \frac{F_c}{F_{max}} \quad \text{(Eq. 6.29)}$$

$$\sigma_{bending} = \frac{\left(\frac{M(R_1) * y}{I}\right)}{2} \quad \text{(Eq. 6.30)}$$

$$\sigma_{max} = K_t * \sigma_{bending} \quad \text{(Eq. 6.31)}$$

$$FOS_{bending} = \frac{\sigma_{max}}{\sigma_F} \quad \text{(Eq. 6.32)}$$

Where E is the material's elastic modulus, L is the height of the support leg, and K is the column effective length factor. The effective length factor was chosen as 2 to represent one fixed end and one end free to move laterally. This factor was chosen as a conservative approach, as there is a chance the surface could be on wheels. Factors of safety have also been determined, where R_{max} is the maximum reaction force as summarised in Table 6.3 combined weight of the surface and the patient. A stress analysis has been carried out on the support legs due to the moment caused by the weight of the surface and patient. Equations 6.30 – 6.32 describe the stress analysis where $M(R_1)$ is the moment acting on the support R_1 from Figure 6.7. All findings from this analysis are summarised in Table 6.9. Materials with factors of safety less than one have been highlighted as inappropriate. Note that for all width sizes, *b*, investigated, the thickness, *h*, of the square hollow section remained at 1.6mm, which is a standard thickness.

Table 6.9: Summary of Analysis of Surface Legs

Size of b (mm)	Material	Weight [kg]	Factor of Safety (Buckling)	Factor of Safety (Bending Moment)
50	Aluminium	3.5	17.4	2.8
	Steel	9.7	50.3	5.8
40	Aluminium	2.8	8.7	1.8
	Steel	7.8	25.0	3.7
30	Aluminium	2.0	3.5	1.0
	Steel	5.7	10.0	2.1
20	Aluminium	1.3	0.9	0.4
	Steel	3.7	2.6	0.8

Local suppliers have been approached to supply quotes for aluminium and steel square hollow sections. A summary of these quotes is included in Table 6.10. Note that these quotes are of the raw material only, and do not include any additional machining or assembly required.

Table 6.10: Material cost for support structure

Material (width)	Company[+]	Quote [NZD exc. GST]
Aluminium (50mm)	Inex Metals	$70.21
	Wakefield Metals	$108.00
Steel (50mm)	Wakefield Metals	$140.00
	Steel & Tube	$124.60

[+]All companies are located in Christchurch, New Zealand
*Excludes machining costs

Both aluminium and steel square hollow sections were found to withstand worst case compressive and bending forces if they were large enough. The cost of both materials were not significantly different and so the lighter aluminium material was chosen to produce the support legs. At a width of 50mm and thickness of 1.6mm, the factor of safety is appropriate for use while the weight of the legs is minimised.

6.3.5 Top Surface Material Selection

The material of the top surface has to be soft for comfort, and also easily and effectively cleaned for hygiene. The material must also be capable of attaching to the flat aluminium surface and preferably supplied locally. Two companies, Nexus (Christchurch, New Zealand) and ACMA (Wellington, New Zealand), have been contacted who supply foam. Both companies produce foam for use in the medical industry or the food processing industry, and they are thus familiar with the standards required.

1.3.5.1 ACMA Foams

Among other work, ACMA foams work alongside manufactures of hospital beds to produce bed-end grab-handles and bed bumpers / pads. ACMA specialise in making integral skin foam, as shown in Figure 6.15. This self-skinning foam can be moulded over metal or plastic inserts. The foam used is a closed cell foam with very similar material properties to the EvaDura foam supplied by Nexus Foams. The advantage of this method of manufacture is the edges of the parts produced are cushioned. In addition, the foam has a strong bond with the insert, and is thus durable.

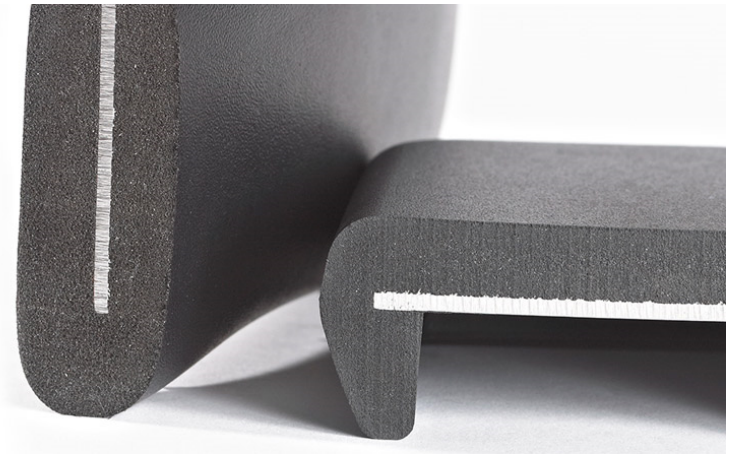

Figure 6.15: Integral skin foam (ACMA(ACMA Industries, 2016), Wellington, New Zealand)

The cost to produce a surface with integral foam has been quoted at $99 plus between $3,000 and $4,000 for initial tooling. Due to the large starting costs, this option will not be utilised immediately. However, if the DIET project becomes commercially viable, where machines will be produced in bulk, this method should be explored further.

1.3.5.2 Nexus Foams

Nexus suggested three types of foam which would be suitable for the DIET surface. One material, HR360-160PL, is an open cell foam, which is less dense and would require additional upholstery to make the material cleanable. The HR360-160PL material is commonly used for applications such as padding for bus seating or cushioning for furniture. The two other materials, EvaDure and KXNitrile, are closed cell. Material properties and cost of each material have been summarised in Table 6.11.

Samples of each foam were provided from Nexus and these have been evaluated with Tiro Medical, the company who is commercialising the DIET system. The open cell, HR360-160PL, foam is required to be at least 30mm thick before it provides the required comfort. Conversely, the two closed cell materials only need to be 10mm. A thick foam material may lead to less of the breast tissue being imaged during operation of the DIET system. The KXNitrile material was thus identified as the most comfortable feeling foam, followed closely by the EvaDura foam. However, the KXNitrile material permanently deforms if an object is placed on top of it, while the Eva Dura foam does not. This situation may occur on the DIET system, particularly when the surface is being stored. Such deformation would cause grooves along the surface and may be a cause of discomfort. For this reason, the EvaDura foam is the preferred foam from the samples provided by Nexus.

Table 6.11: Material properties of materials from Nexus Foam

Material	Foam Type	Density (kg/m^3)	Tensile Strength (kPa)	Elongation (%)	Cost (NZD ex GST and Deliver)
HR360-160PL	Open cell	36	50	90	$72.93
EvaDure	Closed cell	30	270	250	$89.93
KXNitrile	Closed cell	42	310	16 – 25	$109.47

The existing DIET surface is covered by 5mm EvaDura foam. No particular issues, such as permanent deformation, have been observed while using this foam in clinical trials. However, to mitigate discomfort in knees and hips caused by pressing on a hard surface, a 10mm thickness will be used.

6.4 Design Specification

Tiro Medical is a start-up company based in Christchurch, New Zealand working on obtaining the regulatory and reimbursement approval required to commercialise the DIET system, both domestically and internationally. Tiro Medical are also making ongoing advancements to the imaging components of the system. As a result of these changes, the dimensions of the shell are continuously changing. For these reasons, Tiro Medical have requested a design specification for the DIET surface, rather than a manufactured product. The design specification can be referred to and modified, if necessary, once a final machine shell has been designed. A surface compatible with the dimensions of the DIET machine shell can then be produced and used in future clinical trials.

6.4.1 Drawing Specifications

Drawings have been produced which detail all dimensions and materials required to produce the DIET surface. Due to ongoing improvements to the DIET system, some dimensions of the DIET surface are dependent on the final dimensions of the DIET machine shell. All of the variable dimensions have been clearly annotated on drawings. All drawings have been included in Appendix C.

6.5 Summary

Details of the surface of the machine required for manufacture have been determined. This specification includes the dimensions of the surface, as well as the materials chosen. Finally, a design specification has been prepared for the manufacture of the surface when it is required.

The dimensions of the surface were constrained by the dimensions of the shell of the DIET system and also the dimensions of a 95th percentile female body. To confirm the overall dimensions of the DIET surface, various existing medical surfaces were examined and their dimensions summarised. These values were used as a guide when selecting the overall dimensions of the DIET surface.

A mechanical loading analysis was carried out for each of the load bearing parts of the DIET surface. Alongside this, quotes for each material was requested from local suppliers. In addition, various types of foam were investigated for the top surface. A summary of all materials recommended for the DIET surface is summarised in Table 6.12.

Table 6.12: Summary of material recommended for the DIET surface

Surface Part	Recommended Material	Recommended Dimensions	Expected Cost (NZD, ex GST & Shipping)*
Flat Surface	Aluminium	5mm thick	$300
Support Structure	Aluminium	50mm x 50mm x 3mm	$130
Support Legs	Aluminium	50mm x 50mm x 1.6mm	$70
Top Surface	EvaDura	10mm thick	$90

*Approximate cost

Finally, a design specification has been creating, including drawings of each part of the DIET surface. Due to ongoing developments to the internal components of the DIET system, it is not practical to produce a final prototype surface at this stage. However, in future, this surface will be produced and utilised in clinical trials. The design specification summarised important information required to produce an ergonomically designed surface suitable for the DIET machine.

7. Conclusion

The research presented in this thesis has enabled further development of a high performance clinical prototype of the DIET breast cancer screening system. The two main objectives of this report were to: **1)** Develop the machine top surface opening to remove the need for interchangeable breast rings; and **2)** Improve the ergonomics of the DIET surface. Both objectives have been achieved.

A unique shape was chosen for the top surface opening, which allows imaging all parts of the breast tissue, from the breast cup to the Axillary Tail of Spence and chest wall. Anthropometric data was examined and the surface opening was sized to allow for the 95th percentile woman to be screened, thus removing the need for interchangeable breast rings. A portion of a woman's chest will be exposed during screening due to the geometry of the opening. Previously, the breast cup profile could be extracted in images using simple edge segmentation methods due to the significant change in image intensity between the breast cup and the matte black internal walls of the DIET machine. This segmentation was expected to be more difficult due to the exposure of the chest. Therefore, segmentation methods were investigated to mitigate this impact.

Phantom breasts were produced out of silicone and shaped to fit the proposed surface opening, with size based on anthropometric data. Three colours of phantom skin were produced: pale white, Mediterranean and dark brown. These colours represent the wide range of colours seen in the human skin colour spectrum, enabling the DIET machine to be capable of screening all women regardless of ethnic background. All three phantom breasts were used in trial runs in the DIET machine. Images from these trials were then used to determine the extent the breast cup could be isolated from the rest of the image using image processing.

In general, isolating the breast cup in the pale white and Mediterranean phantom breast images was relatively simple because there was a substantial difference in image intensity between the cup and the remainder of the image. This difference was not as apparent in the dark brown phantom images, making segmentation more difficult. However, when image filtering, edge detection and region detection methods were used in combination, clear accurate edges could be determined for all phantom breasts. In addition, by changing the actuator colour to matte black, changing the colour of the internal walls of the DIET machine, or by cropping images prior to image analysis, the segmentation process could be automated. This automation is desirable for processing the many images created during each breast screening.

In parallel with investigating the breast opening, an investigation was carried out on the shape of the top surface of the DIET system. Early results from clinical trials carried out on the DIET machine indicated that improvements could be made to the ergonomics of the machine. In particular, certain areas of the existing top surface were causing discomfort to the rib cage, breast and neck. These discomforts were causing women to shift position during a screening session which, in some cases, lead to compromised data.

Three unique prototype surfaces were designed and built for use in ergonomic trials. An initial trial was carried out until sufficient evidence exposed that modifications to the prototypes were necessary. An additional trial was carried out on two modified surfaces. The second trial concluded there was a clear preference for a simplified surface that felt natural for a woman to lie on. Thus, this prototype was developed further.

Mechanical loading analysis dictated the type of materials that would be appropriate for use on the proposed surface. This analysis, in combination with material weight and cost considerations, concluded that the base structure of the surface should be made from aluminium. In addition, EvaDura foam draped over aluminium sheet metal will provide the top surface of the system.

Ongoing developments are being carried out on the internal components of the DIET system and so it is not practical to produce a final full DIET prototype at this stage. However, in future, this surface will be produced and utilised in clinical trials. A design specification has been created, including drawings of each part of the DIET surface. This specification summarises important information required to produce an ergonomically designed surface suitable for the DIET machine.

In summary, the major requirement of this research was to design an ergonomic surface, which is suitable for use with the DIET machine and has an opening that removes the need for breast rings. The main components of this research were prototyping, ergonomic testing, phantom breast production and image processing. All research requirements were accomplished, and a design specification of the surface has been included. This specification allows for the manufacture of the ergonomically designed surface to be produced when it is required for further clinical trials.

References

ACMA Industries. (2016). 1/17/2017 Polyurethane Integral Skin. Retrieved from http://acma.co.nz/index.php/products/35-integral-skin

Ampil, F., Caldito, G., Henderson, B., Li, B., Kim, R. H., Burton, G., … State, L. (2012). Carcinoma of the Axillary Tail of Spence : A Case Series, *4060*, 4057–4059.

Astner, S., & Anderson, R. R. (2004). Skin Phototypes 2003. *Journal of Investigative Dermatology*, *122*(2), xxx–xxxi. http://doi.org/10.1046/j.1523-1747.2003.22251.x

Beer, F. P., Johnston, E. R., DeWolf, J. T., & Mazurek, D. F. (2012). Mechanics of Materials (Sixth Edition), 838.

Berg, W. A., Blume, J. D., Cormack, J. B., Mendelson, E. B., Lehrer, D., Pisano, E. D., … Marques, H. S. (2008). and Mammography vs Mammography Alone in Women at Elevated Risk of Breast Cancer, *299*(18), 2151–2163.

Berg, W. a., Gutierrez, L., NessAiver, M. S., Carter, W. B., Bhargavan, M., Lewis, R. S., & Ioffe, O. B. (2004). Diagnostic Accuracy of Mammography, Clinical Examination, US, and MR Imaging in Preoperative Assessment of Breast Cancer. *Radiology*, *233*(3), 830–849. http://doi.org/10.1148/radiol.2333031484

Bois, W. E. B. Du, Luschan, F. Von, & Reform, R. (2016). W . E . B . Du Bois , Felix von Luschan , and Racial Reform at the Fin de Siècle Author (s): John David Smith Source : Amerikastudien / American Studies , Vol . 47 , No . 1 , European American Studies Published by : Universitätsverlag WINTER Gmbh Stable, *47*(1), 23–38.

Botterill, T., Lotz, T., Kashif, A., & Chase, J. G. (2014). Reconstructing 3-D Skin Surface Motion for the DIET Breast Cancer Screening System, *33*(5), 1109–1118.

Brand, J., & Mason, J. S. (2000). A comparative assessment of three approaches to pixel-level human skin-detection. *Pattern Recognition, 2000. Proceedings. 15th International Conference on*, *1*, 1056–1059 vol.1. http://doi.org/10.1109/icpr.2000.905653

Brewer. (2016). BrewerElement Treatment Table. Retrieved September 20, 2016, from http://brewercompany.com/product/element-treatment-table/

CIVCO Medical Solutions. (2015).

Clarys, P., Alewaeters, K., Lambrecht, R., & Barel, A. O. (2000). Skin color measurements: comparison between three instruments: the Chromameter(R), the DermaSpectrometer(R) and the Mexameter(R). *Skin Research and Technology : Official Journal of International Society for Bioengineering and the Skin (ISBS) [and] International Society for Digital Imaging of Skin (ISDIS) [and] International Society for Skin Imaging (ISSI)*, *6*(4), 230–238. http://doi.org/srt060407 [pii]

Cochrane, D., & Henzel, M. (2005). Guide to Stainless Steel Finishes. *Euro Inox*, *1*. Retrieved from

http://www.euro-inox.org/pdf/build/Finishes02_EN.pdf

Cowell, C. F., Weigelt, B., Sakr, R. a., Ng, C. K. Y., Hicks, J., King, T. a., & Reis-Filho, J. S. (2013). Progression from ductal carcinoma in situ to invasive breast cancer: Revisited. *Molecular Oncology*, *7*(5), 859–869. http://doi.org/10.1016/j.molonc.2013.07.005

CYRO. (n.d.). Physical Properties of Acrylite FF Acrylic Sheet.

Dempsey, M. F., Condon, B., & Hadley, D. M. (2002). MRI safety review. *Seminars in Ultrasound CT and MRI*, *23*(5), 392–401. http://doi.org/10.1016/S0887-2171(02)90010-7

Dibden, A., Offman, J., Parmar, D., Jenkins, J., Slater, J., Binysh, K., … Duffy, S. W. (2014). Reduction in interval cancer rates following the introduction of two-view mammography in the UK breast screening programme. *British Journal of Cancer*, *110*(3), 560–4. http://doi.org/10.1038/bjc.2013.778

Feig, S. A. (2006). Screening mammography: A successful public health initiative. *Revista Panamericana de Salud Publica/Pan American Journal of Public Health*, *20*(2–3), 125–133. Retrieved from http://www.scopus.com/inward/record.url?eid=2-s2.0-33845506001&partnerID=40&md5=7e31b94791829f2c4785e1a229ec4de9

GmbH, C. + K. electronic. (2016). Courage + Khazaka electronic GmbH Scientific Devices Mexameter ® MX 18 Fields of Application : Retrieved August 1, 2016, from http://www.courage-khazaka.de/index.php/en/products/scientific/130-mexameter

González, F. J., Martínez-Escanamé, M., Muñoz, R. I., Torres-Álvarez, B., & Moncada, B. (2010). Diffuse reflectance spectrophotometry for skin phototype determination. *Skin Research and Technology*, *16*(4), 397–400. http://doi.org/10.1111/j.1600-0846.2010.00450.x

Gonzalez, R. C., Woods, R. E., & Eddins, S. L. (2004). Digital Image Processing Using Matlab - Gonzalez Woods & Eddins.pdf. *Education*. http://doi.org/10.1117/1.3115362

Haghir, H., Mokhber, N., Azarpazhooh, M. R., Haghighi, M. B., & Radmard, M. (2013). A magnetic resonance imaging study of adhesio interthalamica in clinical subtypes of schizophrenia. *Indian Journal of Psychiatry*, *55*(2), 135–139. http://doi.org/10.4103/0019

Hayes, J., Richardson, a., & Frampton, C. (2013). Population attributable risks for modifiable lifestyle factors and breast cancer in New Zealand women. *Internal Medicine Journal*, *43*(11), 1198–1204. http://doi.org/10.1111/imj.12256

Huang, S.-Y., Boone, J. M., Yang, K., Packard, N. J., McKenney, S. E., Prionas, N. D., … Yaffe, M. J. (2011). The characterization of breast anatomical metrics using dedicated breast CT. *Medical Physics*, *38*(4), 2180–2191. http://doi.org/10.1118/1.3567147

Huston, R. L. (2009). *Principles of Biomechanics*. CRC Press.

Inc., C. I. (2016). MEDICAL TABLES & CABINETS. Retrieved September 20, 2016, from

http://www.clinton-ind.com/

Institute, N. C. (2013). Breast Cancer Treatment (PDQ ®) Patient Version. Retrieved August 1, 2016, from https://www.cancer.gov/types/breast/patient/breast-treatment-pdq

Kashif, A. S. (2013). Imaging technology for digital image based motion detection in the DIET breast cancer screening system, (July).

Kashif, A. S., Lotz, T. F., Heeren, A. M. W., & Chase, J. G. (2013). Separate modal analysis for tumor detection with a digital image elasto tomography (DIET) breast cancer screening system. *Medical Physics*, *40*(11), 113503. http://doi.org/10.1118/1.4826168

Kashif, A. S., Lotz, T. F., McGarry, M. D., Pattison, A. J., & Chase, J. G. (2013). Silicone breast phantoms for elastographic imaging evaluation. *Medical Physics*, *40*(6), 63503. http://doi.org/10.1118/1.4805096

Kaysons. (n.d.). Physical Properties of Acrylic Sheets. Retrieved from http://www.builditsolar.com/References/Glazing/physicalpropertiesAcrylic.pdf

Lift, E. Z. (2016). Adapta Summit 7-Section Treatment Platform. Retrieved September 20, 2016, from http://www.djoglobal.com/products/chattanooga/adapta-summit-7-section-treatment-platform

Linda, Q. T. A. (2012). Developing Magnetic resonance elastography (MRE) breast actuation system for detecting breast cancer, (March).

Martini & Nath, J. (2009). *Fundamentals of Anatomy and Physiology*. *Learning* (Vol. 7th). http://doi.org/612

Michaelson, J. S., Silverstein, M., Wyatt, J., Weber, G., Moore, R., Halpern, E., … Hughes, K. (2002). Predicting the survival of patients with breast carcinoma using tumor size. *Cancer*, *95*(4), 713–723. http://doi.org/10.1002/cncr.10742

Ministry of Health. (2013). *Mortality and Demographic Data 2010*.

National Breast Cancer Foundtion. (2016). Breast Cancer Stage 3. Retrieved August 1, 2016, from http://www.nationalbreastcancer.org/breast-cancer-stage-3

New Zealand Breast Cancer Foundation. (2015). Fast facts BREAST CANCER SUPPORT OUR FOCUS GET INVOLVED INVOLVE YOUR BUSINESS New Zealand Breast Cancer Foundation Websitet. http://doi.org/10.111/imj.12256

Ning, R., Conover, D. L., Yu, Y., Zhang, Y., Liu, S., & Neugebauer, J. (2010). Koning cone beam breast CT for breast cancer detection, diagnosis and treatment. *American Journal of Clinical Oncology: Cancer Clinical Trials*, *33*(5), 526–527.

Oakworks Medical. (2016). C-ARM IMAGING TABLES. Retrieved September 20, 2016, from http://www.oakworksmed.com/dtpm300.asp

orfit. (2016), Sagittilt (TM) Prone Breast Solution.

Parvin, S. (2015). polymorphisms in breast cancer patients of Bangladesh.

Peters, A., Chase, G. J., & Van Houten, E. E. W. (2008). Digital image elasto-tomography: Mechanical property estimation of silicone phantoms. *Medical and Biological Engineering and Computing*, *46*(3), 205–212. http://doi.org/10.1007/s11517-007-0275-x

Ravnbak, M. H. (2010). Objective determination of Fitzpatrick skin type. *Danish Medical Bulletin*, *57*(8), B4153. http://doi.org/10.1136/jcp.43.9.787-d

Rong, Z. (2006). *Breast sizing and development of a 3D seamless bra.*

Sachdeva, S. (2009). Fitzpatrick skin typing: applications in dermatology. *Indian Journal of Dermatology, Venereology and Leprology*, *75*(1), 93–96. http://doi.org/10.4103/0378-6323.45238

Samani, A., Zubovits, J., & Plewes, D. (2007). Elastic moduli of normal and pathological human breast tissues: an inversion-technique-based investigation of 169 samples. *Physics in Medicine and Biology*, *52*(6), 1565–1576. http://doi.org/10.1088/0031-9155/52/6/002

Shank, T. (n.d.). AS 2465 Grade 8, 14–15.

Sharpe, H., & Bradburuy, S. (2015). *Understanding Excess Body Weight*. Retrieved from http://www.health.govt.nz/system/files/documents/publications/understanding-excess-body-weight-nzhs-apr15.pdf

Shop, T. F. (2016). The Fibreglass Shop. Retrieved August 16, 2016, from https://www.fibreglassshop.co.nz

Society, A. C. (2015). Breast Cancer Survival Rates. Retrieved May 20, 2008, from https://www.cancer.org/cancer/breast-cancer/understanding-a-breast-cancer-diagnosis/breast-cancer-survival-rates.html

Stryker, U. (2009). EMS Equipment Catalog (stryker). http://doi.org/10.1002/ejoc.201200111

Swiatoniowski, A. K., Quillen, E. E., Shriver, M. D., & Jablonski, N. G. (2013). Technical Note: Comparing von Luschan skin color tiles and modern spectrophotometry for measuring human skin pigmentation. *American Journal of Physical Anthropology*, *151*(2), 325–330. http://doi.org/10.1002/ajpa.22274

Tedeschi-Oliveira, S. V., Melani, R. F. H., de Almeida, N. H., & de Paiva, L. A. S. (2009). Facial soft tissue thickness of Brazilian adults. *Forensic Science International*, *193*(1–3), 1–7. http://doi.org/10.1016/j.forsciint.2009.09.002

The Ministry of Health. (2009). *Clinical Guidelines for Weight Management in New Zealand Adults*.

Valea, F. a, & Katz, V. L. (n.d.). Diagnosis and Treatment of Benign and Malignant Disease, 327–358.

Van Houten, E. E. W., Peters, A., & Chase, J. G. (2011). Phantom elasticity reconstruction with Digital

Image Elasto-Tomography. *Journal of the Mechanical Behavior of Biomedical Materials*, *4*(8), 1741–1754. http://doi.org/10.1016/j.jmbbm.2011.05.031

Visscher, M. O. (2010). Imaging Skin: Past, Present and Future Perspectives. *Imaging of the Skin*, (February), 10–28.

XIEHE Medical Apparatus & Instruments. (2010).

Young, W. C., & Budynas, R. G. (2002). Stress Concentration. *Roarks's Formulas for Stress and Strain*, 259. http://doi.org/10.1002/9780470172681.ch6

Appendix A: Human Ethics Application

This appendix contains the ethics approval documents, sent to the University of Canterbury Human Ethic Committee, listed below.

Document	Detail
1	HEC Application Form
2	Information Sheet
3	Advertisement
4	Consent Form
5	Conformation of Approval
6	Ergonomics Questionnaire

Human Ethics Committee – Student Application

UNIVERSITY OF CANTERBURY
Te Whare Wānanga o Waitaha
CHRISTCHURCH NEW ZEALAND

For Office Use Only –	**HEC Reference:**
Date Received:	**Reviewers:**
Date Approved:	**Approved:** **(HEC Chair)**

HUMAN ETHICS APPLICATION COVERSHEET – STUDENT

Please remember that your audience for this application form, as well as all forms for participants, will include community members and scholars from outside your discipline and therefore must be written in everyday language.
This form should be completed after reading the *Human Ethics Policy* issued by the Human Ethics Committee available at http://www.canterbury.ac.nz/humanethics

Will another ethics committee review this application?

- If a New Zealand Health and Disability Ethics Committee (HDEC) is reviewing your project, please send your HDEC application to us with this coversheet, and then the approval. You do not need to fill out the full University of Canterbury application form.
- If you have ethics approval from another institutional ethics committee (eg another New Zealand or Overseas University ethics committee) and you will conduct your research in the country of that ethics committee, please send this coversheet only with that application and the later approval letter, and an explanatory email. You do not, initially, need to fill out the full University of Canterbury application form.

Please ***Bold*** your answers

Project Title: **Improvements to Ergonomics and Reliability of the Digital Image Elasto-Tomography Breast Cancer Screening Device**

Status of Research: **Masters**

Applicant

Name: **Claire Bewley**

University Programme/ Department: **Mechanical Engineering**

Applicant's Email: **claire.bewley@pg.canterbury.ac.nz**

Primary Telephone No: **(027) 829 2440**

Primary Supervisor Title, given name and family name

Name: **Distinguished Professor Geoff Chase**

University Programme/ Department: **Mechanical Engineering**

Supervisor's Email: **Geoff.chase@canterbury.ac.nz**

Primary Telephone No: **(03) 364 2987 ext 7224**

Other Supervisors

RESEARCHER'S SIGNATURE

I *Claire Bewley* have considered, the various ethical issues involved in this research, I have discussed this proposal with my supervisor(s), and I will conduct this research within the bounds of any approval given by the Human Ethics Committee of the University of Canterbury.

Signed: _____ Dated:

Is the approval of this application a necessary pre-requisite for the Dean of Postgraduate Studies to formally accept your PhD proposal? **NO**

SENIOR SUPERVISOR'S SIGNATURE

As the primary supervisor of *Claire Bewley* research project I, *Geoff Chase* consider that the design and documentation are of a standard appropriate for a research project carried out in the name of the University of Canterbury.

Signed: _____ Dated:

LOW RISK PROCESSES (TO BE COMPLETED BY THE PRIMARY SUPERVISOR)

No issues were raised on the low risk checklist. The research should not encounter any more risk than might be encountered in normal daily life. The project does do not raise any issue of deception, threat, invasion of privacy, mental, physical or cultural risk or stress, and does not involve gathering personal information of a sensitive nature about or from individuals. The testing is done fully clothed and is entirely non-invasive with no risk of any form of injury.

There were no ethical issues raised in the proposal.

Signed (Senior/Primary Supervisor only) _____ Dated:

SUBMISSION INSTRUCTIONS.

Please submit ONE electronic file containing all the necessary documents in a PDF format and ONE fully signed hard copy. Exceptions may be made, but must be discussed first with the HEC Secretary. Processing of HEC applications is unable to begin until a hard copy of the application has been received by the Ethics Office.
Electronic copies should be emailed to human-ethics@canterbury.ac.nz. Hard copies should be sent to the Secretary, Human Ethics Committee (Level 5, Matariki South).

Low Risk application information:

Research may be considered low risk when it arises from

a Masters or PhD theses where the projects do not raise any issue of deception, threat, invasion of privacy, mental, physical or cultural risk or stress, and do not involve gathering personal information of a sensitive nature about or from individuals.

b Masters or PhD level supervised projects undertaken as part of specific course requirements where the projects do not raise any issue of deception, threat, invasion of privacy, mental, physical or cultural risk or stress, and do not involve gathering personal information of sensitive nature about or from individuals.

c Undergraduate and Honours class research projects which do not raise any issue of deception, threat, invasion of privacy, mental, physical or cultural risk or stress, and do not involve gathering personal information of sensitive nature about or from individuals, but do not have blanket approval as specified in Section 4 of the Principles and Guidelines.

3. No research can be counted as low risk if it involves:

(i) invasive physical procedures or potential for physical harm
(ii) procedures which might cause mental/emotional stress or distress, moral or cultural offence
(iii) personal or sensitive issues
(iv) vulnerable groups
(v) Tangata Whenua (if in doubt please see the comments under question 12 on the application form)
(vi) cross cultural research
(vii) investigation of illegal behaviour(s)
(viii) invasion of privacy
(ix) collection of information that might be disadvantageous to the participant
(x) use of information already collected that is not in the public arena which might be disadvantageous to the participant
(xi) use of information already collected which was collected under agreement of confidentiality
(xii) participants who are unable to give informed consent
(xiii) conflict of interest e.g. the researcher is also the lecturer, teacher, treatment-provider, colleague or employer of the research participants, or there is any other power relationship between the researcher and the research participants.
(xiv) deception
(xv) audio or visual recording without consent
(xvi) withholding benefits from "control" groups
(xvii) inducements
(xviii) risks to the researcher

This list is not definitive but is intended to sensitise the researcher to the types of issues to be considered. Low risk research would involve the same risk as might be encountered in normal daily life.

DESCRIPTION OF THE PROJECT

1. What does the project seek to do?

The purpose of the master's thesis is to improve the ergonomics and usability of a digital image elasto tomography (DIET) breast cancer screening machine.

2. What is the research question or hypothesis of this project?

The proposed research will investigate ways to improve a system, which uses digital image elasto-tomography to detect breast cancer, such that the system is ergonomic and the breast opening is shaped appropriately to accommodate for majority of the female population. The question for this project is "*what surfaces are comfortable for women to lie still on for up to 5 minutes at a time?*"

The nature and design of these surfaces will impact on the digital imaging technology used, and thus change the overall DIET technology. Hence, the question needs to be answered.

3. Describe how this project arose

Breast cancer is a major health problem; it is estimated that every year one million women are diagnosed worldwide and 410,000 women die from the disease. Mammography (breast x-ray) is the current conventional method of breast cancer detection. While mammography can detect some breast cancers, the technology has limitations including performance, cost, radiation exposure and patient discomfort.

The cost of equipment and personnel alone puts mammography out of reach for many developing nations. Mammography is also limited to screening women over the age of 45 when the breast tissue is typically less dense. To make breast screening available to all women, regardless of age or location, there is a great and growing need for additional breast screening modalities that address some or all of these limitations.

The digital image-based elasto-tomography (DIET) breast cancer screening technology is a novel technique for breast cancer screening that is based on elastography, which is imaging based on the elastic properties of tissue rather than radio density or another metric. The DIET technology is currently in a working prototype state and is undergoing a clinical study at Canterbury Breastcare to assess the performance and any limitations. Two important areas of development have been exposed from the clinical study to date, and form the focus of this project.

Ergonomics of the system

For the system to perform optimally, women are required to lie very still during the imaging process (up to five minutes for each breast). Any undue motion could result in poor data quality or potentially false positive/negative screening results. Feedback from clinical studies to date have indicated that the top surface of the DIET machine is not comfortable for all women, and on occasion has resulted in women adjusting their position during an imaging session. To ensure the integrity of all data it is therefore very important that the ergonomics of the system are improved.

Breast opening

With the current DIET system, breast rings are used for two main reasons: 1) To isolate the breast tissue to be imaged from the rest of the chest; and 2) To block light from entering the system, causing noise errors due to the sensitivity of the cameras used for imaging. The current breast rings have highlighted two main challenges with using a 'multi-ring' breast ring system.

The first problem relates to the clinical work flow. The sizing and changing of incorrectly sized breast rings consumes time and requires operator skill. Often what appears to be the correct sized ring when a patient is standing, may not be the best size breast ring when the patient lies down. In this case, the patent would have to then stand up again to have the ring size adjusted. This process takes time and makes the screening process less streamlined for both the patient and operator. Additionally, if a poorly sized breast ring is chosen, it can cause wrinkles on the breast surface which may limit the usability of the resulting imaging data.

The second problem is that the breast rings are limiting the imaging area. The result of this issue means that some abnormalities will not be able to be detected in regions of the breast that are not visible to the cameras. In particular, near the chest wall, where manual detection and mammography are also very poor in finding tumors.

4. How will you go about answering the research question?

Three different DIET surfaces will be designed using ergonomic principles and anthropometric data (human dimensions). These surfaces will be prototyped. Female volunteers will test each surface (while fully clothed) and provide ergonomic feedback. The most ergonomic surface, based on volunteer feedback, will then be further developed and manufactured. All imaging technology will then be evaluated in the context of this surface to optimise the overall system.

INFORMATION ABOUT THE PARTICIPANTS

5. Who are the participants and why have they been chosen to be asked to participate?

Breast cancer predominantly effects women. The DIET machine is designed to detect cancer within the breasts of women. For this reason, only women participants shall be participating in this trial. Women of all ages, ethnicities, shapes and sizes shall participate so that substantial ergonomic feedback can be obtained.

6. How many participants will be involved (of each category where relevant)?

Up to 50 women will be involved.

7. What selection criteria and/or exclusion criteria will you use?

Participants will initially be randomly selected from female volunteers. Participants who express interest will be asked what size, age and ethnicity they are. Of the 50 participants there must be at least the following variety:

- **3 participants for each dress size group (6 - 8,10 - 12,14 - 16,18+)**
- **3 participants for each age group (18 – 35, 36 – 50, 50+)**

If the initial response does not have enough variety, additional participants shall be requested. Once all 50 volunteers have been confirmed, additional interested volunteers shall be made aware that all spots have been taken.

8. Describe how potential participants will be identified and recruited?

Email communications shall be sent to staff and students at the University of Canterbury. If the initial response does not have enough variety, additional participants shall be approached via advertisement in the community.

9. Does the project involve recruitment through advertising?

YES, please refer to the attached advert document

10. How much time are participants asked to contribute to the research?

Up to 30 minutes for each participant.

11. Is any form of inducement to be offered?

NO

12. How will the participants be treated?

Initially, after consent, each participant will fill out a privacy declaration and a short survey about themselves. This will include their clothing size, age and ethnicity. A photo of each participant will also be taken if the participant agrees, this photo will only be of the side profile of a participant lying on a surface so will not have their face.

The process of the trial will then be explained to the participants. During this time, they are welcome to ask questions. Participants will be made aware that if any point in the trial they do not feel comfortable with what is being asked of them, they are welcome to withdraw from the trial. Participants will also be told that if a surface causes any pain, they are welcome to come off that surface at any time.

For the trial, each participant shall be asked to lie face down (fully clothed) onto each prototyped surface. The volunteers will lie on each surface for 5 minutes each. Half way through they will be asked to describe discomfort in any parts of their body and what level of discomfort they experience. The same questions will be asked at the end of the five minutes. The participants will also be asked if they experience any pain; if they do experience pain, they will be reminded that they can come off that surface at any time.

After the participant has trialled each surface, they will be asked a quick questionnaire where they will describe their experience and rate each surface based on comfort.

OTHER PARTIES WITH AN INTEREST IN THE RESEARCH

13. Does the project require permission of an organisation, other people, to access participants or information?

NO – All participants will be adult age and will be participating at a time best suited for them.

14. Will the project require Maori consultation?

NO – Ethnicities of participants will be recorded but only for statistical reasons. No ethnicity will be treated differently.

15. Will the project require Community consultation? **NO**

16. Is the project funded externally? **NO**

17. Is the project commissioned by or carried out on behalf of an external organisation(s)? **NO**

18. Is the project to be part of the CEISMIC digital archive? **NO**

19.

DATA COLLECTION

20. Does the project involve a questionnaire? **YES, please see attached interview questions.**

(a) Explain how and why the questionnaire(s) will be anonymous or confidential

The questionnaire will be confidential as the questionnaire will be filled out at the trial. Each participant will be given a participant number. This participant number will be recorded on each page of the questionnaire, rather than the participant's name. No information on the questionnaire could be used to identify a participant. All data from the questionnaire will be stored in encrypted files.

(b) Explain how the questionnaire will be distributed and collected.

The questionnaire will be given to each participant at the trial on paper and will be filled out at the beginning of the trial.

21. Does the project involve a structured or semi-structured interview?

YES – Participants will be asked which surface was the most and least comfortable to lie on and will be asked to provide any other ergonomic feedback. Please refer to attached interview questions.

22. Does the project involve an unstructured interview? **NO**

23. Does the project involve focus groups? **NO**

24. Does the project involve recording of Audio, Video or Images? **YES. Participants will be asked if they give consent to have their photo taken while they are on the surfaces. Because they will be lying face down on the surface, their face will not be in the photo making it difficult to identify the participant. The photos will be used to show what a participant looked like on each surface and to point out if some surfaces have areas which could be improved. Photos of all participants will not be required and this will be made clear to all participants. All photos will be stored in encrypted files which can only be accessed by the primary researcher.**

25. Will participants will be given the opportunity to check the transcript and/or notes of their interview/focus group? **YES**

INFORMED AND VOLUNTARY CONSENT

26. By whom and how will information be given to potential participants?

Once a participant has shown interest in the trial, an information sheet (attached) will be sent to them via email. The participant will then indicate if they are still willing to participate and a meeting time will be arranged. This gives each participant time to consider the trial and means they can say no if they choose to. At the actual trial, participants will be given two hard copies of the consent form to sign there. One will be for the participant to keep and the other for the primary researcher.

27. Are all participants competent to give consent on their own behalf? **YES** If no, please explain,

    (a) why they are not competent to give informed consent on their behalf? **N/A**

    (b) how consent will be obtained in the absence of that competency? **N/A**

    (c) if applicable, how will assent to participate be gained? **N/A**

PRIVACY AND CONFIDENTIALITY

28. Will information pertaining to or about the participants be obtained from any source other than the participant? **NO**

    (a) the identity of the third party or parties.

    (b) why such information is needed.

    (c) how will you obtain consent from the participant and the third party(ies) to gather that data.

    (d) the processes you will use to obtain that data.

29. Is information that identifies participants to be given to any person outside the research team, or if identification of or attribution of comments by participants is sought, please explain how and why. **NO**

30. Please explain how confidentiality of the participants' identities will be maintained in the treatment and use of the data.

Each participant will be given a participation number which will be used on all forms / questionnaires for the participants. The only time the name of a participant will be recorded is for initial contact via email / phone. All contact details of participants will be stored within an encrypted file which only the primary researcher can access.

31. Is an institution (eg, school, business, etc) to which participants belong to be named or be able to be identified in the publication or presentation of this project? **NO**

32. Where will the project be conducted?

The project will be carried out in an office within the civil / mech building at the University of Canterbury or any other free room within the university (depending on availability). Although the trial will take place in a public building, it is intended that the room will only have the participant and the primary researcher.

RISK

33. Is there any risk to physical well-being? **NO**

34. Could participation involve mental stress or emotional distress? **NO**

35. Is there a possibility of causing moral or cultural offence, inadvertently or otherwise? **NO**

36. Is deception involved at any stage of the project? **NO**

37. **NA**

DATA STORAGE AND FUTURE USE

38. Please provide details of how the data will be securely stored, and how you will separate identifying and non-identifying data.

All data relating to participants, including contact details for participants will be stored in encrypted files on the primary researcher's external drive. The external drive will be encrypted with Bit Locker which requires a password to open the drive each time it is used. Only the primary researcher knows the password to the drive.

39. Who, apart from the researcher and their supervisor (where applicable) will have authorised access to the data? **No one**

40. What will happen to the raw data at the end of the project?

All raw data will be kept safely and then destroyed after five years.

41. What plans do you have for the publication of the data?

The data will be summarised in the Master's thesis which may become a public document. There may also be other publications such as journal articles or conference material which references this trial. None of the raw data will released publicly. There will be no way to identify who took part in the study from the results. The summary of results will also be distributed to participants who wish to review it.

42. Please describe plans for future use of the data beyond those already described above.

University of Canterbury

Department of Mechanical Engineering
DIET Breast Screening Device Ergonomic Study

Improvements to Ergonomics and Reliability of the Digital Image Elasto-Tomography Breast Cancer Screening Device

- Information Sheet -

Dear Participant,

You are invited to participate in the research project 'Improvements to Ergonomics and Reliability of the Digital Image Elasto-Tomography Breast Cancer Screening Device'. This research is part of a Master's of Mechanical Engineering project that will be submitted to the University of Canterbury.

Background

Breast cancer is the most common form of cancer in the female population, with new cases expected to represent more than one quarter of all female cancer diagnoses. In New Zealand, every year over 650 women die of breast cancer. Early detection of any lumps in the breast can enable early treatment and greatly improve survival rates.

Current early screening methods usually involve a mammogram, which is a specialised x-ray of the breast. More advanced diagnosis can involve ultrasound or magnetic resonance imaging (MRI) to get a more detailed view of potential lesions. Due to the complexity and cost of these procedures, large scale screening of breast cancer at a younger age is not practical.

About the Study

The new technology that is investigated in this study is a low-cost and non-invasive method to screen the breast for potential abnormalities including cancer. The technology is called Digital Image Elasto-Tomography (DIET), and as the name suggests, the method uses digital images to screen for breast abnormalities. The DIET system induces a small (~1mm) vibration in the breast at up to 100 times per second and images of this motion are captured using an array of digital cameras positioned around the breast. Using sophisticated computer software, these images can then provide information about the likelihood of an abnormality being present in the breast. The technology has been developed to the stage where it is now being clinically tested. A schematic of the DIET system is shown in the figure below.

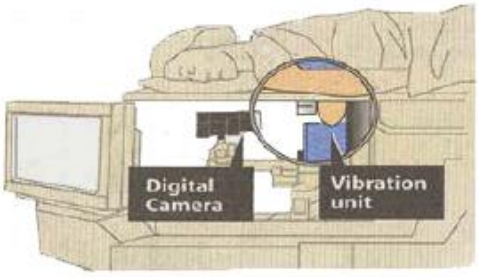

The aim of this project is to design an ergonomic and comfortable surface for women to lie on during breast cancer screening using the device. No participants will undergo screening with the technology during this study. The results will be used to continue development on the technology. We intend to recruit up to 30 volunteers.

Participation

Your involvement in this project will be to trial and evaluate three prototype surface designs. This will be accomplished, with your help, by lying face down on three prototype surfaces. Feedback will be sought regarding comfort and favourability of each design. The entire process is expected to take half an hour.

Participation is voluntary and you have the right to withdraw at any stage without penalty. You may ask for your raw data to be returned to you or destroyed at any time. If you withdraw, any information relating to you will be removed from the database. However, once analysis of raw data starts on the 13th of January 2016, it will become increasingly difficult to remove the influence of your data on the results.

The results of the project may be published, but you can be assured of the complete confidentiality of data gathered in this investigation. The identity of participants will not be made public. To ensure anonymity and confidentiality, each participant will be given a participant number. No questions will be asked which could be used to identify a participant or that require potentially sensitive personal information. All information will be stored on university servers and a password will be required to access the information.

The project is being carried out as a requirement for to complete the mechanical engineering master's thesis under the supervision of Distinguished Professor Geoff Chase, who can be contacted at Geoff.chase@canterbury.ac.nz. He will be pleased to discuss any concerns you may have about participation in the project.

The project has been reviewed and approved by the Department of Mechanical Engineering and the University of Canterbury Human Ethics Committee low risk approval.

If you agree to participate in the study, you are asked to complete the consent form and return this to myself at the trail.

Regards,

Claire Bewley

Masters Student,
The University of Canterbury
(027) 829 2440

I have read and understand the contents of this letter and give consent for the researcher to record and store relevant data about my participation in this research project.

Signed_____ (Participant)

Would you like to help make Breast Cancer Screening more comfortable?

We are looking for females to take part in an ergonomic study for a new breast screening device.

The Project

A new low-cost and non-invasive method to screen the breast for potential cancer is currently being developed. The technology, Digital Image Elasto-Tomography (DIET), involves subtly vibrating the breast and recording digital images of the motion. Using sophisticated computer software, these images can then provide information about the likelihood of an abnormality being present in the breast. The technology has been developed to the stage where it is now being clinically tested. A schematic of the DIET system is shown in the figure below.

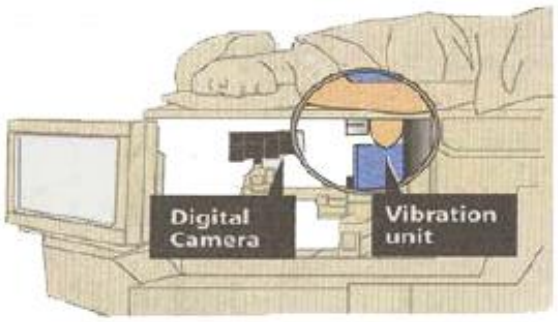

The aim of this project is to design an ergonomic and comfortable surface for women to lie on during breast cancer screening using the device. No participants will undergo screening with the technology during this study.

Who is require for the trial?

Any female aged 18 and above.

What would be required from me?

Lie down (fully clothed) on three prototype surfaces and answer a few questions related to the ergonomics/comfort.

How long would it take?

Less than 30 minutes.

How do I sign up?

Please contact Claire Bewley: claire.bewley@pg.canterbury.ac.nz

- This trial has approval from the Human Ethics Committee of the University of Canterbury (HEC) -

University of Canterbury

Department of Mechanical Engineering
DIET Breast Screening Device Ergonomic Study

UNIVERSITY OF CANTERBURY
Te Whare Wānanga o Waitaha
CHRISTCHURCH NEW ZEALAND

Improvements to Ergonomics and Reliability of the Digital Image Elasto-Tomography Breast Cancer Screening Device

- Consent Form -

- ☐ I have been given a full explanation of this project and have had the opportunity to ask questions.
- ☐ I understand what is required of me if I agree to take part in the research.
- ☐ I understand that participation is voluntary and I may withdraw at any time without penalty. Withdrawal of participation will also include the withdrawal of any information I have provided should this remain practically achievable.
- ☐ I understand that any information or opinions I provide will be kept confidential to the researcher and that any published or reported results will not identify the participants. I understand that a thesis is a public document and will be available through the UC Library.
- ☐ I understand that all data collected for the study will be kept in locked and secure facilities and/or in password protected electronic form and will be destroyed after five years.
- ☐ I understand the risks associated with taking part and how they will be managed.
- ☐ I understand that I am able to receive a report on the findings of the study by contacting the researcher at the conclusion of the project.
- ☐ I understand that I can contact the researcher, Claire Bewley (Claire.bewley@pg.canterbury.ac.nz), or supervisor, Geoff Chase (Geoff.chase@canterbury.ac.nz), for further information. If I have any complaints, I can contact the Chair of the University of Canterbury Human Ethics Committee, Private Bag 4800, Christchurch (human-ethics@canterbury.ac.nz)
- ☐ I would like a summary of the results of the project.
- ☐ By signing below, I agree to participate in this research project.

Name: _____ Signed: _____ Date: _____
Email Address *(for report of findings, if applicable):* _____

This consent form will be collected at the arranged trial time.

Claire Bewley

HUMAN ETHICS COMMITTEE

Secretary, Lynda Griffioen
Email: human-ethics@canterbury.ac.nz

Ref: HEC 2015/85/LR

26 November 2015

Claire Bewley
Department of Mechanical Engineering
UNIVERSITY OF CANTERBURY

Dear Claire

Thank you for forwarding your low risk application to the Human Ethics Committee for the research proposal titled "Improvements to ergonomics and reliability of the digital image elasto-tomography breast cancer screening device".

I am pleased to advise that the application has been reviewed and approved.

Please note that this approval is subject to the incorporation of the amendments you have provided in your email of 26 November 2015.

With best wishes for your project.

Yours sincerely

Lindsey MacDonald
Chair, Human Ethics Committee

DIET Ergonomics Questionnaire

Volunteer Number: Date / Time:

Height	
Weight	
Approximate Cloth Size (Circle)	6 – 8 10 – 12 14 – 16 18+
Ethnicity	
Age Group	18 – 35 36 – 50 50+

Surface 1

		2 Minutes 30	**5 Minutes**
Neck / Head	Is there any pain or discomfort in your head or neck?	Yes No	Yes No
	Level of pain / discomfort in neck / head	1 (Slightly uncomfortable) 2 (Quite uncomfortable) 3 (Unbearable) N/A	1 (Slightly uncomfortable) 2 (Quite uncomfortable) 3 (Unbearable) N/A
	Comments on pain in neck / head		
Chest	Is there any pain or discomfort in your chest?	Yes No	Yes No
	Level of pain / discomfort in chest	1 (Slightly uncomfortable) 2 (Quite uncomfortable) 3 (Unbearable) N/A	1 (Slightly uncomfortable) 2 (Quite uncomfortable) 3 (Unbearable) N/A
	Comments on pain in chest		
Waist	Is there any pain or discomfort in your waist?	Yes No	Yes No
	Level of pain / discomfort in waist	1 (Slightly uncomfortable) 2 (Quite uncomfortable) 3 (Unbearable) N/A	1 (Slightly uncomfortable) 2 (Quite uncomfortable) 3 (Unbearable) N/A
	Comments on pain in waist		

Any other pain or discomfort? Explain

Surface 2

		2 Minutes 30	5 Minutes
Neck / Head	Is there any pain or discomfort in your head or neck?	Yes No	Yes No
	Level of pain / discomfort in neck / head	1 (Slightly uncomfortable) 2 (Quite uncomfortable) 3 (Unbearable) N/A	1 (Slightly uncomfortable) 2 (Quite uncomfortable) 3 (Unbearable) N/A
	Comments on pain in neck / head		
Chest	Is there any pain or discomfort in your chest?	Yes No	Yes No
	Level of pain / discomfort in chest	1 (Slightly uncomfortable) 2 (Quite uncomfortable) 3 (Unbearable) N/A	1 (Slightly uncomfortable) 2 (Quite uncomfortable) 3 (Unbearable) N/A
	Comments on pain in chest		
Waist	Is there any pain or discomfort in your waist?	Yes No	Yes No
	Level of pain / discomfort in waist	1 (Slightly uncomfortable) 2 (Quite uncomfortable) 3 (Unbearable) N/A	1 (Slightly uncomfortable) 2 (Quite uncomfortable) 3 (Unbearable) N/A
	Comments on pain in waist		

Any other pain or discomfort? Explain

Surface 3

		2 Minutes 30	**5 Minutes**
Neck / Head	Is there any pain or discomfort in your head or neck?	Yes No	Yes No
	Level of pain / discomfort in neck / head	1 (Slightly uncomfortable) 2 (Quite uncomfortable) 3 (Unbearable) N/A	1 (Slightly uncomfortable) 2 (Quite uncomfortable) 3 (Unbearable) N/A
	Comments on pain in neck / head		
Chest	Is there any pain or discomfort in your chest?	Yes No	Yes No
	Level of pain / discomfort in chest	1 (Slightly uncomfortable) 2 (Quite uncomfortable) 3 (Unbearable) N/A	1 (Slightly uncomfortable) 2 (Quite uncomfortable) 3 (Unbearable) N/A
	Comments on pain in chest		
Waist	Is there any pain or discomfort in your waist?	Yes No	Yes No
	Level of pain / discomfort in waist	1 (Slightly uncomfortable) 2 (Quite uncomfortable) 3 (Unbearable) N/A	1 (Slightly uncomfortable) 2 (Quite uncomfortable) 3 (Unbearable) N/A
	Comments on pain in waist		

Any other pain or discomfort? Explain

After all surfaces have been tested, each volunteer will be asked the following questions:

1. Which was the most comfortable surface to lie on? _____

2. Which was the least comfortable to lie on? _____

3. Any further comments or suggestions relating to the ergonomics?

_____

Appendix B: Phantom Breast Mould Drawings

This appendix contains drawings, listed below, which detail the phantom breast moulds.

Drawing Number	Detail
B-0010	Typical Mould Assembly
B-0020	5^{th}, 50^{th} and 95^{th} Percentile Breast Moulds
B-0021	5^{th} Percentile Breast Mould
B-0022	50^{th} Percentile Breast Mould
B-0023	95^{th} Percentile Breast Mould
B-0030	Support Plate
B-0040	Support Structure

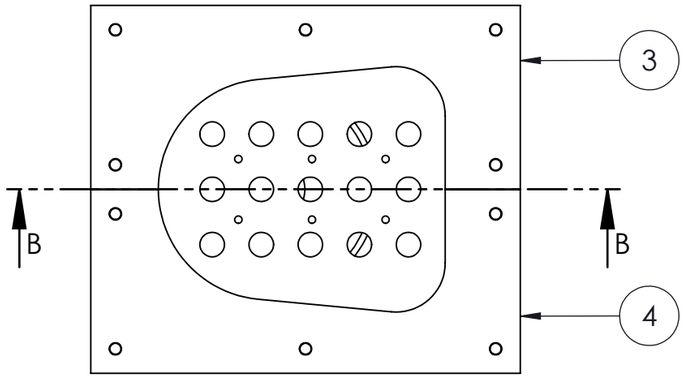

TOP VIEW

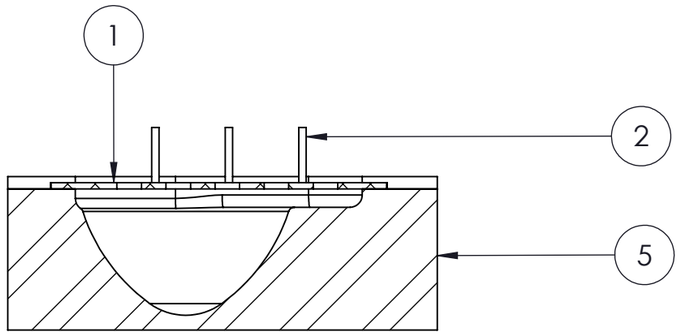

SECTION B-B

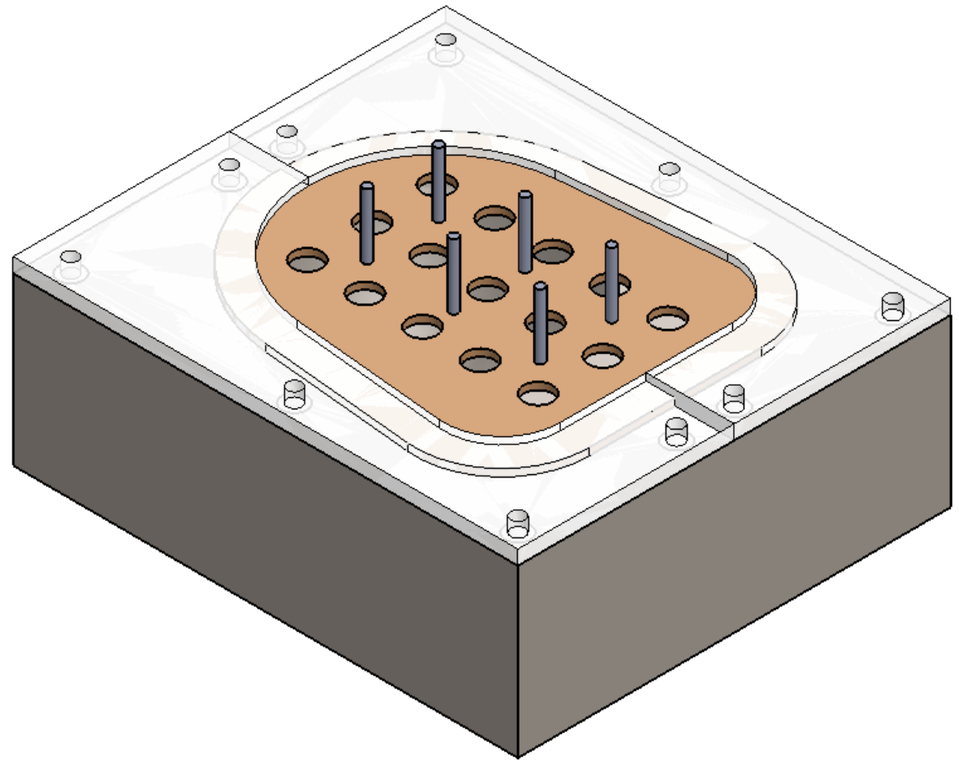

ISOMETRIC VIEW

ITEM NO.	PART NUMBER	MATERIAL	DWG. NO.	QTY.
1	SUPPORT PLATE	PERSPEX	B-0030	1
2	M6 THREADED ROD	STEEL	-	6
3	SUPPORT STRUCTURE - LEFT	PERSPEX	B-0040	1
4	SUPPORT STRUCTURE - RIGHT	PERSPEX	B-0040	1
5	BREAST MOULD	MODELLING BOARD	B-002X	1

THIRD ANGLE PROJECTION

MATERIAL: SEE BILL OF MATERIAL

FINISH:

TOLERANCE (UNLESS OTHERWISE SPECIFIED)

DECIMAL mm

.X ± .XX ± .XXX ± ANG. ± °

UNIVERSITY OF CANTERBURY ©
DEPARTMENT OF MECHANICAL ENGINEERING

TYPICAL MOLD ASSEMBLY

DESIGN: C. H. BEWLEY	DWG NO.: B-0010		REV: 1
DRAWN: C. H. BEWLEY	PROJECT: DIET BREAST CANCER SCREENING SYSTEM		
SUPERVISOR: G. CHASE	ISSUE DATE: 25-09-2015	DRAWING NOT TO SCALE	SHEET: 1 OF 1

5TH PERCENTILE BREAST MOLD

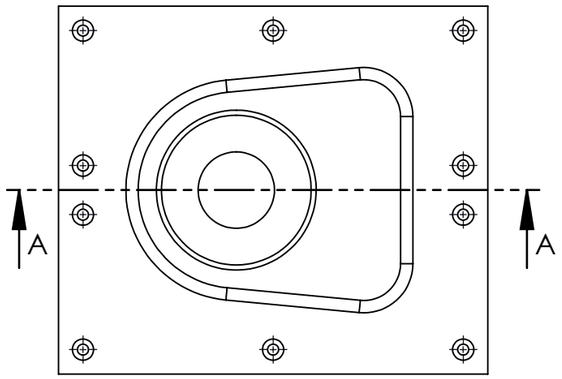

50TH PERCENTILE BREAST MOLD

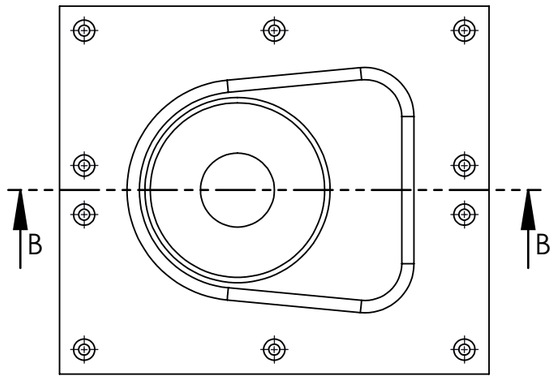

95TH PERCENTILE BREAST MOLD

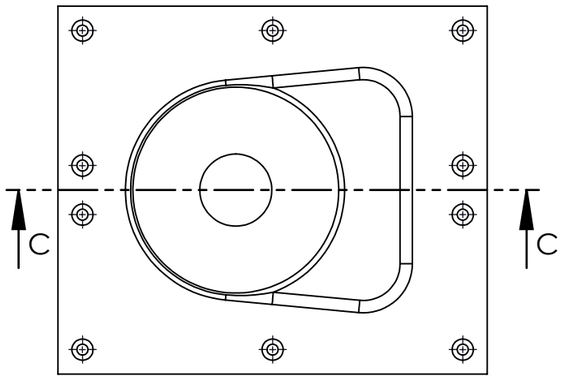

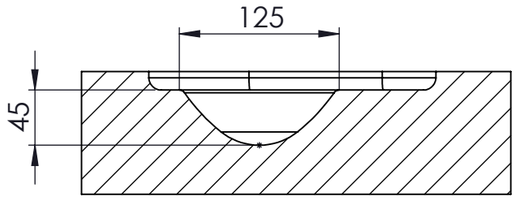

SECTION A-A

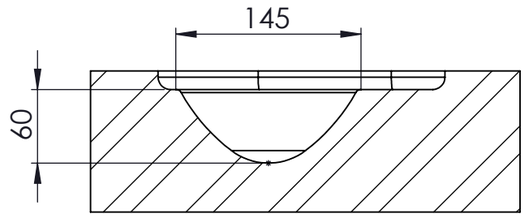

SECTION B-B

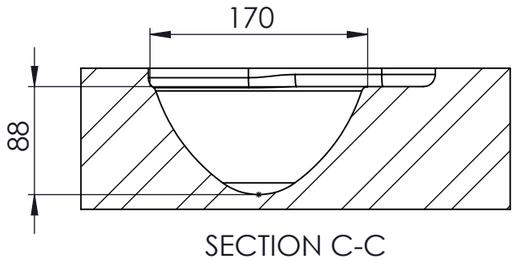

SECTION C-C

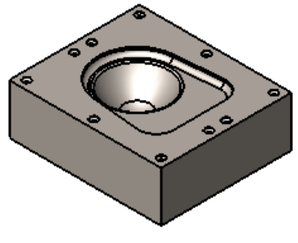

3D VIEW OF 50TH
PERCENTILE BREAST MOLD

THIRD ANGLE PROJECTION

MATERIAL: MODELLING BOARD

FINISH:

TOLERANCE (UNLESS OTHERWISE SPECIFIED)
DECIMAL mm
.X ± .XX ± .XXX ± ANG. ± °

UNIVERSITY OF CANTERBURY ©
DEPARTMENT OF MECHANICAL ENGINEERING

5TH, 50TH AND 95TH PERCENTILE BREAST MOULDS

DESIGN: C. H. BEWLEY	DWG NO.: B-0020		REV: 1
DRAWN: C. H. BEWLEY	PROJECT: DIET BREAST CANCER SCREENING SYSTEM		
SUPERVISOR: G. CHASE	ISSUE DATE: 25-09-2015	DRAWING NOT TO SCALE	SHEET: 1 OF 1

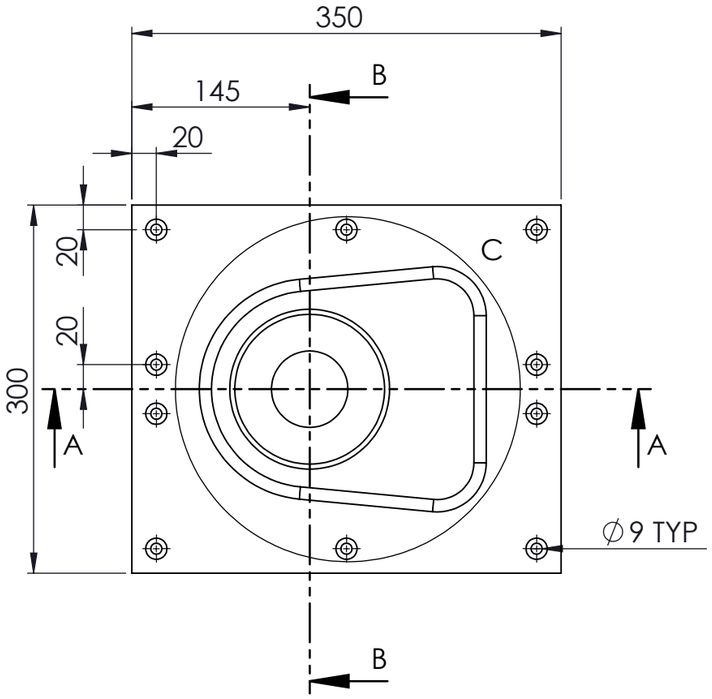

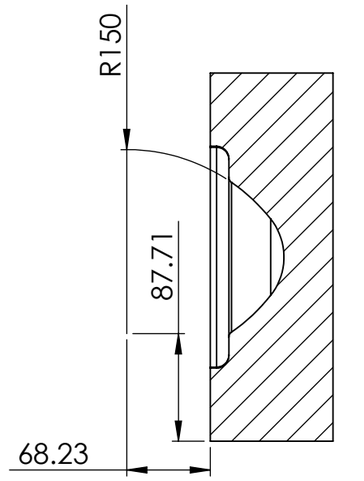

SECTION B-B

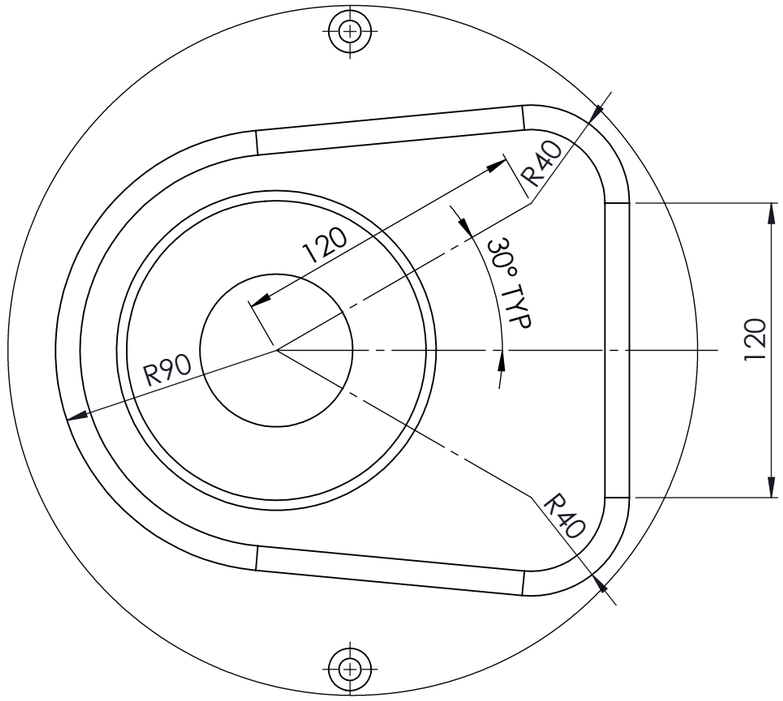

DETAIL C
SCALE 2 : 5

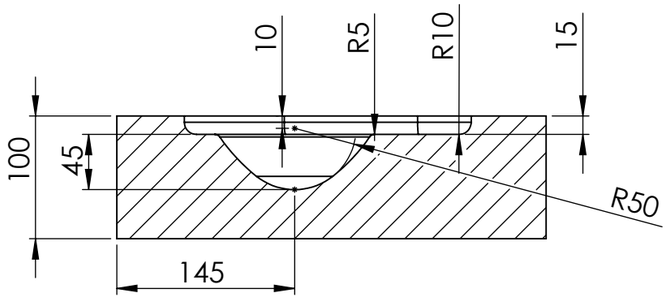

SECTION A-A

THIRD ANGLE PROJECTION	THIS DOCUMENT IS ISSUED IN STRICT CONFIDENCE ON CONDITION THAT IT IS NOT COPIED, REPRINTED, OR DISCLOSED TO A THIRD PARTY EITHER WHOLLY OR IN PART WITHOUT THE WRITTEN CONSENT OF UNIVERSITY OF CANTERBURY	UNIVERSITY OF CANTERBURY © DEPARTMENT OF MECHANICAL ENGINEERING	UNIVERSITY OF CANTERBURY
MATERIAL: MODELLING BOARD		5TH PERCENTILE BREAST MOULD	
FINISH		DESIGN: C. H. BEWLEY	DWG NO.: B-0021
TOLERANCE (UNLESS OTHERWISE SPECIFIED) DECIMAL mm		DRAWN: C. H. BEWLEY	PROJECT: DIET BREAST CANCER SCREENING SYSTEM
.X ± .XX ± .XXX ± ANG. ± 1°		SUPERVISOR: G. CHASE	ISSUE DATE: 25-09-2015
		DRAWING NOT TO SCALE	SHEET: 1 OF 1

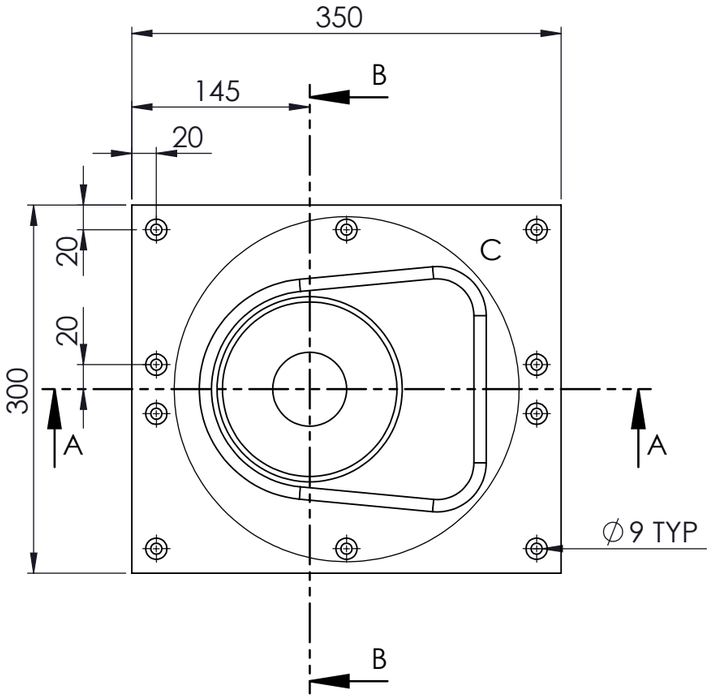

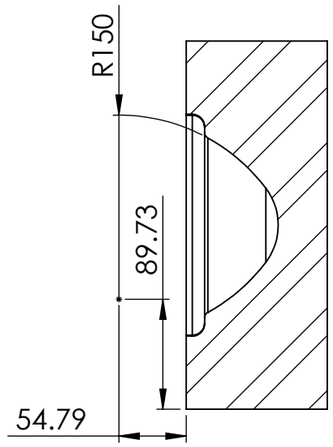

SECTION B-B

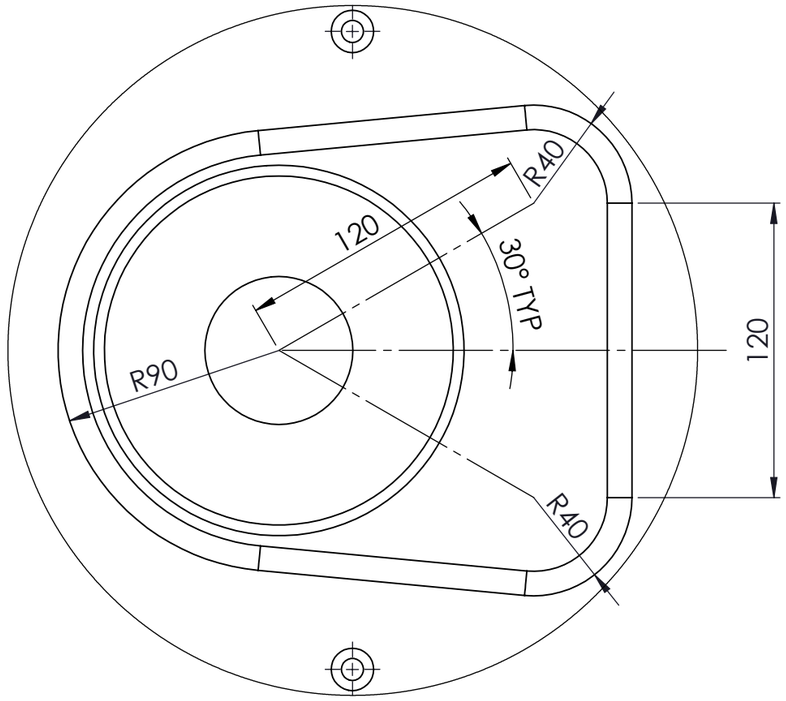

DETAIL C
SCALE 2 : 5

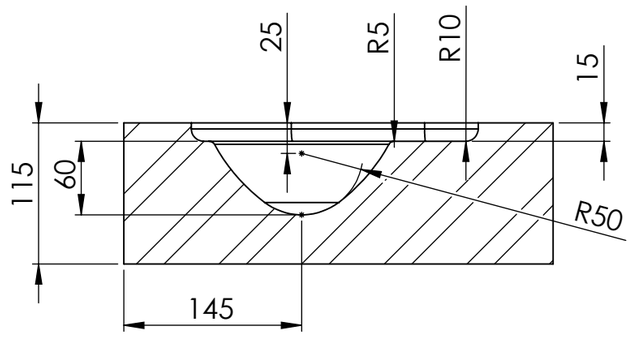

THIRD ANGLE PROJECTION	THIS DOCUMENT IS ISSUED IN STRICT CONFIDENCE ON CONDITION THAT IT IS NOT COPIED, REPRINTED, OR DISCLOSED TO A THIRD PARTY EITHER WHOLLY OR IN PART WITHOUT THE WRITTEN CONSENT OF UNIVERSITY OF CANTERBURY	UNIVERSITY OF CANTERBURY © DEPARTMENT OF MECHANICAL ENGINEERING	UNIVERSITY OF CANTERBURY
MATERIAL: MODELLING BOARD		50TH PERCENTILE BREAST MOULD	
FINISH		DESIGN: C. H. BEWLEY	DWG NO.: B-0022
TOLERANCE (UNLESS OTHERWISE SPECIFIED) DECIMAL mm: .X ± .XX ± .XXX ± ANG. ± 1°		DRAWN: C. H. BEWLEY	PROJECT: DIET BREAST CANCER SCREENING SYSTEM
		SUPERVISOR: G. CHASE	ISSUE DATE: 25-09-2015
		DRAWING NOT TO SCALE	SHEET: 1 OF 1

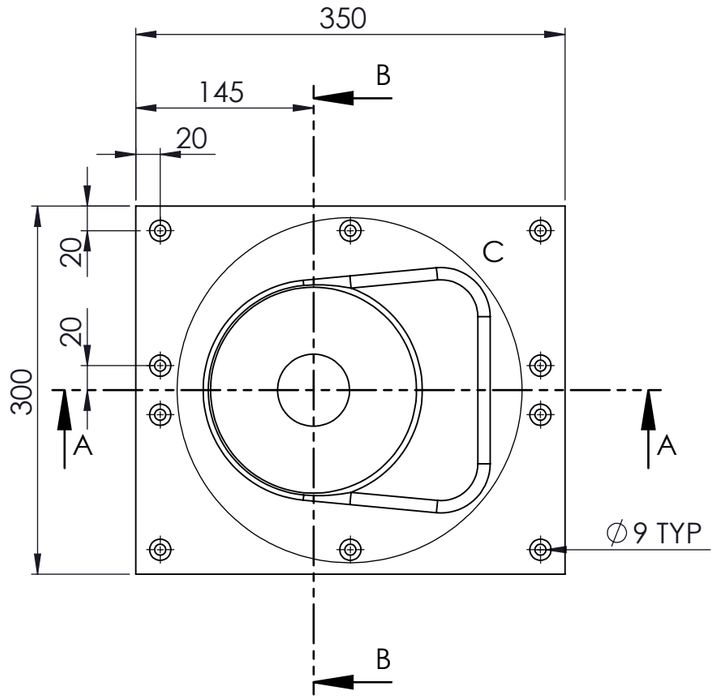

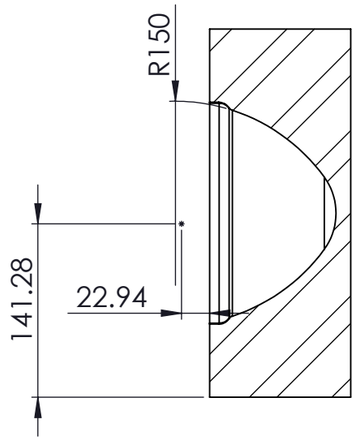

SECTION B-B

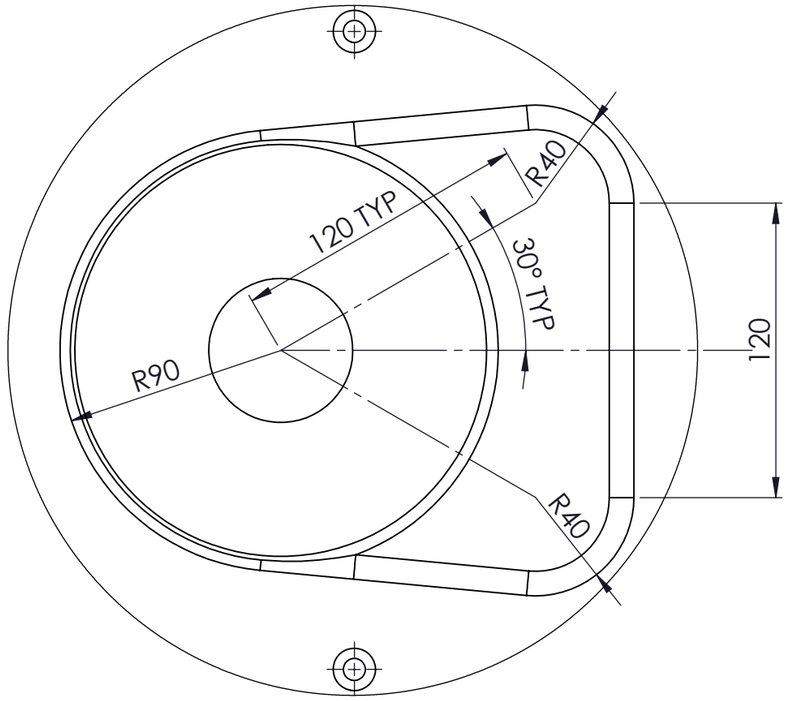

DETAIL C
SCALE 2 : 5

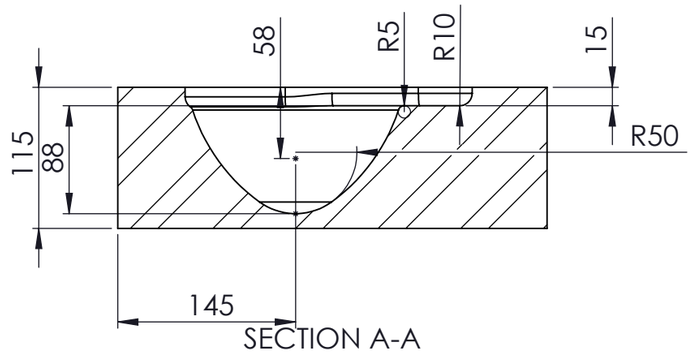

SECTION A-A

THIRD ANGLE PROJECTION	THIS DOCUMENT IS ISSUED IN STRICT CONFIDENCE ON CONDITION THAT IT IS NOT COPIED, REPRINTED, OR DISCLOSED TO A THIRD PARTY EITHER WHOLLY OR IN PART WITHOUT THE WRITTEN CONSENT OF UNIVERSITY OF CANTERBURY	UNIVERSITY OF CANTERBURY © DEPARTMENT OF MECHANICAL ENGINEERING	UNIVERSITY OF CANTERBURY
MATERIAL: MODELLING BOARD		95TH PERCENTILE BREAST MOULD	
FINISH		DESIGN: C. H. BEWLEY	DWG NO.: B-0023
TOLERANCE (UNLESS OTHERWISE SPECIFIED) DECIMAL mm: .X ± .XX ± .XXX ± ANG. ± 1°		DRAWN: C. H. BEWLEY	PROJECT: DIET BREAST CANCER SCREENING SYSTEM
		SUPERVISOR: G. CHASE	ISSUE DATE: 25-09-2015
		DRAWING NOT TO SCALE	SHEET: 1 OF 1

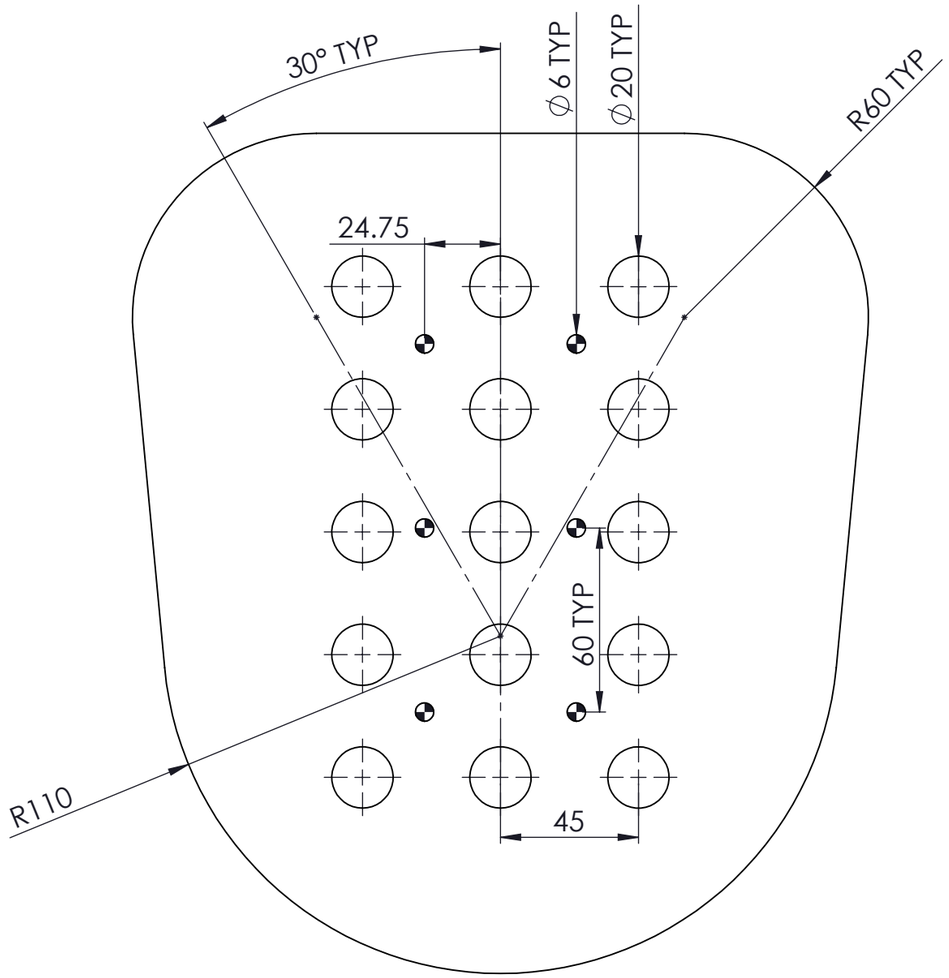

TOP VIEW

SIDE VIEW

UNIVERSITY OF CANTERBURY ©
DEPARTMENT OF MECHANICAL ENGINEERING

UNIVERSITY OF CANTERBURY

MATERIAL: PERSPEX

FINISH:

TOLERANCE (UNLESS OTHERWISE SPECIFIED)
DECIMAL mm
.X ± .XX ± .XXX ± ANG. ± °

SUPPORT PLATE

DESIGN	DWG NO.	REV
C. H. BEWLEY	B-0030	1
DRAWN: C. H. BEWLEY	PROJECT: DIET BREAST CANCER SCREENING SYSTEM	
SUPERVISOR: G. CHASE	ISSUE DATE: 25-09-2015	DRAWING NOT TO SCALE / SHEET: 1 OF 1

LEFT SUPPORT

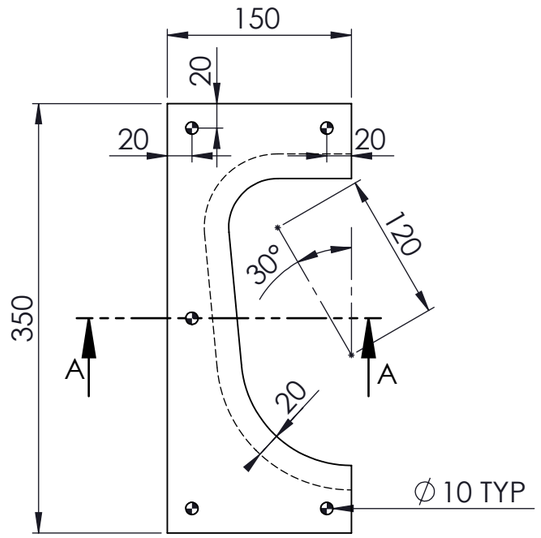

RIGHT SUPPORT

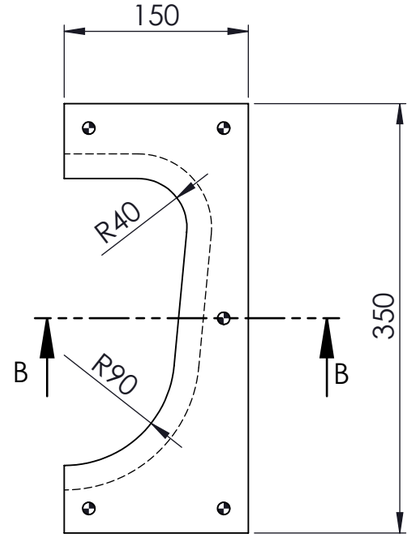

SECTION A-A

SECTION B-B

THIRD ANGLE PROJECTION	THIS DOCUMENT IS ISSUED IN STRICT CONFIDENCE ON CONDITION THAT IT IS NOT COPIED, REPRINTED, OR DISCLOSED TO A THIRD PARTY EITHER WHOLLY OR IN PART WITHOUT THE WRITTEN CONSENT OF UNIVERSITY OF CANTERBURY	UNIVERSITY OF CANTERBURY © DEPARTMENT OF MECHANICAL ENGINEERING	UNIVERSITY OF CANTERBURY
MATERIAL: PERSPEX		SUPPORT STRUCTURE	
FINISH		DESIGN: C. H. BEWLEY	DWG NO.: B-0040
			REV: 1
TOLERANCE (UNLESS OTHERWISE SPECIFIED)		DRAWN: C. H. BEWLEY	PROJECT: DIET BREAST CANCER SCREENING SYSTEM
DECIMAL mm		SUPERVISOR: G. CHASE	ISSUE DATE: 25-09-2015
.X ± .XX ± .XXX ± ANG. ±1 °		DRAWING NOT TO SCALE	SHEET: 1 OF 1

Appendix C: DIET Surface Design Specification

This appendix contains drawings, listed below, which detail the proposed new DIET Surface.

Drawing Number	Detail
D-0010	Overall Assembly
D-0011	Assembly Parts
D-0020	Support Structure
D-0021	Support Structure – Left Support
D-0022	Support Structure – Right Support
D-0023	Support Structure – Width Support
D-0024	Support Structure – Flat Support
D-0025	Support Structure – Connection Plate
D-0030	Support Leg
D-0040	Flat Surface
D-0050	Foam Surface

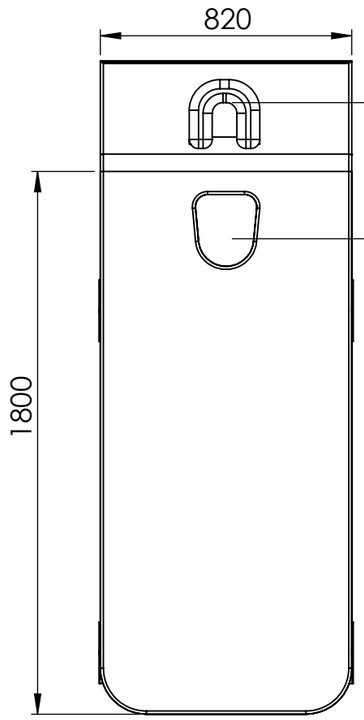

DISTANCE BETWEEN BREAST CENTER AND HEAD REST TO BE BETWEEN 350mm AND 450mm. FINAL DIMENSION TO BE CONFIRMED WITH FINAL DIET SHELL DESIGN

TOP VIEW

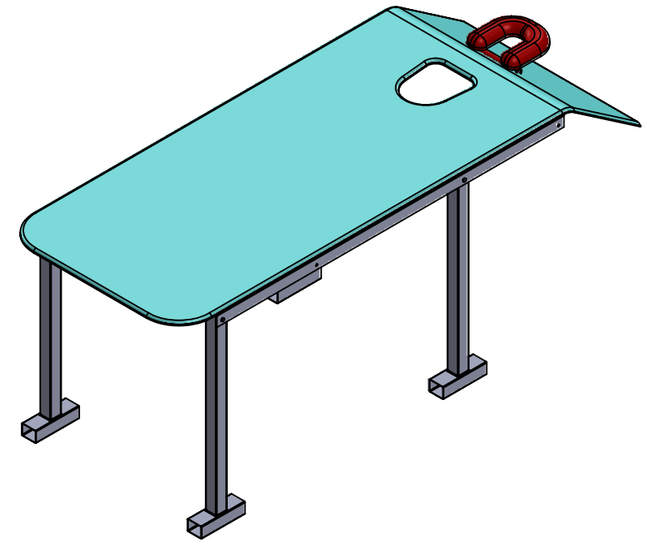

ISOMETRIC VIEW

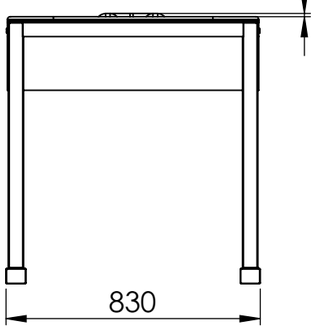

HEIGHT DIFFERENCE BETWEEN HEADREST AND FOAM SURFACE TO BE NO GREATER THAN 50mm. FINAL DIMENSION TO BE CONFIRMED WITH FINAL DIET SHELL DESIGN

SIDE VIEW

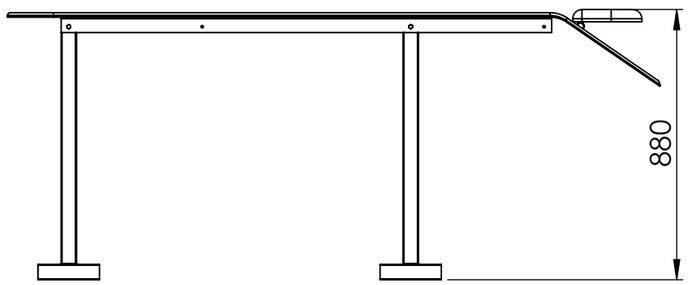

FRONT VIEW

THIRD ANGLE PROJECTION

MATERIAL: SEE BILL OF MATERIALS (D-0011)

FINISH: SEE PARTS

TOLERANCE (UNLESS OTHERWISE SPECIFIED)

DECIMAL mm

.X ± .XX ± .XXX ± ANG. ± °

UNIVERSITY OF CANTERBURY ©
DEPARTMENT OF MECHANICAL ENGINEERING

DIET SURFACE OVERALL ASSEMBLY

DESIGN	DWG NO.	REV
CHB	D-0010	1
DRAWN: CHB	PROJECT: DIET BREAST CANCER SCREENING SYSTEM	
SUPERVISOR: GJC	ISSUE DATE: 13.01.17	DRAWING NOT TO SCALE
		SHEET: 1 OF 1

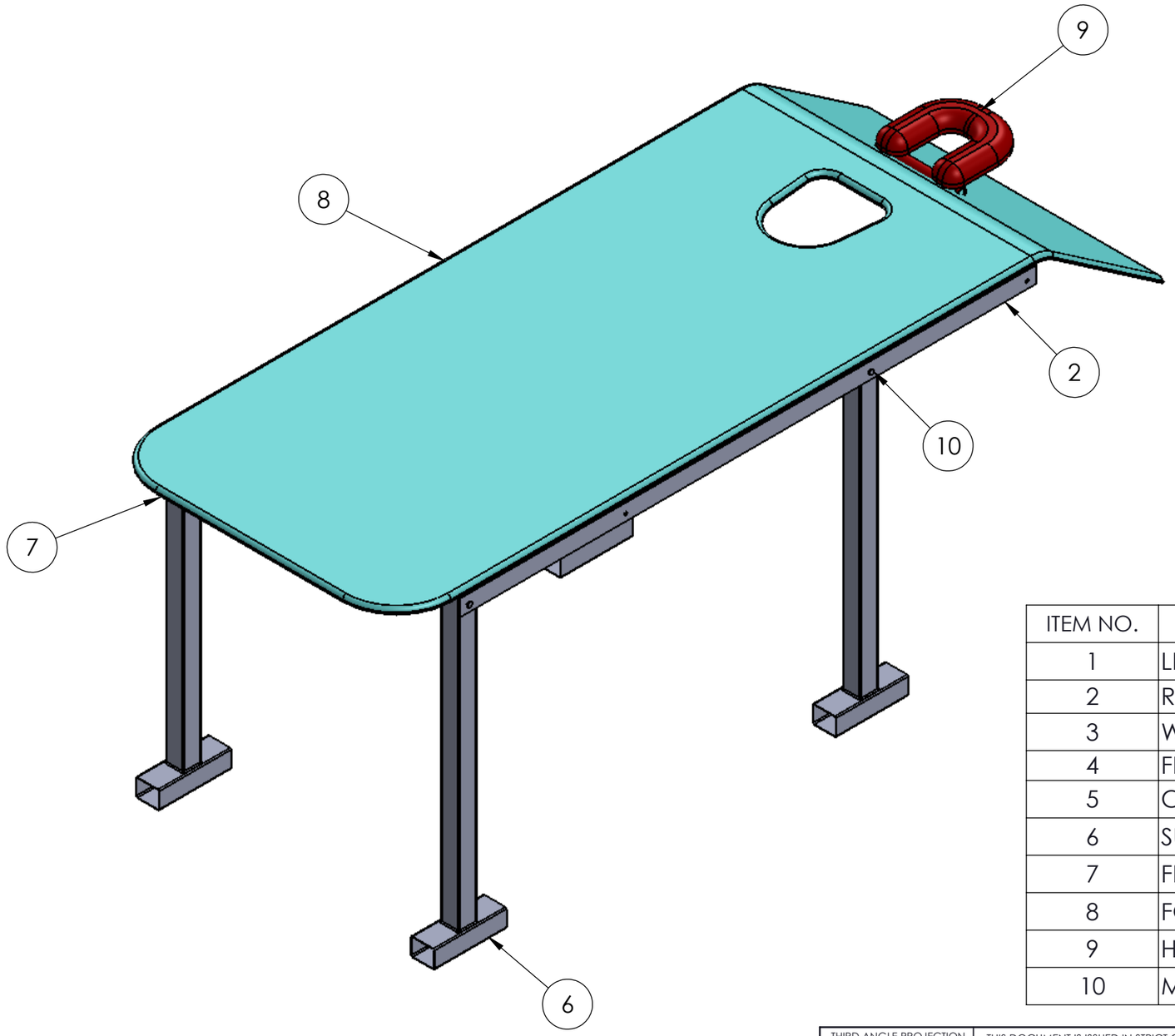

ISOMETRIC VIEW

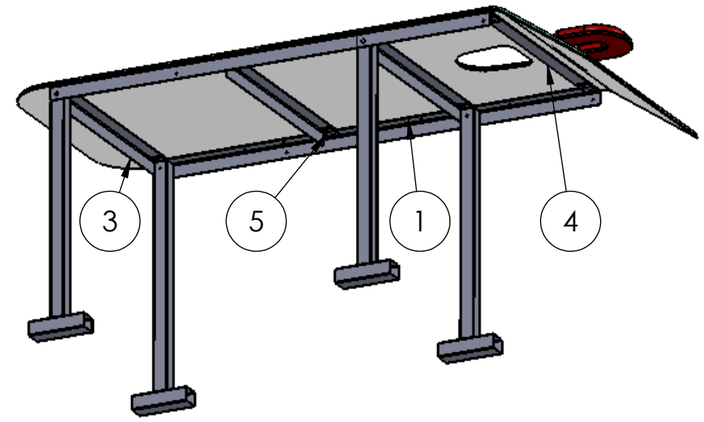

VIEW OF ASSEMBLY FROM BELOW

ITEM NO.	PART	MATERIAL	DWG NO.	QTY.
1	LEFT SUPPORT	ALUMINIUM	D-0021	1
2	RIGHT SUPPORT	ALUMINIUM	D-0022	1
3	WIDTH SUPPORT	ALUMINIUM	D-0023	3
4	FLAT SUPPORT	ALUMINIUM	D-0024	1
5	CONNECTION PLATE	ALUMINIUM	D-0025	8
6	SUPPORT LEG	ALUMINIUM	D-0030	4
7	FLAT SURFACE	5mm ALUMINIUM SHEET	D-0040	1
8	FOAM SURFACE	10MM EVA-DURA FOAM	D-0050	1
9	HEADREST	VINYL FACE CRADLE	-	1
10	M8 BOLTS	STEEL	-	20

THIRD ANGLE PROJECTION

MATERIAL: SEE BILL OF MATERIAL

FINISH: SEE PARTS

TOLERANCE (UNLESS OTHERWISE SPECIFIED)

DECIMAL mm

.X ± .XX ± .XXX ± ANG. ± °

UNIVERSITY OF CANTERBURY ©
DEPARTMENT OF MECHANICAL ENGINEERING

DIET SURFACE ASSEMBLY PARTS

DESIGN	DWG NO.	REV
CHB	D-0011	1

DRAWN	PROJECT
CHB	DIET BREAST CANCER SCREENING SYSTEM

SUPERVISOR	ISSUE DATE		SHEET
GJC	13.01.17	DRAWING NOT TO SCALE	1 OF 1

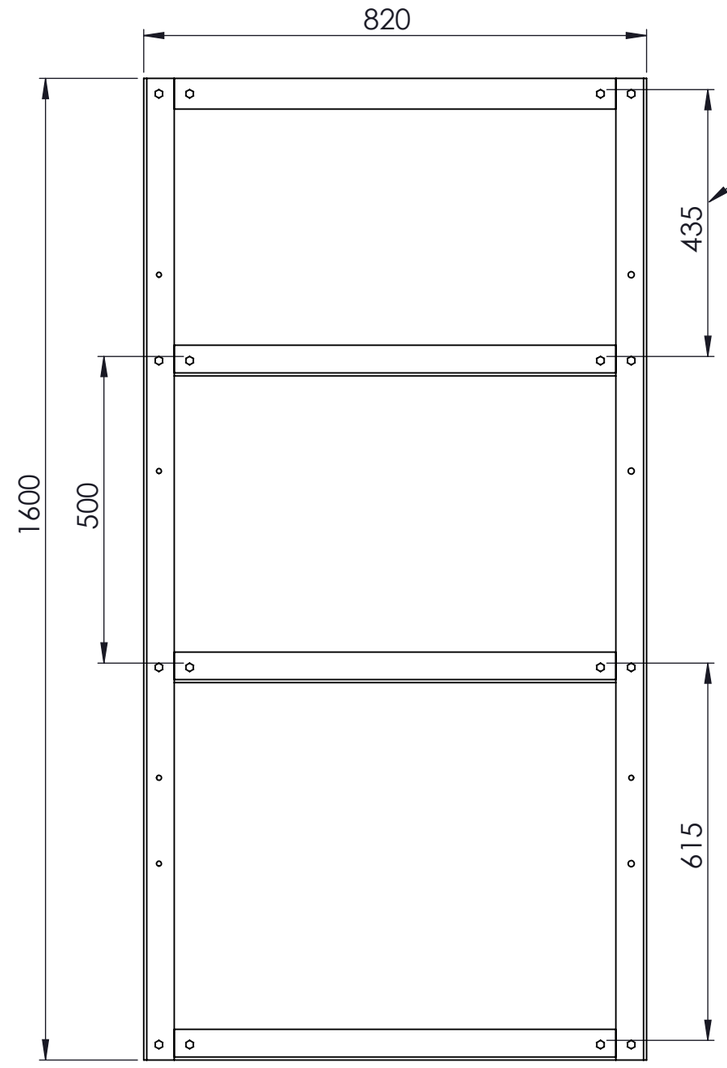

TOP VIEW

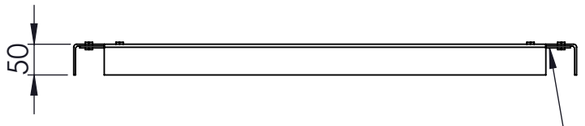

SIDE VIEW

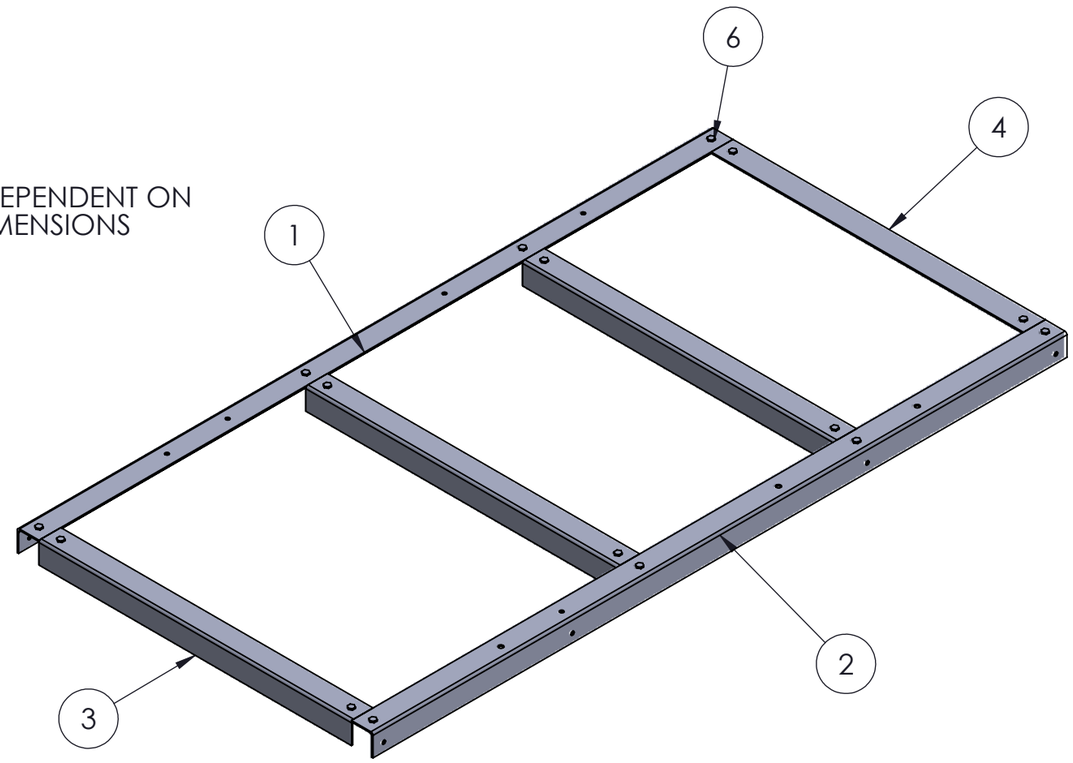

ISOMETRIC VIEW

ITEM NO.	PART	MATERIAL	DWG NO.	QTY.
1	LEFT SUPPORT	6060 ALUMINIUM	D - 0021	1
2	RIGHT SUPPORT	6060 ALUMINIUM	D - 0022	1
3	WIDTH SUPPORT	6060 ALUMINIUM	D - 0023	3
4	FLAT SUPPORT	6060 ALUMINIUM	D - 0024	1
5	CONNECTION PLATE	6060 ALUMINIUM	D - 0025	8
6	M8 BOLTS	STEEL	-	16

THIRD ANGLE PROJECTION

MATERIAL: SEE PARTS

FINISH: SEE PARTS

TOLERANCE (UNLESS OTHERWISE SPECIFIED)

DECIMAL mm

.X ± .XX ± .XXX ± ANG. ± °

UNIVERSITY OF CANTERBURY ©
DEPARTMENT OF MECHANICAL ENGINEERING

DIET SURFACE SUPPORT STRUCTURE

DESIGN	DWG NO.	REV
CHB	D-0020	1
DRAWN: CHB	PROJECT: DIET BREAST CANCER SCREENING SYSTEM	
SUPERVISOR: GJC	ISSUE DATE: 10.01.17	DRAWING NOT TO SCALE / SHEET: 1 OF 1

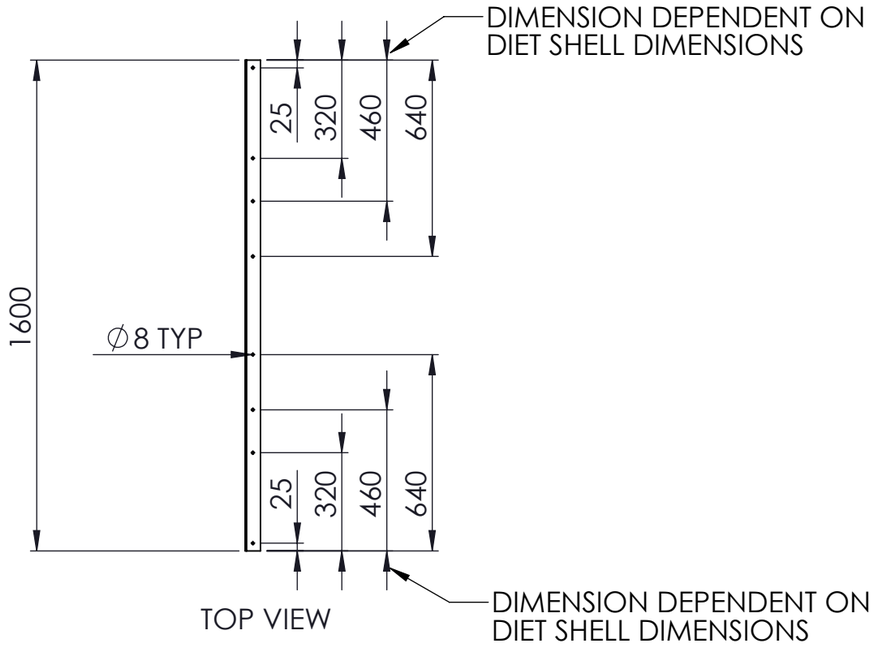

TOP VIEW

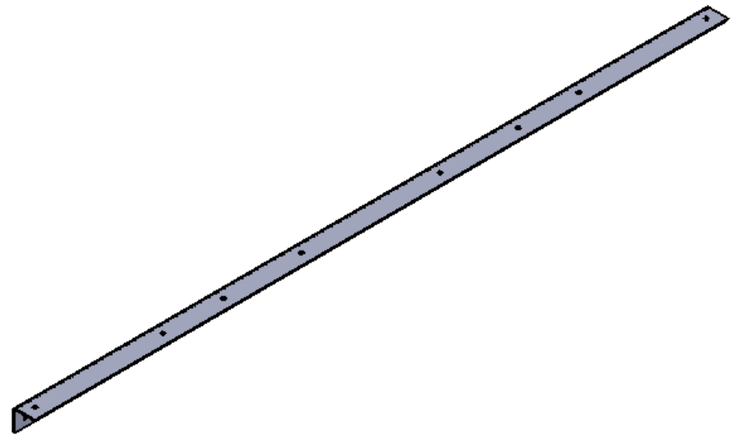

ISOMETRIC VIEW

A

SIDE VIEW

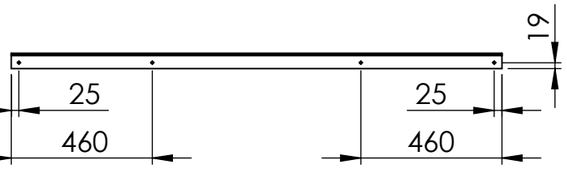

FRONT VIEW

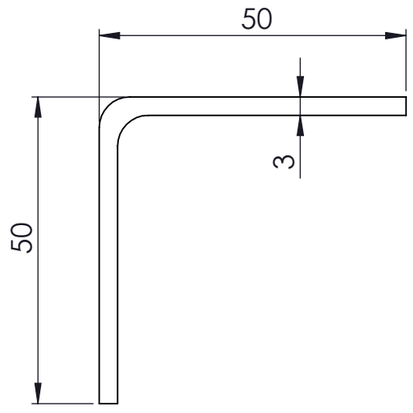

DETAIL A
SCALE 1 : 1

THIRD ANGLE PROJECTION

MATERIAL: 6060 ALUMINIUM

FINISH: ANODISED

TOLERANCE (UNLESS OTHERWISE SPECIFIED)
DECIMAL mm
.X ± .XX ± .XXX ± ANG. ± °

UNIVERSITY OF CANTERBURY ©
DEPARTMENT OF MECHANICAL ENGINEERING

DIET SURFACE SUPPORT STRUCTURE - LEFT SUPPORT

DESIGN	DWG NO.	REV
CHB	D-0021	1
DRAWN: CHB	PROJECT: DIET BREAST CANCER SCREENING SYSTEM	
SUPERVISOR: GJC	ISSUE DATE: 10.01.17	DRAWING NOT TO SCALE / SHEET: 1 OF 1

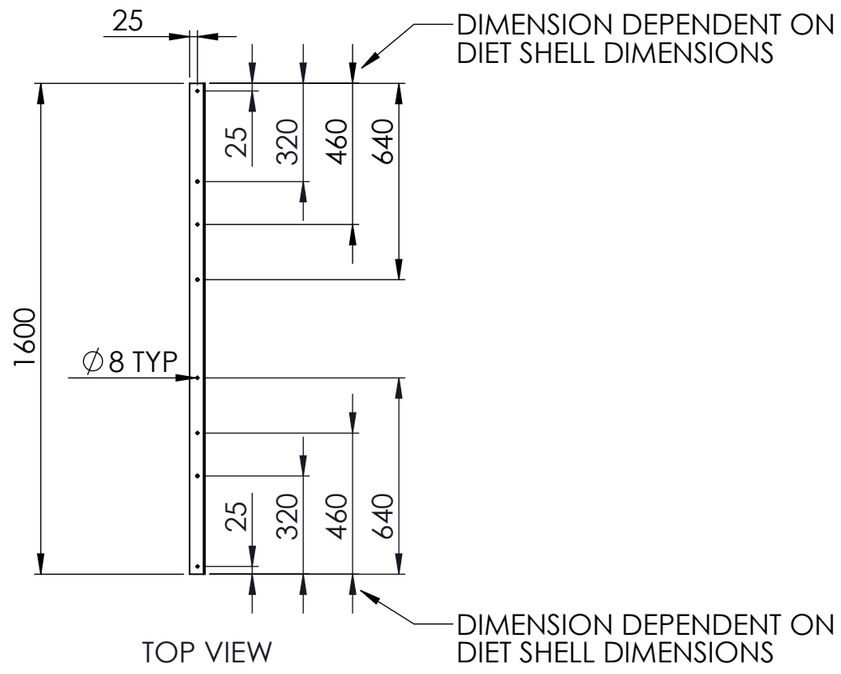

TOP VIEW

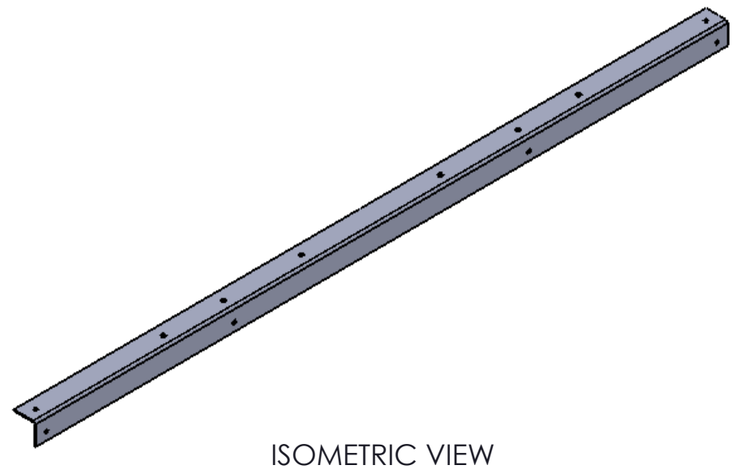

ISOMETRIC VIEW

A

SIDE VIEW

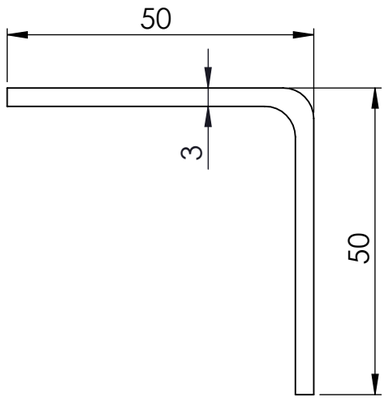

DETAIL A
SCALE 1 : 1

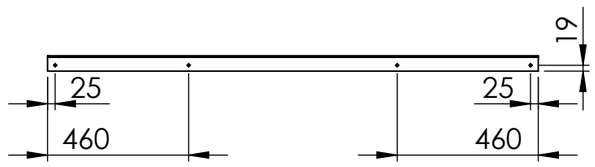

FRONT VIEW

THIRD ANGLE PROJECTION	THIS DOCUMENT IS ISSUED IN STRICT CONFIDENCE ON CONDITION THAT IT IS NOT COPIED, REPRINTED, OR DISCLOSED TO A THIRD PARTY EITHER WHOLLY OR IN PART WITHOUT THE WRITTEN CONSENT OF UNIVERSITY OF CANTERBURY	UNIVERSITY OF CANTERBURY © DEPARTMENT OF MECHANICAL ENGINEERING	UNIVERSITY OF CANTERBURY
MATERIAL: 6060 ALUMINIUM		DIET SURFACE SUPPORT STRUCTURE - RIGHT SUPPORT	
FINISH: ANODISED		DESIGN: CHB / DWG NO.: D-0022	REV: 1
TOLERANCE (UNLESS OTHERWISE SPECIFIED) DECIMAL mm: .X ± .XX ± .XXX ± ANG. ± °		DRAWN: CHB / PROJECT: DIET BREAST CANCER SCREENING SYSTEM	
		SUPERVISOR: GJC / ISSUE DATE: 10.01.17 / DRAWING NOT TO SCALE	SHEET: 1 OF 1

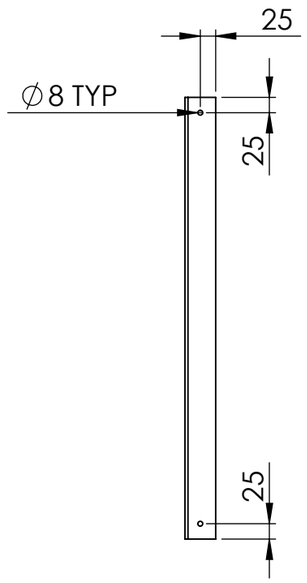

TOP VIEW

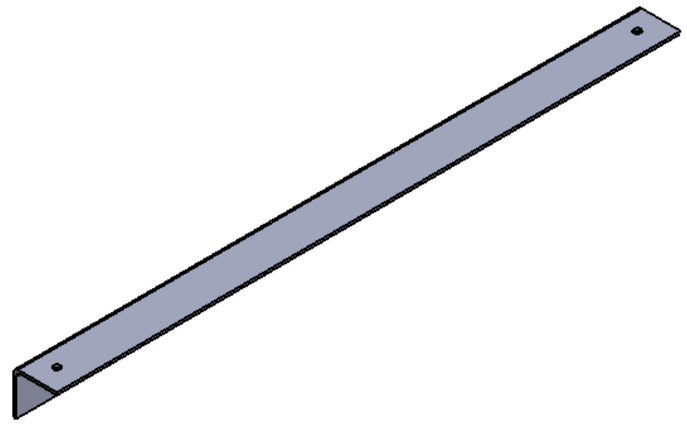

ISOMETRIC VIEW

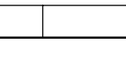

SIDE VIEW

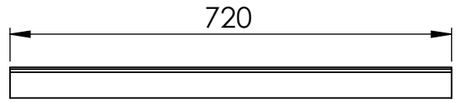

FRONT VIEW

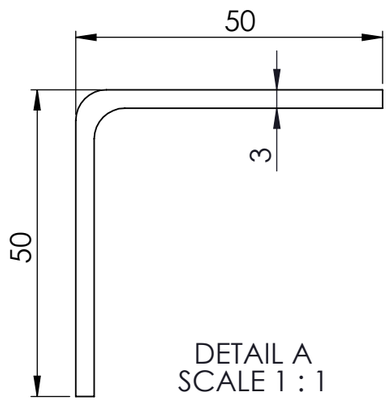

DETAIL A
SCALE 1 : 1

THIRD ANGLE PROJECTION

MATERIAL: 6060 ALUMINIUM

FINISH: ANODISED

TOLERANCE (UNLESS OTHERWISE SPECIFIED)

DECIMAL mm

.X ± .XX ± .XXX ± ANG. ± °

UNIVERSITY OF CANTERBURY © DEPARTMENT OF MECHANICAL ENGINEERING

DIET SURFACE SUPPORT STRUCTURE - WIDTH SUPPORT

DESIGN	DWG NO.	REV
CHB	D-0023	1
DRAWN: CHB	PROJECT: DIET BREAST CANCER SCREENING SYSTEM	
SUPERVISOR: GJC	ISSUE DATE: 10.01.17	DRAWING NOT TO SCALE / SHEET: 1 OF 1

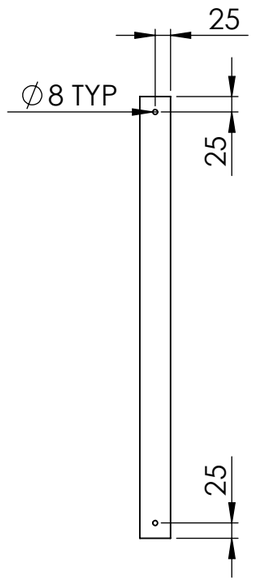

TOP VIEW

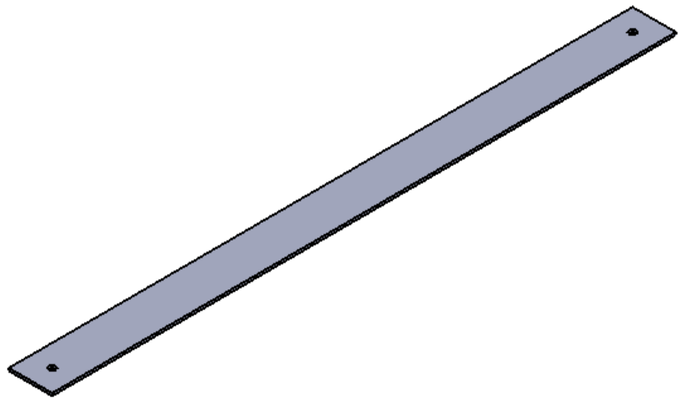

ISOMETRIC VIEW

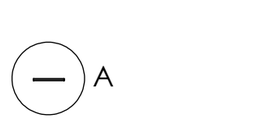

SIDE VIEW

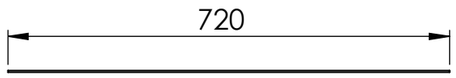

FRONT VIEW

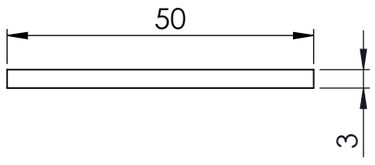

DETAIL A
SCALE 1 : 1

THIRD ANGLE PROJECTION

MATERIAL: 6060 ALUMINIUM

FINISH: ANODISED

TOLERANCE (UNLESS OTHERWISE SPECIFIED)
DECIMAL mm
.X ± .XX ± .XXX ± ANG. ± °

UNIVERSITY OF CANTERBURY ©
DEPARTMENT OF MECHANICAL ENGINEERING

DIET SURFACE SUPPORT STRUCTURE - FLAT SUPPORT

DESIGN	DWG NO.	REV
CHB	D-0024	1
DRAWN: CHB	PROJECT: DIET BREAST CANCER SCREENING SYSTEM	
SUPERVISOR: GJC	ISSUE DATE: 10.01.17	DRAWING NOT TO SCALE / SHEET: 1 OF 1

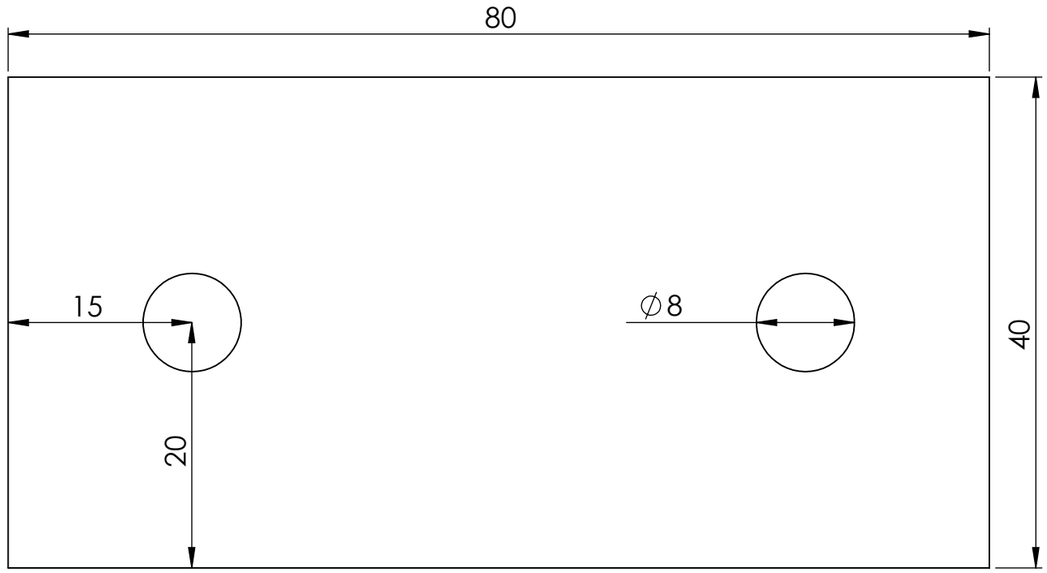

TOP VIEW

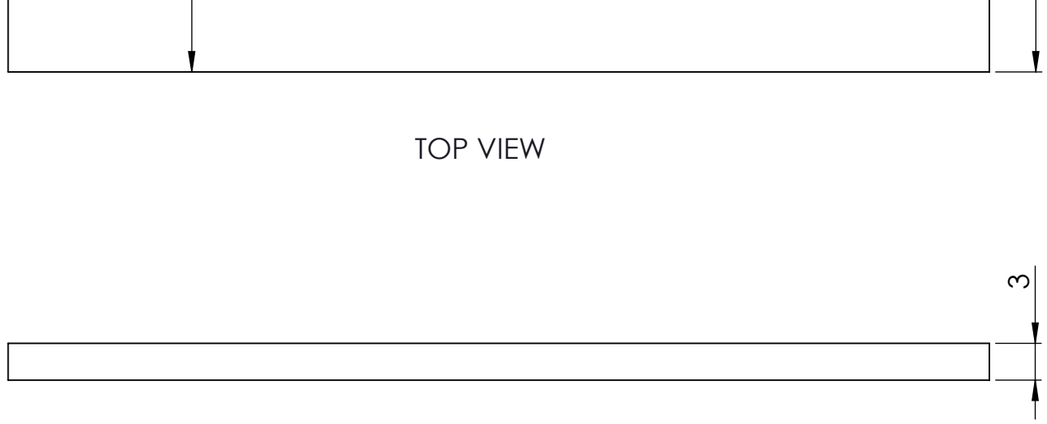

SIDE VIEW

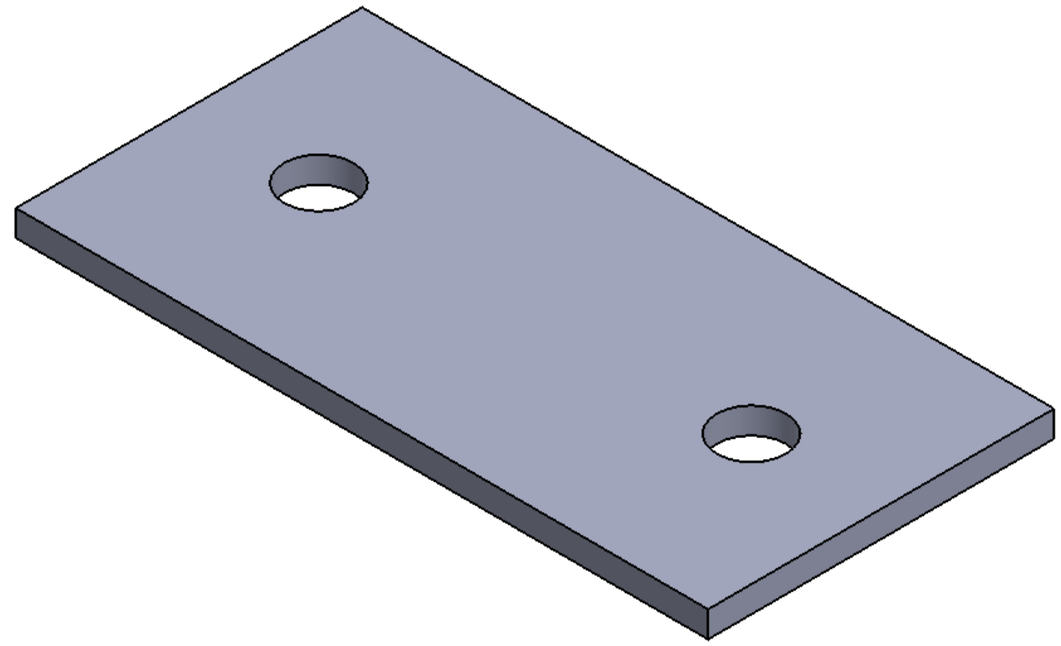

ISOMETRIC VIEW

THIRD ANGLE PROJECTION

MATERIAL: 6060 ALUMINIUM

FINISH: ANODISED

TOLERANCE (UNLESS OTHERWISE SPECIFIED)

DECIMAL mm

.X ± .XX ± .XXX ± ANG. ± °

UNIVERSITY OF CANTERBURY ©
DEPARTMENT OF MECHANICAL ENGINEERING

DIET SURFACE SUPPORT STRUCTURE - CONNECTION PLATE

DESIGN	DWG NO.	REV
CHB	D-0025	1
DRAWN: CHB	PROJECT: DIET BREAST CANCER SCREENING SYSTEM	
SUPERVISOR: GJC	ISSUE DATE: 10.01.17	DRAWING NOT TO SCALE
		SHEET: 1 OF 1

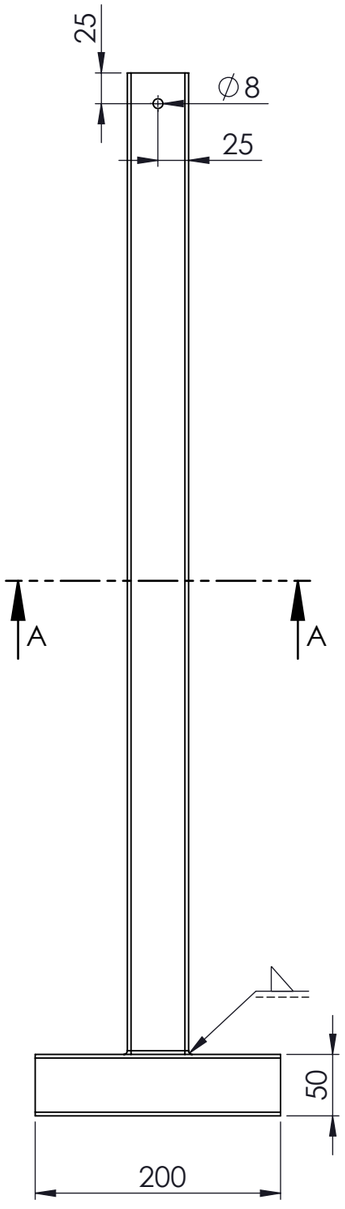

FRONT VIEW

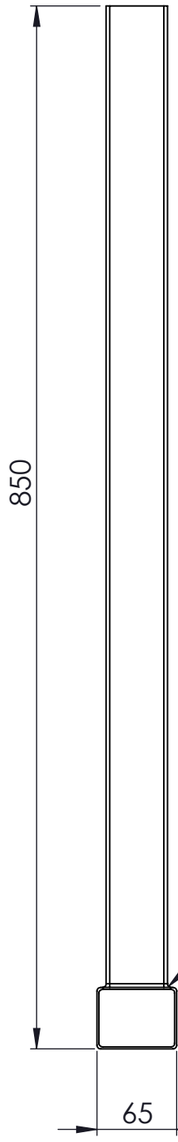

SIDE VIEW

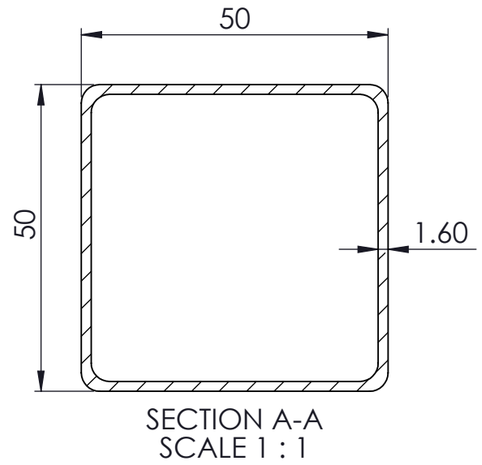

SECTION A-A
SCALE 1 : 1

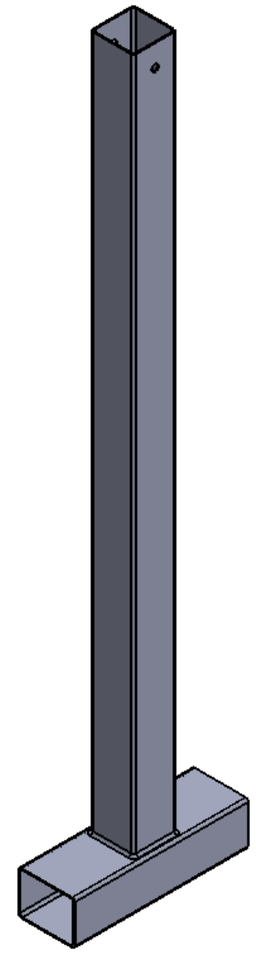

ISOMETRIC VIEW

THIRD ANGLE PROJECTION

UNIVERSITY OF CANTERBURY ©
DEPARTMENT OF MECHANICAL ENGINEERING

UNIVERSITY OF CANTERBURY

MATERIAL: ALUMINIUM

FINISH: ANODISED

TOLERANCE (UNLESS OTHERWISE SPECIFIED)
DECIMAL mm
.X ± .XX ± .XXX ± ANG. ± °

DIET SURFACE SUPPORT LEG

DESIGN	DWG NO.	REV
CHB	D-0030	1
DRAWN: CHB	PROJECT: DIET BREAST CANCER SCREENING SYSTEM	
SUPERVISOR: GJC	ISSUE DATE: 14.12.16	DRAWING NOT TO SCALE / SHEET: 1 OF 1

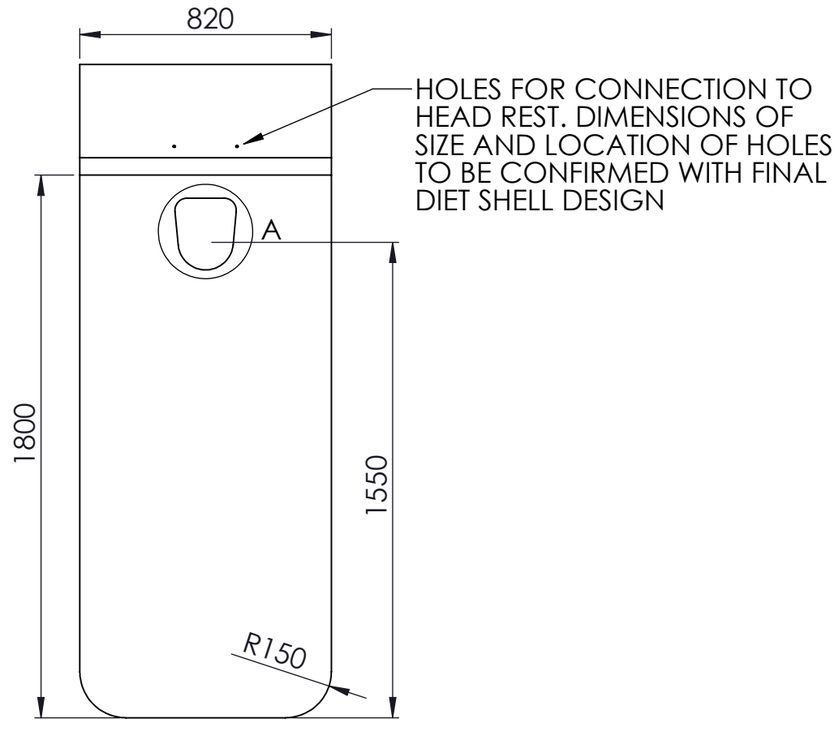

TOP VIEW
SCALE 1:20

SIDE VIEW
SCALE 1:20

ANGLE TO BE BETWEEN 130° AND 160°. FINAL DIMENSION TO BE CONFIRMED WITH FINAL DIET SHELL DESIGN

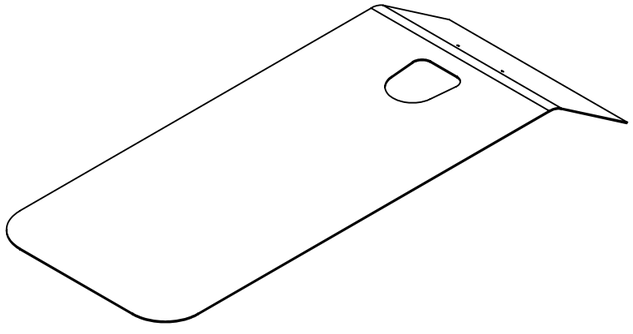

ISOMETRIC VIEW
SCALE 1:20

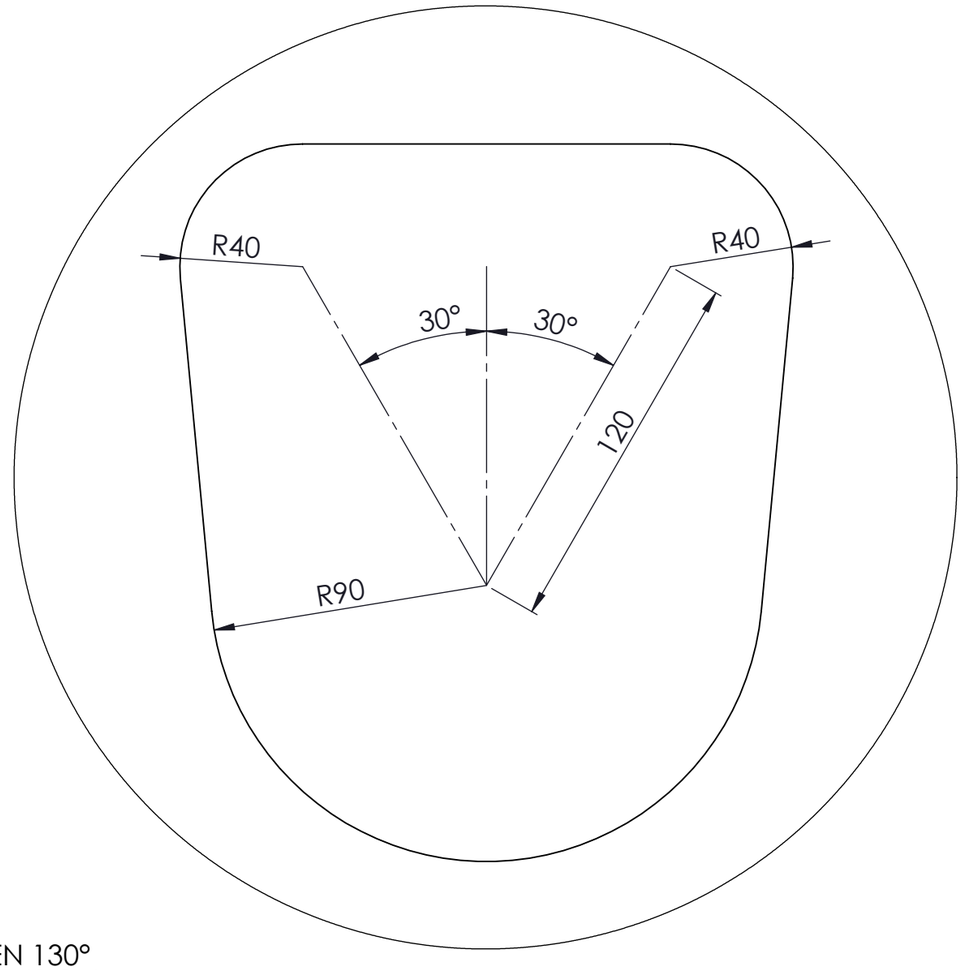

DETAIL A
SCALE 1 : 2

THIRD ANGLE PROJECTION

UNIVERSITY OF CANTERBURY ©
DEPARTMENT OF MECHANICAL ENGINEERING

MATERIAL: 5mm ALUMINIUM SHEET

FINISH: ANODISED IN BLACK

TOLERANCE (UNLESS OTHERWISE SPECIFIED)
DECIMAL mm
.X ± .XX ± .XXX ± ANG. ± °

DIET SURFACE FLAT SURFACE

DESIGN	DWG NO.	REV
CHB	D-0040	1
DRAWN: CHB	PROJECT: DIET BREAST CANCER SCREENING SYSTEM	
SUPERVISOR: GJC	ISSUE DATE: 14.12.16	DRAWING NOT TO SCALE / SHEET: 1 OF 1

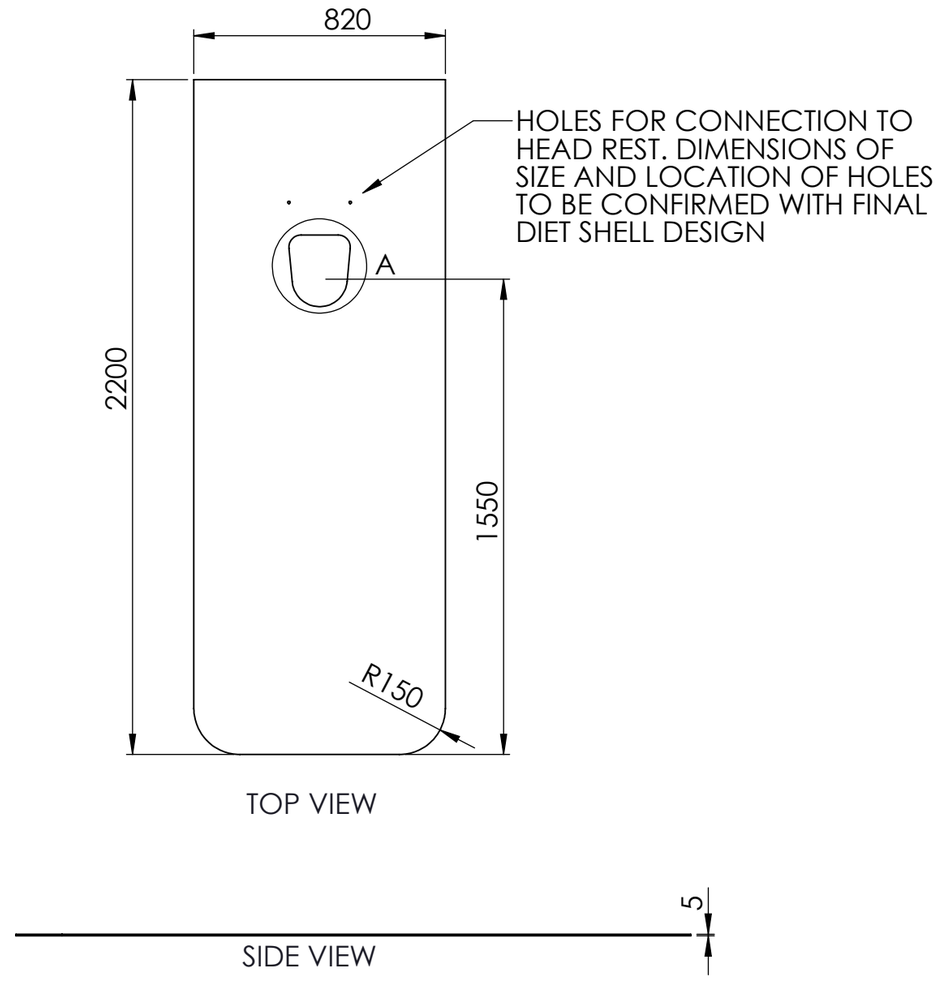

TOP VIEW

SIDE VIEW

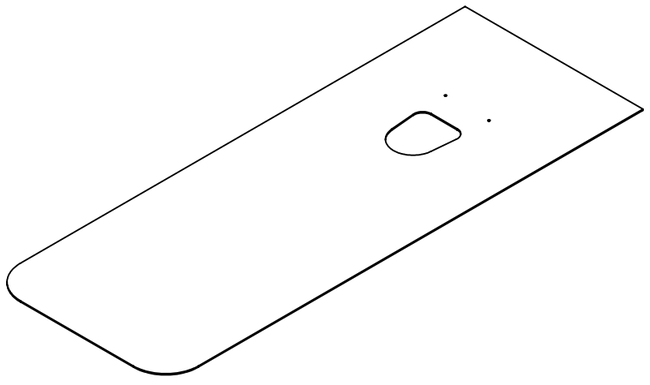

ISOMETRIC VIEW

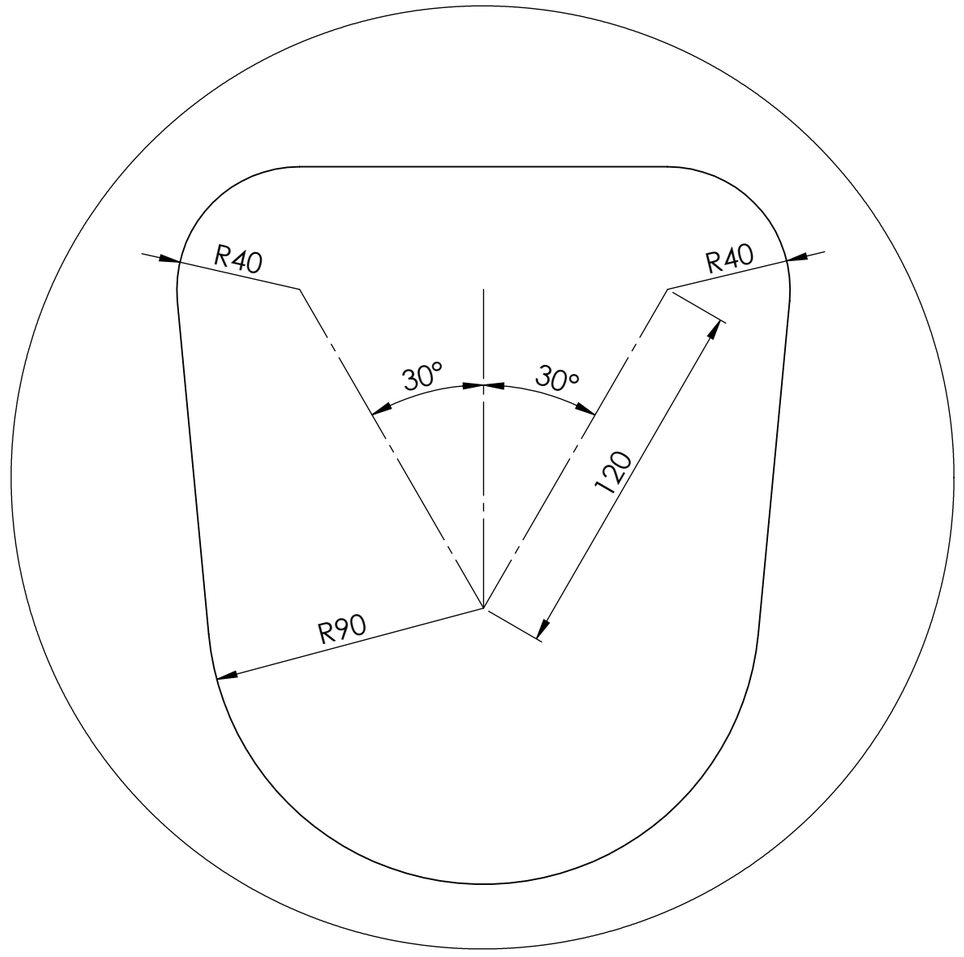

DETAIL A
SCALE 1 : 2

THIRD ANGLE PROJECTION

UNIVERSITY OF CANTERBURY ©
DEPARTMENT OF MECHANICAL ENGINEERING

MATERIAL: 10mm EVA-DURA FOAM

FINISH: NA

TOLERANCE (UNLESS OTHERWISE SPECIFIED)
DECIMAL mm
.X ± .XX ± .XXX ± ANG. ± °

FOAM SURFACE

DESIGN	DWG NO.	REV
CHB	D-0050	1

DRAWN	PROJECT
CHB	DIET BREAST CANCER SCREENING SYSTEM

SUPERVISOR	ISSUE DATE		SHEET
GJC	14.12.16	DRAWING NOT TO SCALE	1 OF 1